Tau protein exerts noncanonical functions in aging disorders: focus on Neurodegeneration and Cancer

A doctoral dissertation presented by

Claudia Magrin

Under the supervision of

Prof. Dr. Paolo Paganetti

Dr. Stéphanie Papin

Submitted to the

Faculty of Biomedical Sciences

Università della Svizzera italiana

For the degree of

PhD in Biomedical Sciences

July 2023

To my future

Summary

This thesis recapitulates the main findings obtained from January 2019 to June 2023. My PhD studies assessed the overall **hypothesis that the protein Tau exerts noncanonical functions in modulating chromatin maintenance**. This poorly investigated role of the microtubule binding protein Tau, linked to neurodegenerative disorders, collectively defined as tauopathies, may contribute to the pathogenesis of human aging-associated disorders through a loss-of-function mechanism. The entire research project was performed at the Laboratory for Aging Disorders (Laboratories for Translational Research, Ente Ospedaliero Cantonale, Bellinzona, Switzerland). The thesis director and group leader Prof. Dr. Paolo Paganetti and the senior scientist Dr. Stephanie Papin supervised the project.

The focus of my research was to investigate in cultured cells the role of the protein Tau in cellular pathways associated to aging disorders such as neurodegeneration and cancer. The thesis is organized as follows: in the Introduction (***Chapter 1)*****,** I describe the status of what is known about the biology of Tau and its implication in the two major disorders neurodegeneration and cancer. I present the overall rationale and hypothesis of the thesis (***Chapter 2)*** which is divided in two different parts: the first part of the project (***Chapter 3***) reports a newly discovered function of Tau in regulating the p53/MDM2 axis and cell fate. These results were published in my co-first author publication: *Sola, M. and* ***Magrin C.,*** *et al.; Tau affects P53 function and cell fate during the DNA damage response. Commun Biol 3, 245 (2020);* https://doi.org/10.1038/s42003-020-0975-4. The second part of the project (***Chapter 4***) reports a newly identified role of Tau in regulating gene expression and senescence through the modulation of PRC2, a chromatin remodeling complex, and of IGFBP3. These results were compiled in a first author publication: ***Magrin, C****., et al.; Tau protein modulates epigenetic-mediated induction of cellular senescence.* https://doi.org/10.1101/2023.06.05.543662. *Fr Cell Dev Biol (submitted 2023)*. The last part of the thesis (***Chapter 5***) includes the overall discussion and conclusion, and an outlook of the field based on my findings.

Throughout this thesis the use of the pronoun “we” has been employed to represent the collaborative nature of this research.

Index

Chapter 1

1. Neurodegenerative diseases

It is estimated that more than 44 million of people in the world are affected by neurodegenerative diseases. This number is constantly increasing due to the life-span increase and the unmet medical need. Alzheimer's disease (AD) and dementia are the most prevalent neurodegenerative disease (60-80%). The prediction of the non-profit group Alzheimer's Disease International is that there will be around 135 million of cases worldwide by the mid-century[1]. The World Health Organization (WHO) announces that by the 2040 neurodegenerative diseases and dementia will overtake cancer to become the second leading cause of death after cardiovascular diseases. Consequently, this group of disorders has a dramatic impact not only on affected people but also on their caregivers and the entire society. It cannot be ignored that the financial burden caused by neurodegenerative diseases amounts only in the U.S. at around US$200 billion year and this number is expected to increase to US$ 1.1 trillion by 2050[2]. The incidence rate of the disease increases from 1% annually in individuals aged 65 to 70 years to 6% to 8% for people over age 85[1,3,4]. The number of affected people is higher in female compared to male, but it is not clear whether it is due to higher risk or to the higher life expectance in women[4].

Currently, the diagnosis is based on measuring clinical performance of cognition and memory, where taking AD as an example the accuracy of diagnosis is below 80%. However, the accuracy can improve to about 90% with the analysis of disease-associated biomarkers in the corticospinal fluid, coupled to neuroimaging techniques such as position emission tomography (PET), single-photon emission computed tomography (SPECT)[5,6] and functional magnetic resonance imaging (fMRI), which inform on the anatomy, metabolism and the presence of protein deposits in the brain[7]. In fact, different studies demonstrate that one of the earliest indicators in AD is the metabolic decline, which represents a possible approach for a preclinical diagnosis of neurodegeneration[8]. Nevertheless, the gold standard for the diagnosis is based on the neuropathological evaluation at autopsy.

Several neurodegenerative disorders, including AD, Parkinson's disease (PD), Huntington's disease (HD) and frontotemporal dementia (FTD), are characterized by the accumulation and the aggregation of specific disease-related proteins such as α-synuclein, Tau, β-amyloid peptide (Aβ), TAR DNA-binding protein 43 (TDP-43), huntingtin (Htt), and others[9]. In general, neurodegenerative diseases are associated with progressive neuronal dysfunction

and death and are classified by their major clinical symptoms, the protein forming the deposits, the biochemical modifications or the cellular compartment affected by the protein deposits[10,11].

The deposition of abnormal forms of Tau characterizes the variety of neurodegenerative diseases known as tauopathies[12,13], which are classified as primary or secondary[14,15]. The primary tauopathies, in which the abnormal aggregation is considered the primary pathological feature, are mainly caused by genetic mutations or abnormalities in the *MAPT* gene[15–17]. The secondary tauopathies are associated with various causes and in this case the accumulation of Tau protein is the secondary consequence of other underlying conditions or diseases[14,15]. The classification of tauopathies is based on the distribution of Tau pathology in different cell populations of the brain: neuronal (Pick disease (PID); AD and neurofibrillary tangle (NFT)-dementia); neuronal and glial (progressive supranuclear palsy (PSP); corticobasal degeneration (CBD); argyrophilic grain disease (AGD)) and glial form (globular glial tauopathies (GGT))[10]. In hereditary form of tauopathies such as FTD-Tau, PSP or CBD, different mutations in the *MAPT* gene encoding for Tau were identified. These mutations are classified as missense mutations or as splicing mutations, which are present mainly in or near the microtubule binding domain and leads to the reduction of the affinity of Tau for microtubules and/or increase the tendency for aggregation[18,19]. The majority of *MAPT* mutations in coding regions are detected in the carboxyl terminal end of Tau containing the microtubule-binding domain and the most common is the P301L[20].

The molecular mechanisms of Tau-induced neurodegeneration and tauopathies is still poorly understood and their characterization is crucial for the development of efficacious drug treatments[21].

2. Tau: from physiology to pathology

2.1 Physiological Functions of Tau

Tau was discovered as a microtubule-associated protein, which is responsible for the maintenance of the organization and the dynamics of microtubules[22,23]. In particular, the stability of microtubules is maintained by the equilibrium of phosphorylation and dephosphorylation of Tau[24]. The majority of Tau in the cells is associated to microtubules through its microtubule-binding domain (MBD) and the flanking regions[25]. Tau is considered a multi-functional protein with distinct roles in different subcellular compartments. Tau is regulating the transport of organelles and biomolecules in the cells and along the neuronal axon through different mechanisms[26]. Actually, Tau is influencing

the function of the motor protein dynein and kinesin[27,28] and it competes for the binding frequency, and it reduces the motile fraction and the run length, thereby slowing both the anterograde and the retrograde transport. In addition, it was demonstrated that Tau is essential for axonal elongation and maturation as shown in cultured rat neurons where the knockdown of Tau promotes the formation of neurites even in non-neuronal cells[29]. However, this function of Tau needs to be confirmed. For example, only a high overexpression of Tau can alter the transport in axons[30], whereas deletion of Tau does not affect the axonal transport in primary neuronal cultures or *in vivo*[31].

Tau is also found to distribute in dendritic spines[32] but the function of Tau in dendrites is not well characterized and defined.

2.2 Structure of Tau and domains

Tau is encoded by the *MAPT* gene located on chromosome 17q21[33] and comprises 16 exons[34]. Tau is a natively unfolded protein and presents little tendency for aggregation[35]. Tau is a hydrophilic protein[36] stable under acidic conditions and at high temperatures. Overall, Tau is a basic protein; however, the 120 N-terminal residues are predominantly acidic, and the 40 C-terminal residues are neutral. The heterogenous distribution of charges is important for the interaction of Tau with microtubules, its folding, but also for the pathogenic aggregation of the protein. Tau is composed of different domains (**Figure 1**) characterized by their different biochemical properties; the projection domain (N-terminal), the proline-rich domain, the MBD and the assembly domain (C-terminal)[37].

In the brain, Tau is synthesized through alternative splicing of exons 2, 3 and 10 in at least six different forms, which range from 352 to 441 amino acids in length (**Figure 1**) and a molecular weight between 45 and 65 kDa[38]. The difference between Tau splice variants is based on the presence of either none, one or two amino-terminal inserts (0N, 1N or 2N) and either three or four microtubule binding repeats (3R or 4R) in the MTB[38–40]. Tau is expressed mainly in neurons[41] but it is also present in astrocytes of human brain[42], oligodendrocytes of rat brains[43], and to low levels also in many peripheral cells.

The expression of Tau spliced forms is regulated during the development: all six Tau variants are expressed in the human adult central nervous system (CNS), whereas the predominant variant present in the embryonic brain is 0N3R, demonstrating that the regulation of Tau splicing is important during the development of the brain[44]. Tauopathies involving the 4R repeat forms are PSP, CBD and AGD where Tau aggregates are found in medial temporal lobe, cortex, basal ganglia subthalamic neurons and substantia nigra. The 3R repeat form is found in the hippocampus and dentate fascia in PID and Pick bodies.

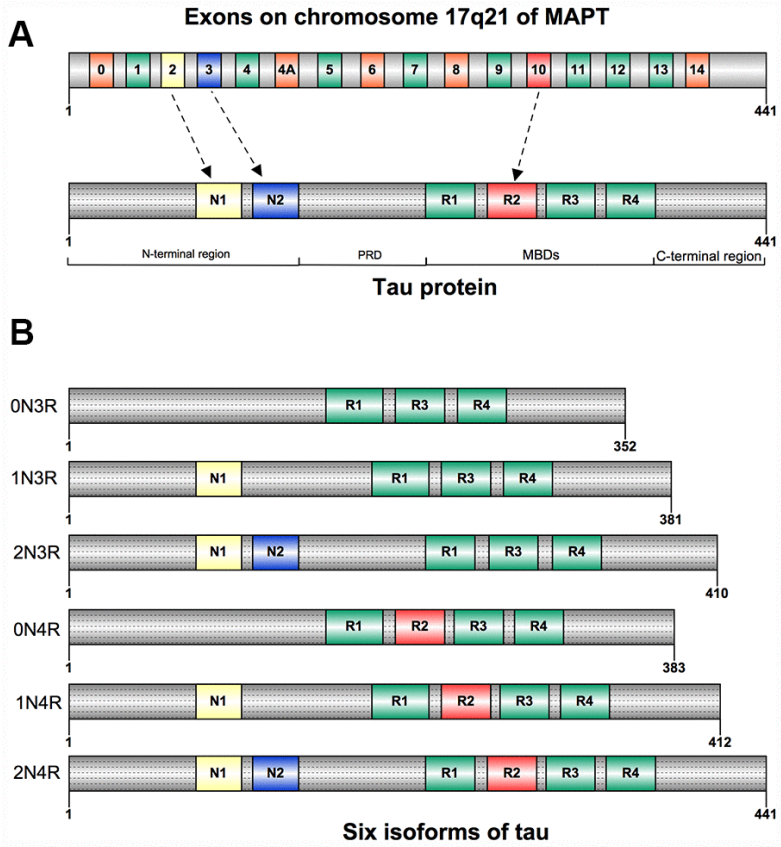

Figure 1. (**A**) The human *MAPT* gene encoding for Tau protein; the structure of human Tau protein with the N-terminal projection region, a proline-rich domain (PRD), a microtubule-binding domain (MBD), and a C-terminal region. (**B**) The alternative splicing generates six different forms in the adult brain, which are different in the number of N-terminal inserts (0N, 1N, or 2N) and C-terminal repeats (3R or 4R). The length of each isoform in terms of amino acid number is also given [45].

2.3 Post-translational modifications (PTMs)

In addition to splicing, the function of Tau is regulated by many post-translational modifications (PTMs)[46] including phosphorylation, acetylation, ubiquitination, nitration, glycation, and protein cleavage. The biological activity of Tau is known to be regulated by phosphorylation status. There are 85 potential phosphorylation sites (80 Ser or Thr, and 5 Tyr) in the longest Tau isoform (2N4R) [46] ; approximately 20 of them can be phosphorylated in physiological conditions and more than double as many are phosphorylated in pathological conditions[47]. These phosphorylations are involved in the control of the biological function of Tau and its pathological ability to self-assemble into paired helical filaments (PHF) and neurofibrillary tangles (NFTs) in neurodegenerative diseases[47]. Notably, phosphorylation at one site facilitates that at other sites, which may correlate with disease progression and may represent a diagnostic marker[48]. Beside the increment in the

number of phosphorylated epitopes on each Tau molecule, the pathogenesis of tauopathies may also be affected by an increase phosphorylation at amino acids that are normally phosphorylated[49]. Animal studies revealed similar pattern of hyperphosphorylation in AD and in the developing brain[50]. Despite there are data suggesting that human fetal Tau is transiently hyperphosphorylated[51,52], the lack of characterization and anatomic data leave the possible role of hyperphosphorylated Tau in fetal brain as an open question. A possibility is that splicing to 3R Tau and hyperphosphorylation both decrease the affinity of Tau to microtubule conferring these latter more flexibility during a phase of intense neurite growth. Understanding the differences in toxicity between the hyperphosphorylated Tau in neurodegeneration and fetal brain would be important to understand the mechanism of Tau aggregation and it would be helpful for the identification of potential treatments for neurodegenerative diseases comprising AD.

Tau phosphorylation is tightly regulated by the presence of protein kinases from the proline-directed protein kinase (PDPK) family such as the mitogen activated protein kinase (MAPK) and the glycogen synthase kinase 3 (GSK3)[53,54]. Moreover, the activity of kinases is counterbalanced by the presence of different phosphatases such as the PP2A[53].

Another Tau post-translational modification is acetylation, which is important both in physiological and pathological conditions[55,56]. The main mediator of Tau acetylation is cAMP-response binding protein and (CREB)-binding protein. Moreover, Tau presents an intrinsic acetyltransferase activity leading to the auto-acetylation mediated by cysteine residues 291 and 322[57].

This auto-acetylation increases the fragmentation of Tau and intensifies the autophagic degradation of Tau[58]. Recent findings demonstrate that the acetylation of Tau at Lys174, identified also in the AD brain, seems to delay the turnover of Tau and is critical for Tau-induced toxicity[59]. In general, depending on the site, the acetylation of Tau can delay or facilitate its degradation and repress the phosphorylation and aggregation of Tau[60,61].

It is not known which Tau phosphorylation sites is essential for the pathology, but different studies shown that mimicking a permanent phosphorylation of Tau lead to a reproduction of the structural and functional characteristics of pathological Tau in AD brain[62].

2.4 Tau spreading

The neuropathological hallmark of tauopathies is the accumulation of aggregated and misfolded forms of Tau protein in the brain. Tau pathology in AD starts from the layer II of entorhinal cortex and then progressively spreads to the cortical regions by a prion-like process. In fact, pathologically folded Tau transfers form one cell to another and induces the

same conformation and toxic properties to Tau molecules present in healthy cells. It was demonstrated that the injection of aggregated Tau extracted from transgenic mouse carrying one of the FTD-Tau mutations into healthy mice led to the de novo development of Tau inclusions[63]. Furthermore, Tau seeding, and propagation was also demonstrated in a number of studies e.g., for Tau extracted from human AD brains[64] or mice, which were exposed to traumatic brain injury (TBI)[65–67]. TBI is considered as a risk factor for tauopathies, and recent study shown that moderate or severe TBI can mediate the formation of pathological Tau and its spreading[67].

The use of Tau pre-formed fibrils (PFF) facilitated the investigation of Tau propagation mechanism[68] and gave the evidence that Tau propagates trans-synaptically between neurons[69,70]. However, Kayed *et al.* showed that different Tau species are taken up from cortical neurons through distinct pathways. For example, endocytosis can mediate the uptake of extracellular Tau[71]. Also, Tau propagation can occur in both retrograde and anterograde direction indicating the existence of other mechanism than only via synaptic transmission[72]. Moreover, the phosphorylation state of Tau can affect the transmission and is associated with the disease progression and severity[73].

Recently, our laboratory demonstrated that a pro-fibrillogenic form of Tau can be transported to a healthy cell through extracellular vesicles (EVs), and the interaction with endogenous Tau occurs in an acidic compartment. These findings open a possible contribution of autophagy in the spreading of Tau pathology and suggest that a dysfunction of acidic degradative compartments of the cells may contribute to disease[74].

3. New functions of Tau: From the nucleus to epigenetic regulation

In addition to the functions of Tau described above, this protein has also been observed in nuclei of neuronal and in non-neuronal cells[75,76], where it plays an important role in maintaining the integrity of genomic deoxyribonucleic acid (DNA), cytoplasmic ribonucleic acid (RNA) and nuclear RNA[77]. In particular, *in vitro* assays showed that Tau has a preference in binding to the AT-rich DNA regions in contrast to GC-rich DNA sequences. Moreover, Tau binds single and double strands DNA and Tau phosphorylation and aggregation affect this interaction. The existence of both non-phosphorylated and phosphorylated Tau is reported in the nucleus, but the majority of nuclear Tau appears to be in a non-phosphorylated form[78,79]. The Tau-DNA binding is associated with the capacity of Tau to protect against hydroxyl free radical-induced DNA breakage[80.] Different studies

demonstrated that in stressful situations, Tau translocates to the nucleus protecting the integrity of neuronal DNA[81]. In Tau knockout mice, heat stress conditions increase the number of DNA breaks compared to wild-type mice whereas similar DNA damage level is observed in basal conditions [82].

Different studies in Tau knockout mice suggest an indirect effect of Tau on gene transcription probably through compensatory changes in gene expression[83–86].

Tau colocalization with pericentromeric heterochromatin associated with HP1 and H3K9me3[86,87] has been observed in Hela cells, human skin fibroblast and also in Tau transgenic drosophila and mice, and in AD brain[88,89]. In particular, Tau interacts with gene-coding and intergenic sequences in euchromatin regions whereas in heterochromatin Tau binds with repetitive sequences of long non-coding RNA in GC repeats[90]. Moreover, phosphorylated Tau has been found to interact with global chromatin in pyramidal and granular neurons and also in epithelial cells of colorectal mucosa[91]. Chromatin abnormalities have been described in drosophila and mouse tauopathy models and in human AD brains. Specifically, in drosophila and mouse models the overexpression of mutant Tau led to the loss of H3K9me2 and altered the distribution of heterochromatin-associated protein HP1α[89]. Supporting this new function of Tau, it was demonstrated that peripheral cells from patients with Tau mutations contain aberrations and abnormalities in chromosome number and chromatin structure[92,93].

As reported Tau is involved in genome integrity[94], protects DNA[95] and is highly sensitive to different kind of stressors[96,97]. Furthermore, it was demonstrated that the absence of Tau induces DNA double-strand breaks (DSBs) and the phosphorylation of histone H2AX[98]. On the other hand, Violet et al. demonstrated that the presence of Tau improves a slow repair of hippocampal DSBs[99] . The possible mechanism related to the role of Tau on protecting the genome could be related to the site-specific Tau hyperphosphorylation: phosphorylation of Thr212, Ser214, Ser202 and Thr205[100,101] are uniformly distributed within the nucleus and associated to high levels of H4K16ac. As a consequence, this epigenetic modification blocks the folding of the 30 nm chromatin fiber[102] leading to an aging-associated decrease of histones[103]. Moreover, Tau regulates pericentromeric heterochromatin (PCH)[104] in non-neuronal cells possibly due to its colocalization with H3K9me2-rich DNA sequences[105].

Epigenetic modification could represent one of the mechanisms related to neurodegenerative diseases such as AD. It was demonstrated that the amyloid precursor gene promoter is hypomethylated with age, thereby enhancing Aβ production[106]. However, more recent data demonstrated no difference in the methylation level of APP gene promoter in Alzheimer's

disease models[107]. Alterations of histone acetylation profile have been related with change in gene transcription[108]. Lee *et al.* investigated the chromatin modification and histone change in AD monozygotic twin compared to the healthy tween. They found that the trimethylation of histone H3 (K9) was greatly increased in the anterior temporal neocortex and hippocampus of the AD twin[109].

4. From Tau to aging-related mechanisms and disorders

The laboratory where I conducted the entire PhD project is investigating the potential role of Tau in various aging processes. In particular, the research focus is on uncovering novel aspects of Tau functions and its involvement in aging-related disorders. Whilst the canonical function of Tau in stabilizing microtubule is clearly associated with the nervous system and neurodegeneration, emerging non-canonical functions of Tau extend beyond the brain with likely implications for cancer. The link between Tau and aging is becoming a prominent area of research.

The age-related increase in the post-translational modifications of Tau is also associated with changes in the function of Tau and its localization. For example, increased phosphorylation of Tau, which may impact on its ability to bind to microtubules and stabilize the cytoskeleton, has been observed with age[110].

Moreover, aging is associated with increased cellular stress and it is characterized by factors like oxidative stress and compromised protein quality mechanisms. Correlated with that, Tau can be affected by these stressors, leading to altered protein function and aggregation[111,112]. Furthermore, aging is characterized by cellular senescence and apoptosis, which are interconnected processes playing essential roles in health and function of the organism[113–115]. Senescence and apoptosis are cellular mechanisms influencing positively the aging process by eliminating damaged cells, preventing their proliferation. However, imbalances in these processes can also contribute to age-related diseases and tissue dysfunction[114,116]. Tau has been found to interact with various cellular components and signaling pathways, which may influence cell fate decisions, including apoptosis and senescence[117].

These aging-related processes are known to be shared for the development of cancer and neurodegeneration. Investigating the role of Tau in various tissues and its interactions with other cellular processes during aging could lead to new therapeutic strategies for aging-related conditions. Understanding these complex relationships is essential for developing strategies to promote healthy aging and prevent or treat aging-related conditions.

5. Aging

Aging is characterized by physical deterioration and biological changes that are associated with an increased risk of diseases and death[118]. Aging is likely due to the exposure of external insults such as UV light, air pollution and poor diet[119] , as well as to the accumulation of internal insults derived from metabolic activities of the cell. Not surprisingly, aging is also associated to human disease, such as neurodegeneration and cancer, which are the most frequent disorders nowadays.

Several evidences support an association between brain aging and the development of AD and PD[120,121]. Brain tissue from older individuals presents abnormal deposits of aggregated proteins such as hyperphosphorylated Tau (p-Tau), Aβ and α-synuclein. Moreover, the effects of aging are more evident in tissues composed by postmitotic cells such as brain. In fact, postmitotic neurons and oligodendrocytes are more vulnerable to DNA damage, which is known to increase with aging[122,123].

Biomarkers associated with aging are divided into primary, antagonistic and integrative hallmarks (**Figure 2**).

The primary hallmarks are genomic instability, telomere attrition and epigenetic alterations. [124,125]. In particular, aged chromatin is characterized by decrease of heterochromatin, histone loss, and increase post-translational modifications of histones[126–128]. In general, these chromatin changes lead to an aberrant gene expression and a dysregulated histone methylation pattern[128]. The antagonistic hallmarks include mitochondrial dysfunction, cellular senescence and deregulated nutrient sensing. Finally, the functional decline associated with aging is based on the cumulative damage and comprises the integrative hallmarks[129,130] (**Figure 2**).

Figure 2. Different hallmarks of aging such as genomic instability, epigenetic alterations, cellular senescence and mitochondrial dysfunction [115].

6. Neurodegeneration and Cancer

Neurodegeneration and cancer appear as unrelated diseases; one due to premature cell dysfunction and cell death, and the other due to resistance to cell death associated to uncontrolled proliferation, genome instability and inflammation. Considering this standpoint, it is possible that a loss of regulation of processes associated to cell fate may either favor uncontrolled cell death in neurodegeneration or uncontrolled cell division in cancer. In fact, evidence exists demonstrating an inverse comorbidity between these two distinct human disorders. Epidemiological studies suggest and inverse correlation between the risk of developing neurodegeneration or cancer[131,132]. For example, several case-controls of PD individuals have reported a reduced risk of cancers[133]. As an exception, an increased risk of malignant melanoma is found to positively correlate with PD [134–137]. Fewer data are available for the link between AD or HD and cancer; a study showed that a diagnosis of AD was associated with a reduced risk of cancer[138].

Interestingly, a recent study based on transcriptome meta-analyses of three neurodegenerative diseases (AD, PD and schizophrenia) and three different cancers (lung,

prostate and colorectal cancer) demonstrated that genes up regulated in cancer are often downregulated in neurodegeneration and vice versa[139].

Different signaling pathways involved in the regulation of cell death have been well investigated in cancer and recently also in neurodegenerative diseases[140–142]. In addition, mutations or aberrant expression of genes important in neurodegeneration are also observed in cancer e.g., *SNCA, phosphatase and tensin homolog (PTEN), PTEN induced kinase 1 (PINK1; parkinsonism associated deglycase 6, PARK6), MAPT, APP*[140]. Moreover, the regulator of cell division PIN1[143] is overexpressed in cancers whereas it is reduced in AD and its knockout in mice leads to neurodegeneration[144].

P53 is amply studied in cancers and is known as the main tumor suppressor involved in 50% of malignancies. In cancer, p53 presents missense mutations affecting its tumor suppressor activity[145–147]. On the contrary, the level and the activity of p53 is increased in neurodegenerative diseases[148] and the dysregulation of p53 may contribute to disease progression through multiple mechanisms. For example, p53-mediated apoptosis can lead to the loss of neurons, contributing to the neurodegenerative phenotype. Additionally, p53 has been shown to interact with other proteins implicated in neurodegenerative diseases, such as amyloid-beta and Tau in Alzheimer's disease, α-synuclein in Parkinson's disease, and mutant huntingtin protein in Huntington's disease. These interactions may influence protein aggregation, cellular toxicity, and neuroinflammation[149,150].

In PD brains the increased level of p53 is associated with an increased apoptosis and related proteins such as Bcl-2 and Caspase-3[151,152]. Although genetic mutations in p53 have not been reported in neurodegeneration some p53 variants with altered tertiary structure have been observed in AD patients[153,154]. Human neuroblastoma cell line SH-SY5Y overexpressing APP present also an increase in unfolded p53 and lack of pro-apoptotic activity[155]. Recent evidence indicates that genetic mutations in *MAPT* gene are involved not only in neurodegeneration but also increase the risk of developing cancer[156]: family with *MAPT* mutations show an increased risk for hematological, lung, breast, and colorectal cancers[156]. These data suggest that *MAPT* gene mutations may predispose to both neurodegeneration and cancer[156,157].

Chemotherapeutic drugs such as taxanes act on microtubules altering the dynamic assembly and impairing the cell cycle in the G1/G2 phase of mitosis. Different studies demonstrate that the modulation of Tau expression has an effect on the response to taxanes in cancer cells[158] and it has been proposed that taxanes and Tau may compete for the same binding site on microtubules.

7. Apoptosis or senescence: cell death or cell cycle arrest

Apoptosis was first described by Kerr, Wyllie, and Currie in 1972 and it is defined as the process of programmed cell death[159]. Apoptosis is considered as a homeostatic mechanism that occurs normally during development and aging to maintains cell populations in tissues. On the other hand, apoptosis acts also as a defense mechanism in immune reactions or when cells are damaged[160]. It can be triggered by different physiological or pathological stimuli such as irradiation or drugs that cause DNA damage[161] **(Figure 3)**. The main characteristic of apoptosis is the formation of apoptotic bodies, which are involved in a process named efferocytosis or clearance of apoptotic cells[162]**(Figure 3)**. This mechanism is important because the uncontrolled release of cell content promotes an inflammatory response[162]. The morphology of apoptotic cells in the early phase of the process is characterized by cell shrinkage and pyknosis [163]: cells are smaller, the cytoplasm is dense and the organelles straightly packed, chromatin is more condensed, and DNA is fragmented. In the late phase of apoptosis, the atypic presence of phosphatidylserine on the extracellular side of the plasma membrane allows the recognition and phagocytosis of apoptotic cells by macrophages. The core of the mechanism linked to apoptosis are the proteases known as caspases (cysteinyl, aspartate-specific proteases)[164], which are considered the initiators and the executors of cell death[165]. Once activated, the initiator caspases (pro-caspase) auto-activate themselves and the executor caspases though proteolysis[166], whereby they can cleave specific substrates[167]. Caspase-8 and -9 are the initiators while caspase-3 is the main effector, accompanied by caspase-6 and -7[164,166,167].

Furthermore, there are two different type of apoptotic program: the extrinsic apoptotic pathway and the intrinsic apoptotic pathway. The extrinsic one is initiated by the interaction of tumor necrosis factor receptor (TNFR) with their TNF protein ligands[168], leading to the release of death signal in the extracellular space[169]. The intrinsic pathway is activated by internal stimuli such as hypoxia, high concentrations of Ca^{+} and irreparable genetic damage[170] and is mediated by intracellular signals that converge to mitochondria[170]. After the activation of pro-apoptotic BH3 members belonging to the Bcl-2 family, antiapoptotic proteins such as Bcl-2 or Bcl-xL are neutralized, and the mitochondrial outer membrane permeability is damaged with the consequent release in the cytosol of intermembrane space proteins[171] such as cytochrome-c, which represents the crucial factor for the activation of mitochondrial-dependent death[171].

Necrosis is an alternative to apoptotic death and is characterized by a toxic process leading to karyiolysis and cell swelling. The decision of the cells to die by necrosis or apoptosis depends on the nature of the cell death signal and the tissue type[172] **(Figure 3)**.

In physiological conditions, apoptosis is responsible for the maintenance of homeostasis in adult tissue and is necessary during developmental processes. For instance, during the development of the nervous system there is an overproduction of cells and thus it is fundamental that these cells are eliminated through an apoptotic mechanism[173]. Apoptosis is also important for the removal of inflammatory cells and in the wound healing process[174]. Due to its importance, alteration of the apoptosis process is involved in different diseases such as cancer, neurodegeneration, infection and autoimmune disease. In cancer the inhibition of apoptosis leads to an excessive proliferation and/or a decreased elimination of damaged cells thereby representing the basis for tumorigenesis. On the contrary, excessive apoptosis is observed in neurodegenerative diseases: in AD the exposure to toxic β-amyloid peptides may induce Tau-mediated apoptosis[175,176].

Senescence is defined as a stable cell cycle arrest and is involved in the prevention of the accumulation of DNA damage and genomic instability[177,178] **(Figure 3)**. There are two different type of senescence: replicative senescence (RS) or stress-induced premature senescence (SIPS)[179]. The RS results from telomere shortening and affects all the proliferating somatic cell types in the organism[180,181]. Instead, the SIPS is independent from telomere shortening and is caused by insults such as genotoxic stress or metabolic shock.

The understanding of the mechanisms and the hallmarks of senescent cells is crucial for developing new therapeutic drugs, but senescence cells present a highly heterogeneous and dynamic phenotype. The principal hallmark of senescence is the cell cycle arrest, which correlates with higher amounts of cell cycle inhibitors such as p16INK4a, p21CIP1 and p27[113]. Other biomarkers of senescence are p19ARF, p53 and plasminogen activator type 1 (PAI-1)[182] .

Senescence cells are characterized by an increased activity of the lysosomal enzyme senescence-associated β-galactosidase (SA-β-gal, which can be measured at pH of 6.0[183,184]. Senescent cells acquire a specific phenotype called senescence-associated secretory phenotype (SASP), which is associated with the secretion of cytokines and other biomolecules with pro-inflammatory activity[185]. Interestingly, senescent cells show alterations in epigenome and chromatin structure. Senescence-associated heterochromatin foci (SAHF) are repressive chromatin regions characterized by the presence of marks including trimethylated Lys9 of histone H3 (H3K9me3), heterochromatin protein 1 (HP1),

and high mobility group protein A (HMGA1 and HMGA2) factors[186,187]. Initially, SAHF were considered to repress genes promoting cell cycle progression[188,189]. In addition, it was observed that senescent cells present unfolded constitutive heterochromatin domains marked by distended pericentromeric satellite sequences[190]. These alterations in chromatin structure are linked to the loss of nuclear lamina[190]. Besides all the features described, senescence cells present altered cell size and a smoothed shape[191]. Another characteristic of senescent cells is a lower but active metabolism and the production of factors that alter the tissue microenvironment[192].

Senescence is considered a strong defense against tumorigenesis[193] and senescent cells are considered as positive regulators of tissue remodeling and repair during development and adulthood[194,195]. Nevertheless, the uncontrolled and aberrant accumulation of senescent cells can initiate a proinflammatory state responsible for the onset of various age-related diseases[193,196] and studies demonstrated that persistent senescence could acquire pro-tumorigenic properties. An increase of senescent cells is found in aged and diseased tissues[197] suggesting that senescence cells may cause many age-related phenotypes. A possible link between senescence and neurodegeneration is based on recent studies describing that, in a mouse model of PD, senescent astrocytes contribute to neurodegeneration[198]. Instead, the elimination of senescence cells is sufficient to delay cognitive impairment[198] and this was also demonstrated in a tauopathy mouse model[199].

Recent studies revealed that senescence has a role in the initiation and progression of Tau-mediated disease using the *MAPT*^{P301S}PS19 mouse model, which accumulates p16^{INK4A}-positive senescent astrocytes and microglia[200].

Generally, the identification of compounds called senolytics that can eliminate senescent cells may provide a strategy for the treatment of these pathologies **(Figure 3)**.

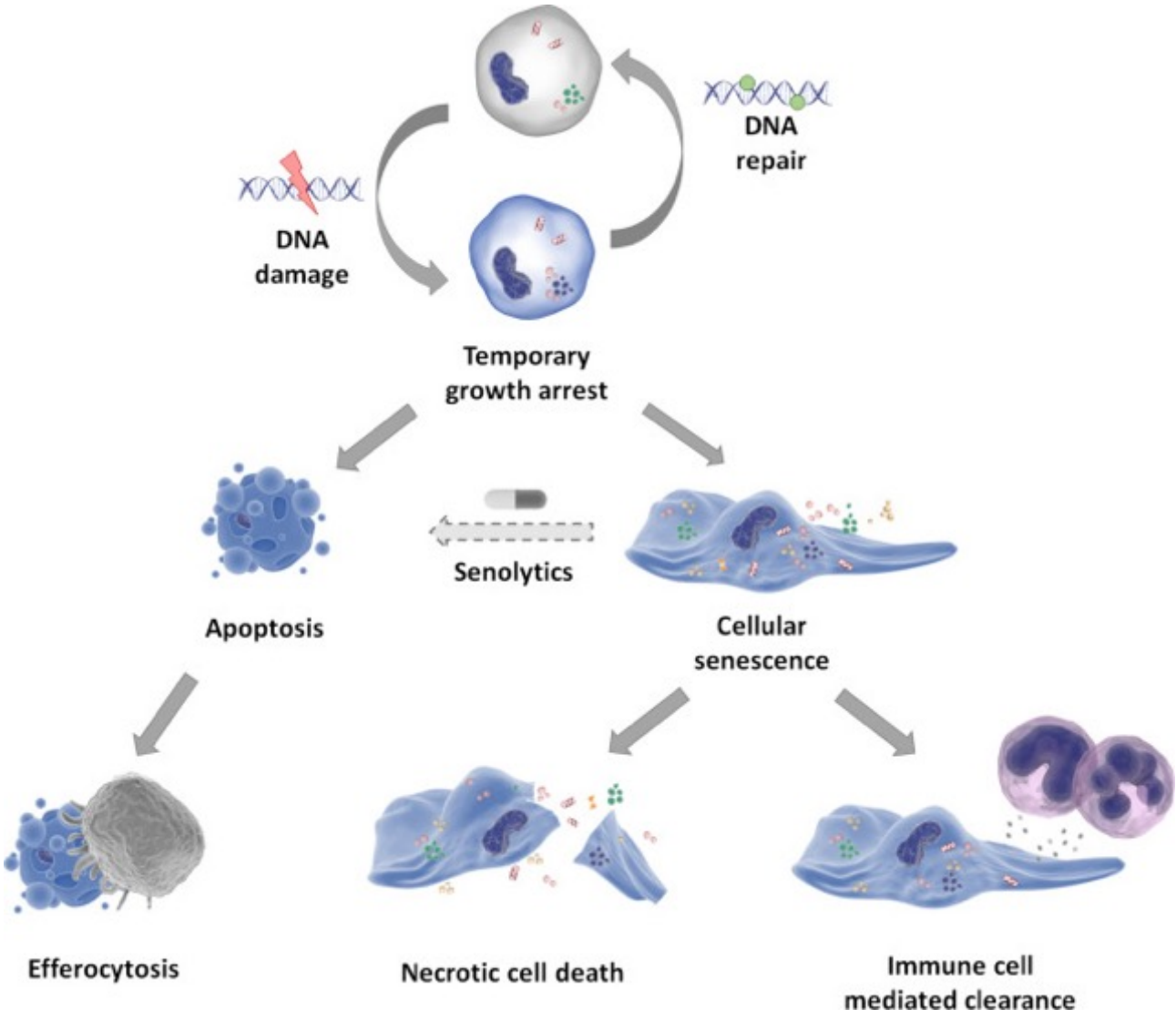

Figure 3. After DNA damage, normal cells stop dividing and try to repair the DNA. If the DNA is not repaired cells initiate apoptosis or other forms of regulated cell death. Otherwise, damaged cells may become senescent or targeted to necrotic cell death. Senolytic drugs aim to initiate pro-apoptotic pathways in senescent cells without affecting normal cells [201].

Chapter 2

Rationale and hypothesis

Tau protein has been extensively studied in the context of its role in microtubule stabilization. However, recent evidence suggests that Tau might also exert noncanonical functions beyond its well-known cytoskeletal role. Recent studies have shown that a fraction of Tau protein can translocate into the nucleus. However, the functional significance of Tau's nuclear presence remains largely unexplored. **The hypothesis of this study is that the protein Tau exerts noncanonical functions by modulating chromatin maintenance.** In particular, we propose to investigate whether Tau plays a central role in modulating chromatin maintenance within the nucleus. We hypothesize that Tau may interact with chromatin-associated proteins and epigenetic regulators, influencing chromatin structure, transcriptional regulation, and ultimately impacting cellular homeostasis. Understanding the potential noncanonical functions of Tau in chromatin maintenance might unveil new regulatory mechanisms and could shed light on novel therapeutic strategies for neuro-degenerative diseases and other conditions where chromatin dysregulation is implicated.

To test our hypothesis, we decided for the following experimental approaches:

The first part of my PhD project focused on investigating whether a loss-of-function of Tau may contribute to the regulation of the DDR, possibly impacting on human disorders associated with aging. In fact, the accumulation of DNA damage is one of the main hallmarks of aging and it represents a risk factor for aging-related diseases such as cancer and neurodegeneration. Thus, we first generated and characterized neuroblastoma cell lines knocked-out or knocked-down for Tau. Then, we induced an acute DNA damage and we compared the DDR in Tau-expressing and Tau-depleted cells. The data collected demonstrated that the depletion of Tau in cells had little impact on the first steps of the DDR but had a dramatic effect on the stability of p53 and its activity as the key factor balancing the induction of apoptosis and senescence. Strikingly, this regulatory function of Tau was clearly exposed when the cells were subjected to an acute DNA damage. However, we observed that Tau knockout cells displayed a tendency to enter a senescent status.

The second part of the thesis assessed whether senescence induction in Tau knockout cells was due to an epigenetic-mediated transcriptional program. For this, we performed a transcriptome analysis obtained from the comparison between neuroblastoma cell lines expressing Tau or knocked-out for Tau. We then questioned the transcriptome data for a

bioinformatic analysis aim at identifying a mechanism activated by Tau-depletion and possibly involved in the induction of senescence. Among the transcripts deregulated in a Tau-dependent manner, we found an enrichment of target genes for the PRC2. we then analyzed the PRC2 core components and its activity in our cellular model. We found a decreased level of the core components of the PRC2 complex and a lower H3K27 methylation activity in Tau deficient cells. Moreover, IGFBP3, a specific target gene of PRC2 involved in senescence was increased in Tau deficient cells we provided evidence that increased senescence in Tau knockout cells is due to decreased repression of IGFBP3 expression by PRC2.

Considering the unmet medical need with heavy personal and economic impact, the understanding of the molecular mechanism and the cellular bases of these disorders offers a great hope for the future.

Chapter 3

Tau affects P53 function and cell fate during the DNA damage response

1. Introduction

1.1 The DNA damage response pathway (DDR)

Cells are subjected every day to a high number of DNA lesions, which are caused by single or double strand breaks, alkylation, crosslinking and base deletion[202,203]. The sources of damage are both intrinsic (e.g., reactive oxygen species) or extrinsic (e.g., by ionizing radiation, ultraviolet radiation)[114]. Nature has therefore evolved a complex molecular mechanism in order to appropriately protect cells from the possible noxious consequences of DNA damage, a mechanism defined as the DNA Damage Response (DDR)[204,205]. The complexity of this process is due to versatile sensing, signal transduction and effector systems (**Figure 4**). The purpose of the DDR is first of all to stop the cell cycle and to activate DNA repair mechanisms. This allows the cell to first try to repair the DNA before reactivating cell division without propagating the DNA lesion. Nevertheless, if the cell fails to repair the DNA damage, the DDR will eventually activate the cell death pathway (apoptosis) or induce cellular senescence[206]. Deregulation of the DDR is linked to many diseases such as tissue dysfunction, immunodeficiency, premature aging, neurodegeneration and cancer[204]. For this reason, it is extremely important that the DDR cell fate response is well balanced, and its modulation appears to be a promising approach for the treatment of these diseases.

The DDR starts with the recognition of a damage to DNA, which coordinates the activation of two kinases, ataxia telangiectasia mutated (ATM) and RAD3-related (ATR) proteins. Specifically, ATM is activated by double-strand breaks, whereas ATR is recruited following damages such as nucleotide damage, and single-strand breaks[207]. The activation of these kinases leads to the initiation of DNA repair mechanisms like non homologous end joining (NHEJ), homologous recombination, nucleotide excision repair, and base excision repair. Precisely, ATM phosphorylates the histone variant H2AX at Ser 139 (γH2AX) in the proximal region of the DNA break[208]. The H2AX phosphorylation leads to the spreading of DNA damage signal along chromatin[209]. In turn, the activation of ATM results in the

initiation of the downstream checkpoint kinase 2 (Chk2), which then leads to an arrest of the cell cycle at the G2/M phase transition[210]. In contrast, ATR orchestrates the activation of checkpoint kinase 1 (Chk1), which leads to the production of DNA repair enzymes[211].

As a next step, Chk1 and Chk2 stabilize effector proteins such as the p53 tumor suppressor protein[210]. P53 is one of the most important regulators of DNA damage-induced cell death (apoptosis) or cell cycle arrest (senescence) (**Figure 4**). The p53 pathway also promotes the intercellular communication by promoting the secretion of proteins that change the cellular environment[212]. Stress signals are transmitted to p53 through post-translational modifications such as phosphorylation, acetylation, methylation and ubiquitination[213,214]. In the absence of stress, normally proliferating cells keep p53 at very low amounts. This is due to its continuous proteasomal degradation through the action of distinct E3 ubiquitin ligases[215]. One of the most characterized p53 E3 ligases is Murine Double Minute 2 (MDM2), which ubiquitinates p53 and targets p53 for degradation, but also function as an antagonist for the binding of p53 to the DNA thus repressing its transcriptional activity[216]. As a consequence of stress, such as a DNA damage, P53 is phosphorylated at Ser15 and Ser20 by ATM and ATR and by their downstream mediators Chk2 and Chk1[217]. This causes p53 to dissociate from MDM2, resulting in p53 stabilization and the binding of p53 to its target gene promoters[218,219]. P53 activation leads to the initiation of a transcriptional program that reflects the nature of the stress signal, the type of protein modifications and the choice of proteins associated with p53. The genes in the p53 network initiate one of three programs that result in cell cycle arrest, cellular senescence or apoptosis. Interestingly, MDM2 transcription is enhanced by p53 through an auto regulatory feedback loop, which is critical to control the balance of p53 and MDM2. Furthermore, MDM2 activity is regulated by MDMX (MDM4), which is a negative regulator of p53, and it is important for the stabilization of MDM2 and p53[220,221]. MDM2 is an unstable protein and it is subject to regulation by phosphorylation and acetylation. Depending on the site and the modifying kinase, these modifications can inhibit or activate the activity of MDM2[221,222]. Post-translational modifications affecting the p53/MDM2 feedback loop have a critical role, in fact the acetylation of eight different lysine residues on p53 prevents the interaction between p53 and MDM2[223].

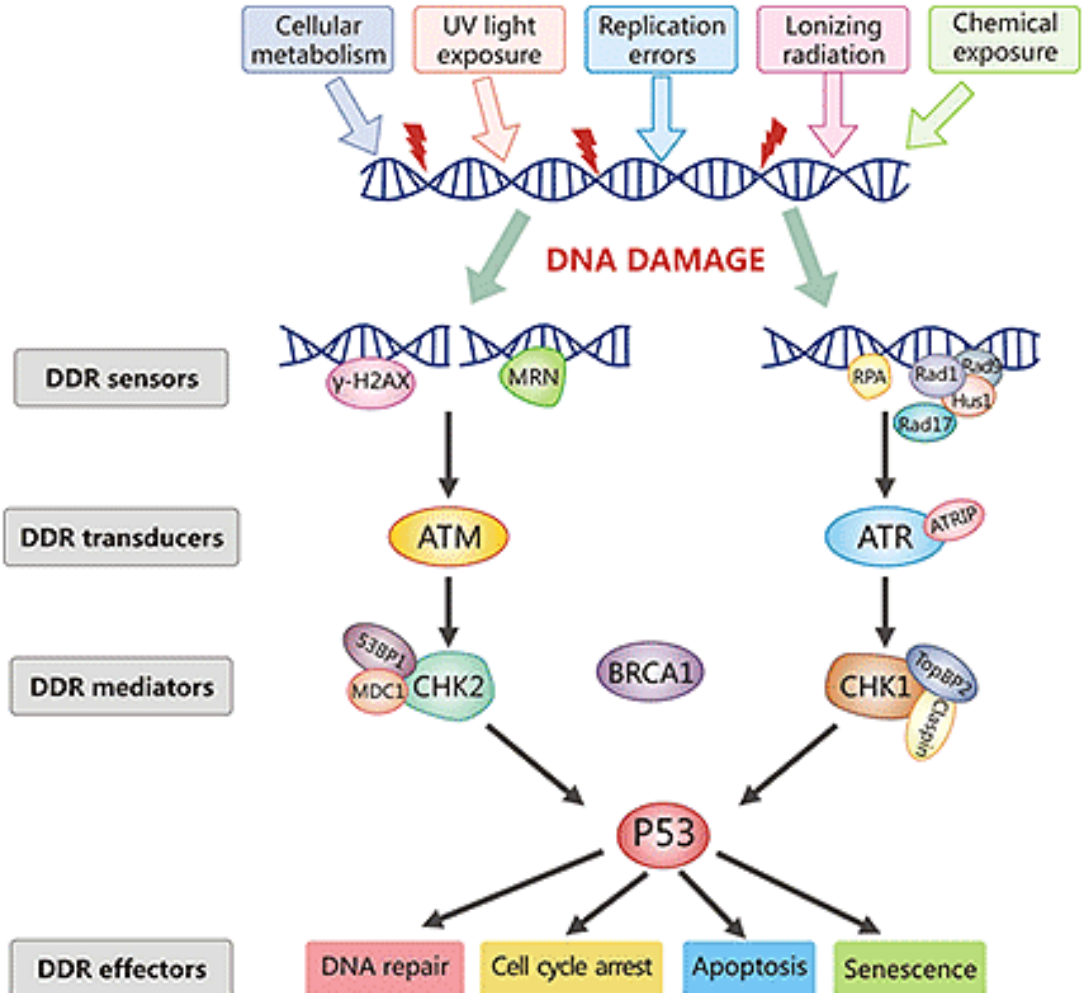

Figure 4. DNA damage response pathway (DDR) scheme [224]

2. Results

COMMUNICATIONS BIOLOGY

ARTICLE

https://doi.org/10.1038/s42003-020-0975-4 OPEN

Tau affects P53 function and cell fate during the DNA damage response

Martina Sola[1,2,5], Claudia Magrin[1,2,5], Giona Pedrioli[1,3], Sandra Pinton[1], Agnese Salvadè[1], Stéphanie Papin[1,6] & Paolo Paganetti[1,4,6]✉

Cells are constantly exposed to DNA damaging insults. To protect the organism, cells developed a complex molecular response coordinated by P53, the master regulator of DNA repair, cell division and cell fate. DNA damage accumulation and abnormal cell fate decision may represent a pathomechanism shared by aging-associated disorders such as cancer and neurodegeneration. Here, we examined this hypothesis in the context of tauopathies, a neurodegenerative disorder group characterized by Tau protein deposition. For this, the response to an acute DNA damage was studied in neuroblastoma cells with depleted Tau, as a model of loss-of-function. Under these conditions, altered P53 stability and activity result in reduced cell death and increased cell senescence. This newly discovered function of Tau involves abnormal modification of P53 and its E3 ubiquitin ligase MDM2. Considering the medical need with vast social implications caused by neurodegeneration and cancer, our study may reform our approach to disease-modifying therapies.

[1] Neurodegeneration Research Group, Laboratory for Biomedical Neurosciences, Ente Cantonale Ospedaliero, Torricella-Taverne, Switzerland. [2] Faculty of Biomedical Sciences, Members of the PhD in Neurosciences Program, Università della Svizzera Italiana, Lugano, Switzerland. [3] Member of the International PhD Program of the Biozentrum, University of Basel, Basel, Switzerland. [4] Faculty of Biomedical Sciences, Università della Svizzera italiana, CH-6900 Lugano, Switzerland. [5] These author contributed equally: Martina Sola, Claudia Magrin. [6] These authors jointly supervised this work: Stéphanie Papin, Paolo Paganetti. ✉email: paolo.paganetti@eoc.ch

Tauopathies are disorders of Tau protein deposition best represented by Alzheimer's disease (AD), where Tau accumulation in neurofibrillary tangles of the brain correlates with the clinical course in terms of number and distribution[1,2]. Also, mutations in the *MAPT* gene encoding for Tau lead to frontotemporal dementia with Parkinsonism 17[1,2]. Since Tau is a microtubule-associated protein, an accepted concept explaining the pathogenesis of tauopathies is that abnormal phosphorylation and folding cause Tau detachment from microtubules, Tau accumulation, and neuronal dysfunction[3,4]. In addition to microtubule association, Tau localizes in the cell nucleus and binds DNA[5–8] and also forms a complex together with P53, Pin1, and PARN regulating mRNA stability through polyadenylation[9]. Nuclear Tau was shown to have a role in DNA protection, whereby heat or oxidative stress cause nuclear Tau translocation[10]. Enhanced DNA damage was observed in Tau-KO neurons when compared to normal neurons[11]. We reported that drug-induced DNA damage also causes Tau nuclear translocation and affects Tau phosphorylation[12]. Notably, checkpoint kinases controlling DNA replication and cell cycle following a DNA damage phosphorylate Tau[13]. Together with chromosomal abnormalities found in AD-derived fibroblasts[14] and increased DNA damage in AD brains[15,16], the emerging function of Tau in DNA stability offers an alternative role of Tau in neurodegeneration and, importantly and insufficiently investigated, also in the DNA damage response (DDR). DNA is continuously damaged by genotoxic agents originating from the environment or generated intracellularly. The integrity of the genome is ensured by an efficient DDR signaling network regulating cell cycle and the DNA repair machinery, but also the activation of cell death or senescence when DNA damage persists. DDR deregulation causes accumulation of DNA errors and genomic instability, both implicated in age-related pathologies as cancer and neurodegenerative disorders[17].

In order to evaluate a role of Tau in this process, we depleted Tau in human cells and then carefully analyzed the DDR. We demonstrate that Tau deficiency renders cells less sensitive to DNA damage-induced apoptosis, which is counterbalanced by increased senescence. We show that this activity of Tau is mediated through a P53 modulation. Overall, our findings propose a role of P53 in tauopathies and a role of Tau in P53 dysregulation, a key event in oncogenesis.

Results

Generation and characterization of Tau-KO and Tau-KD cells. We opted the use of human SH-SY5Y neuroblastoma cells for generating Tau knock-out (Tau-KO) cells by the CRISPR-Cas9 technology and Tau knock-down (Tau-KD) cells by shRNA interference (Fig.1). For disruption of the *MAPT* gene, we designed gRNAs targeting Cas9 endonuclease to two sequences in the first coding *MAPT* exon. CRISPR-Cas9 cell lines were screened for Tau expression by fluorescent confocal microscopy and immune protein blotting with the human-specific N-terminal Tau13 antibody. So, we identified cell lines devoid of Tau (Fig.1a and Supplementary Fig. 7a). Since the Tau13 epitope is within the Cas9-targeted exon, false negatives may perhaps result from in-frame indels or abnormal mRNA processing. With the HT7 antibody against amino acid 159–164 of Tau_{441}, we confirmed the isolation of Tau-KO lines lacking full-length or truncated Tau expression (Fig. 1a and Supplementary Fig. 7a). We finally selected the cell lines 232P and 231K presenting alleles modified at the expected gRNA-sites by indels causing frame-shifts into stop codons within the same exon (Fig.1a). The 231A cell line underwent an unsuccessful CRISPR-Cas9 procedure and had normal Tau expression (Fig. 1a).

To obtain Tau-KD cells, we screened shRNAs targeting the coding sequence or the 3′ untranslated region of the Tau mRNA. Culturing shRNA transduced cells in the presence of puromycin resulted in the isolation of cell populations with constitutive down-regulation of Tau for three shRNAs as shown by immune staining and western blot (Fig.1b and Supplementary Fig. 7b).

Tau deficiency protects against DNA damage-induced apoptosis. Persistent DNA damage induces cell death or senescence. Thus, as a functional readout for the DDR, we assessed the cytotoxicity following a mild exposure to etoposide[18], a DNA topoisomerase II inhibitor causing double-stranded DNA breaks (DSBs). Cell viability was first tested with the well-established LDH and the MTS assays. Tau-KO cells exposed to a short (30 min) 60 µM etoposide treatment did not release LDH in the culture medium and more efficiently converted MTS when compared to Tau-expressing cells, which exhibited substantial etoposide-dependent cytotoxicity in both assays (Fig. 2). To test the involvement of apoptosis, we immune-stained cells for cleaved active caspase-3 (clCasp3), an initiator of apoptosis. Whilst <1% of the untreated Tau-expressing cells were positive for clCasp3, etoposide exposure increased the apoptotic population to 13–15%, apoptosis was induced in only 4–5% of Tau-KO cells (Fig.2). The presence of activated clCasp3 in Tau-expressing cells exposed to etoposide and its almost complete absence in Tau-KO cells was confirmed by western blot analysis with the same antibody for the cleaved enzyme form (Fig. 2 and Supplementary Fig. 8). As a whole, we found a positive association between Tau expression and DSB-induced apoptosis in SH-SY5Y cells.

Tau depletion induces cellular senescence. In alternative to cell death, unresolved DNA damage may provoke cellular senescence[17]. Inhibition of cyclin-dependent kinase by p21 causes cell cycle arrest and induction of senescence[19,20]. When compared to untreated conditions, at three recovery days after etoposide exposure (Fig. 3a), higher amounts of p21 were detected by western blot in both Tau-expressing and Tau-KO cells (Fig. 3b). When comparing the extent of this effect in the absence or the presence of Tau, we found that Tau depletion increased p21 both at basal conditions as well as after etoposide treatment when compared to wt cells (Fig. 3b). The increased amount of p21 present in Tau-KO cells suggests that Tau-depletion may prone cells to enter a senescence state further accelerated in the presence of DSBs. We determined the number of cells entering in a senescent state based on their mean cell size and by the senescence-associated β-galactosidase (SA-βGal) staining procedure at mild acidic conditions. When compared to untreated conditions, significantly increased cell size and SA-βGal-positive cells were found at three recovery days after etoposide exposure both for wt and Tau-KO cells (Fig. 3b). Again, Tau-depleted cells at basal conditions displayed a larger proportion of senescent cells in terms of cell size, SA-βGal staining and p21 expression (Fig. 3b). A consistent observation was made also for Tau-KD cells when compared to control shRNA cells (Fig. 3c, d). We concluded that reduced expression of endogenous Tau changed the fate of SH-SY5Y cells as a consequence of DSBs, favoring cellular senescence induction at the expense of activation of programmed cell death.

DNA damage and DDR activation are not reduced. DSBs lead to rapid recruitment and phosphorylation of the H2A histone family member at the site of DNA damage, and so the presence of γH2A-X is utilized as a surrogate marker of DNA damage. We first performed an accurate etoposide dose-response by in-cell

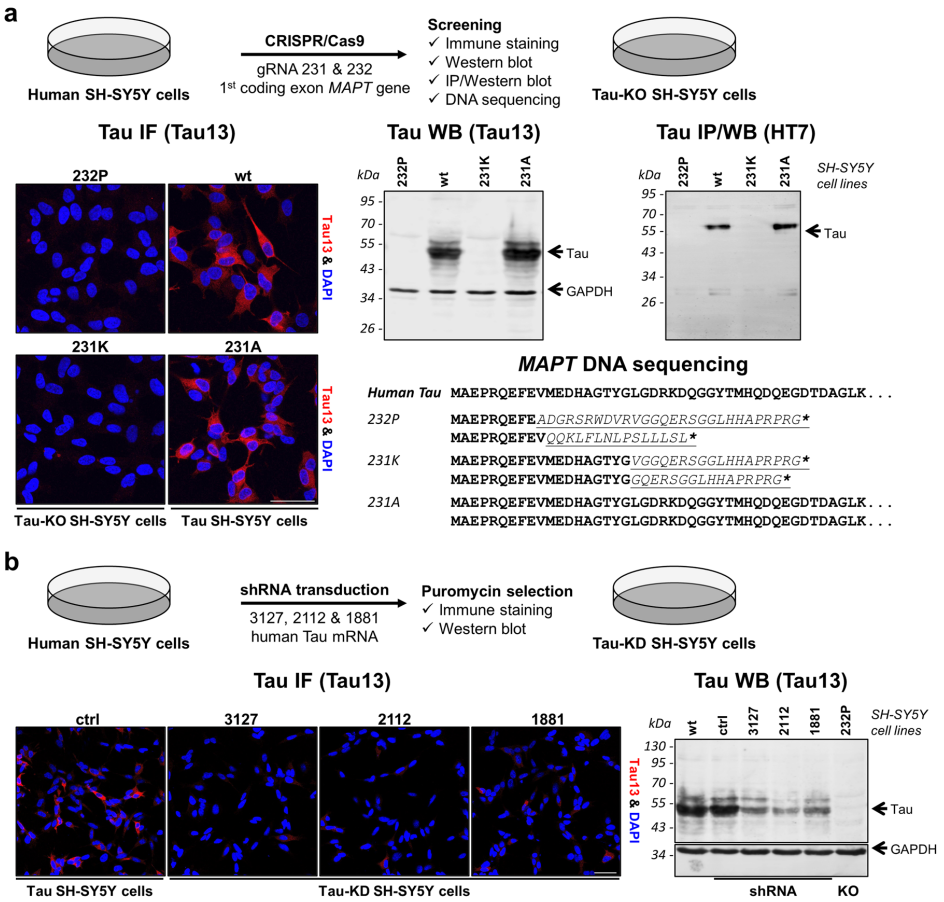

Fig. 1 Generation of Tau-KO and Tau-KD SH-SY5Y cells. a Scheme of the procedure used to generate CRISPR-Cas9-targeted cells and their characterization. Immune staining was performed with Tau13 antibody and nuclear staining with DAPI, western blot with Tau13 (loading control GAPDH) and immune precipitation and western blot with HT7 antibody, parental cells (wt) served as control. Amino acid sequences of the first *MAPT* coding exon in all lines demonstrate successful CRISPR-Cas9-editing causing frameshift (underlined in italics) into early stop codons (asterisks) for both alleles of 232P and 231K cells. **b** Scheme of procedure used to generate Tau-KD cell lines and their characterization by immune staining and western blot for Tau expression when compared to parental cells (wt) or cells transfected with the parental shRNA plasmid (ctrl). Scale bar 50 µm.

western for γH2A-X staining normalized by nuclear DAPI staining and observed an increase detection of γH2A-X total staining in Tau-KO cells when compared to control cells (Fig. 4a). The Comet assays is a direct measure of the magnitude of DSBs in single cultured cells. No difference between control and Tau-KO cells was found at the end of the etoposide treatment or during the recovery, which was rapid and complete before the 6 h washout time point independently on the presence or absence of Tau. However, Tau deletion led to more DSBs at basal conditions (Fig. 4b). Our data were thus consistent with a role of Tau in DNA-protection[10,11]. In contrast, the relatively small increase in etoposide-mediated DNA damage in Tau-KO cells inadequately explained reduced DNA damage-induced cell death in Tau-depleted cells. To corroborate this observation, we performed an etoposide dose-response and determined by confocal microscopy the presence of immune-stained nuclear γH2A-X and of the DSB-activated forms of ATM and Chk2[21,22]. This demonstrated a robust and dose-dependent induction of all three markers at 30 min after etoposide treatment (Fig. 4c). The difference between wt and Tau-KO cells was relatively minor and suggested a slightly stronger activation of the early DDR in Tau-KO cells, although the results obtained at 0 and 6 h recovery were less conclusive (Fig. 4d). Overall, the modest and somehow opposite effect of Tau depletion on the early DDR when compared to cell death induction, suggested a downstream contribution of Tau in modulating cell death.

Tau modulates DDR-dependent stabilization of P53 protein. A key DDR regulator is the tumor suppressor protein P53, which first halts cell division and then dictates cell fate when DNA damage persists[23,24]. To check the requirement of P53 for apoptosis induction in our cell model, we transduced cells with viral pseudoparticles and isolated stable P53 shRNA expressing cells (Supplementary Fig. 1a). The effect of the shRNA was negligible at basal conditions, i.e. when the cells maintain a minimal amount of P53 due to its efficient degradation. In

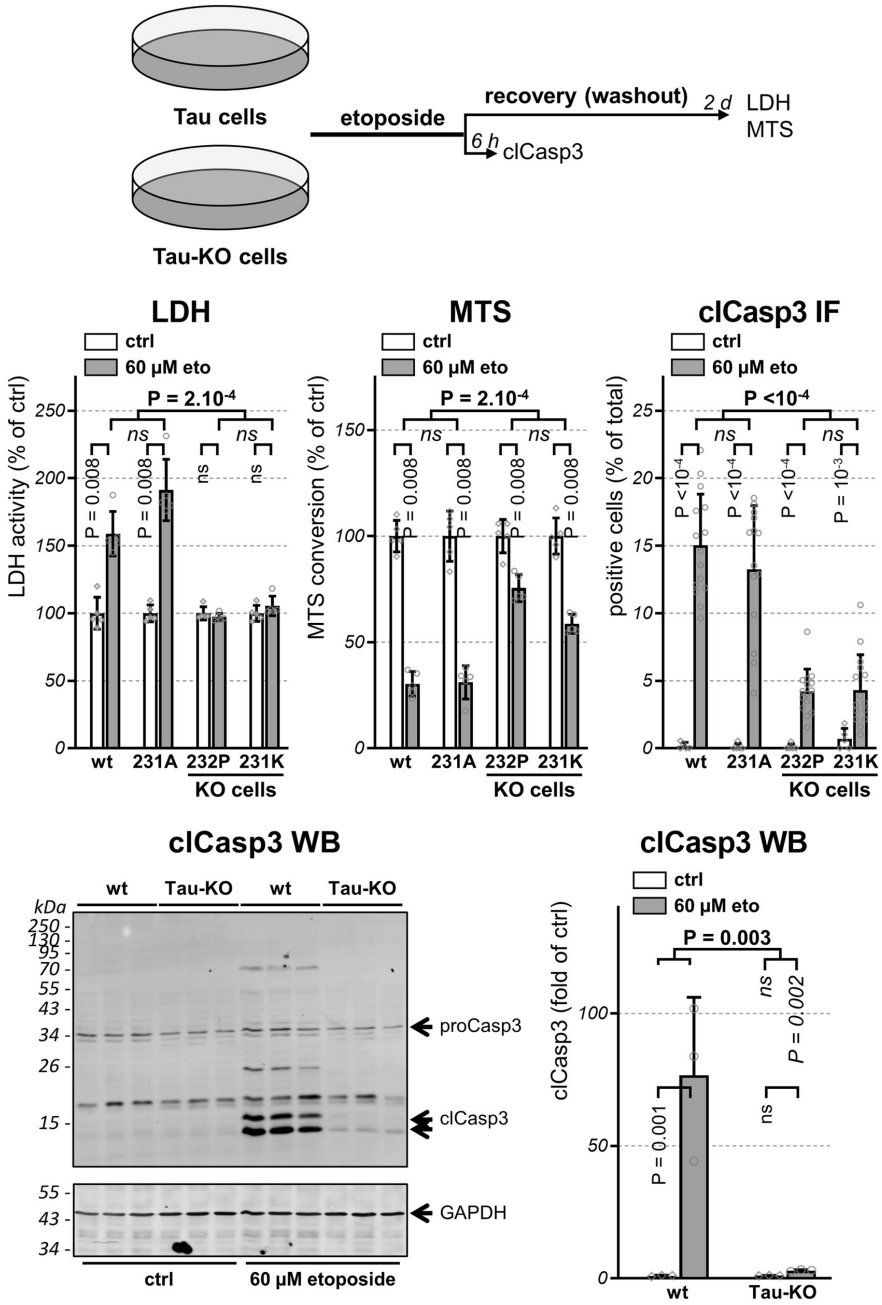

Fig. 2 Tau deficiency confers resistance to etoposide-induced apoptosis. Scheme representing the design of the experiment with parental and 231A (Tau) cells compared to 232P and 231K (Tau-KO) cells treated 30 min with 60 µM etoposide and recovered as indicated before analysis. LDH and MTS values are shown as percentage of parental cells (wt), mean ± SD of five biological replicates. To measure activation of apoptosis, percent positive cells for cleaved-caspase-3 (clCasp3) is determined on confocal microscope images and normalized for total DAPI-positive cells, mean ± SD of five images for the untreated cells (ctrl) and of 15 images for etoposide-treated cells (60 µM eto), $n > 500$ cells/condition, representative experiment of $n > 3$ biological replicates. Activated clCasp3 was also analyzed by western blot with GAPDH as loading control and 15 and 17 kDa clCasp3 quantified by normalization with GAPDH, mean ± SD ($n = 3$ biological triplicates). Statistical analysis by independent measures ordinary two-way ANOVA, source of variation for cell lines (in bold), multiple Bonferroni pairwise comparisons for treatment between lines (in italics) or for each line (in vertical).

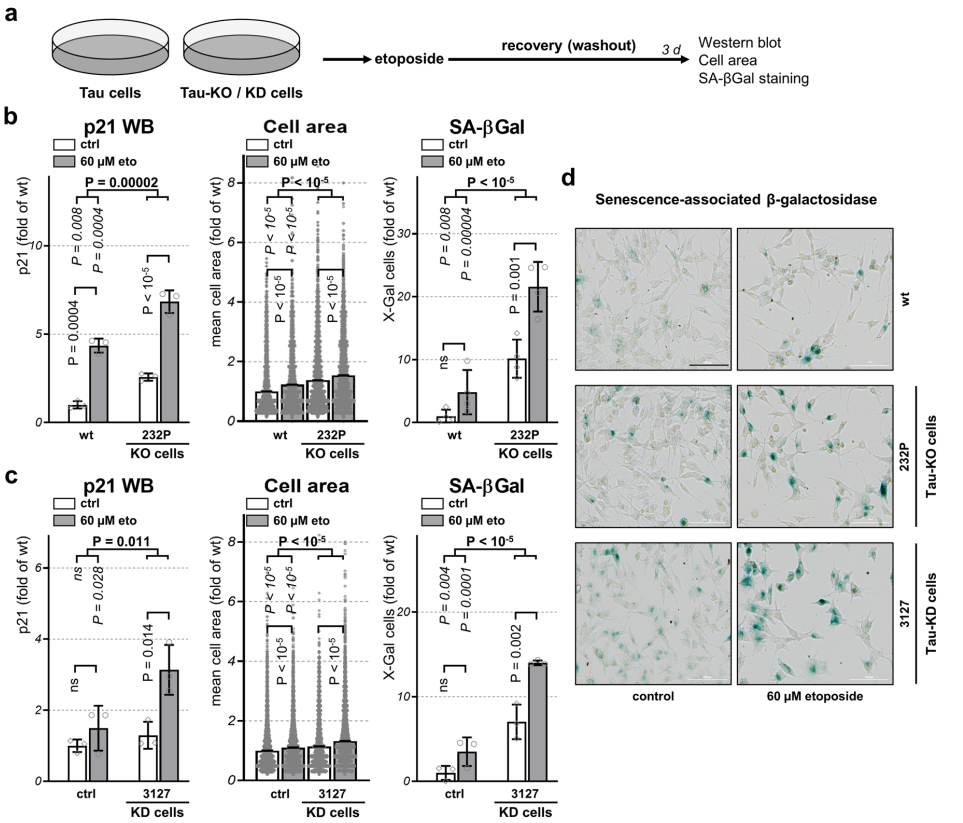

Fig. 3 Tau depletion increases cellular senescence. a Scheme of the procedure followed to assess cellular senescence upon 30 min treatment with 60 µM etoposide followed by 3 days of recovery. **b** Quantification of p21 amount in cell lysates by western blot in parental (wt) or 232P (Tau-KO) cells under control conditions (ctrl) or following etoposide treatment (60 µM eto) normalized for GAPDH, mean ± SD of three biological replicates. Quantification of mean cell area and percent positive cells for senescence-associated β-galactosidase (SA- βGal) determined with a high-content microscope scanner, mean ± sem of four (Tau-KO cells) or three (Tau-KD) independent experiments, $n > 8000$ cells. Data are shown as fold of wt cells at basal conditions. **c** Same as in **b** for mock shRNA (ctrl) or Tau 3127 shRNA (Tau-KD) cells. **d** Representative images of SA-βGal staining (in blue), bright-field, scale bar = 100 µm. Statistical analysis by independent measures ordinary two-way ANOVA, source of variation for cell lines (in bold), multiple Bonferroni pairwise comparisons for treatment between lines (in italics) or for each line (in vertical).

contrast, P53-KD cells displayed reduced etoposide-dependent P53 stabilization when compared to control cells as demonstrated by western blot analysis with the monoclonal antibodies DO-1 and Pab 1801 and confirmed by immune staining with DO-1 (Supplementary Fig. 1b, c). Cell lysates obtained from the neuroblastoma cell line SK-N-AS carrying a homozygous deletion in the *TP53* gene and therefore not expressing P53[25], were used as a negative control for P53 immune detection. Etoposide treatment induced apoptosis in ~2% P53-KD cells compared to ~14% of the control cells (Supplementary Fig. 1d). These data confirmed the involvement of P53 in DSB-induced apoptosis also in SH-SY5Y cells.

Having exposed the contribution of P53 and Tau in modulating DNA damage-dependent apoptosis in SH-SY5Y cells, we next asked whether Tau may modulate P53 activation. Tau-KO cells presented reduced DNA damage-induced nuclear P53 when compared to Tau-expressing cells as shown by immune staining and western blot (Fig. 5a and Supplementary Fig. 2a, b). Reduced P53 was observed when Tau-KO cells were exposed to 30, 60 or 90 µM etoposide and let recover for 30 min or 6 h (Fig. 5a). Reduced etoposide-induced apoptosis in Tau-KO cells displayed a similar dose-dependent effect (Fig. 5b).

Further documenting the role of Tau in etoposide-induced cytotoxicity, re-expressing high levels of human Tau_{441} in Tau-KO cells (Supplementary Figs. 3a and 11) increased P53 stabilization in etoposide-treated cells (Supplementary Fig. 3b) and restored sensitivity in the LDH and clCasp3 assays (Supplementary Fig. 3c). In order to obtain reconstituted Tau expression at a level similar to that of endogenous Tau, in a second set of experiments Tau-KO cells were transiently transfected with a 1:10 mixture of Tau_{410} and GFP plasmids or of empty and GFP plasmids. Tau expression was then analyzed in GFP-positive cells co-transfected either with the Tau_{410} or the empty plasmid by immune staining. This led to determine a level of ectopic expression corresponding to ~2-fold that of endogenous Tau determined in parental SH-SY5Y cells (Supplementary Fig. 3d). Under these conditions, 6 h after etoposide exposure Tau_{410}-transfected Tau-KO cells displayed increased P53 stabilization

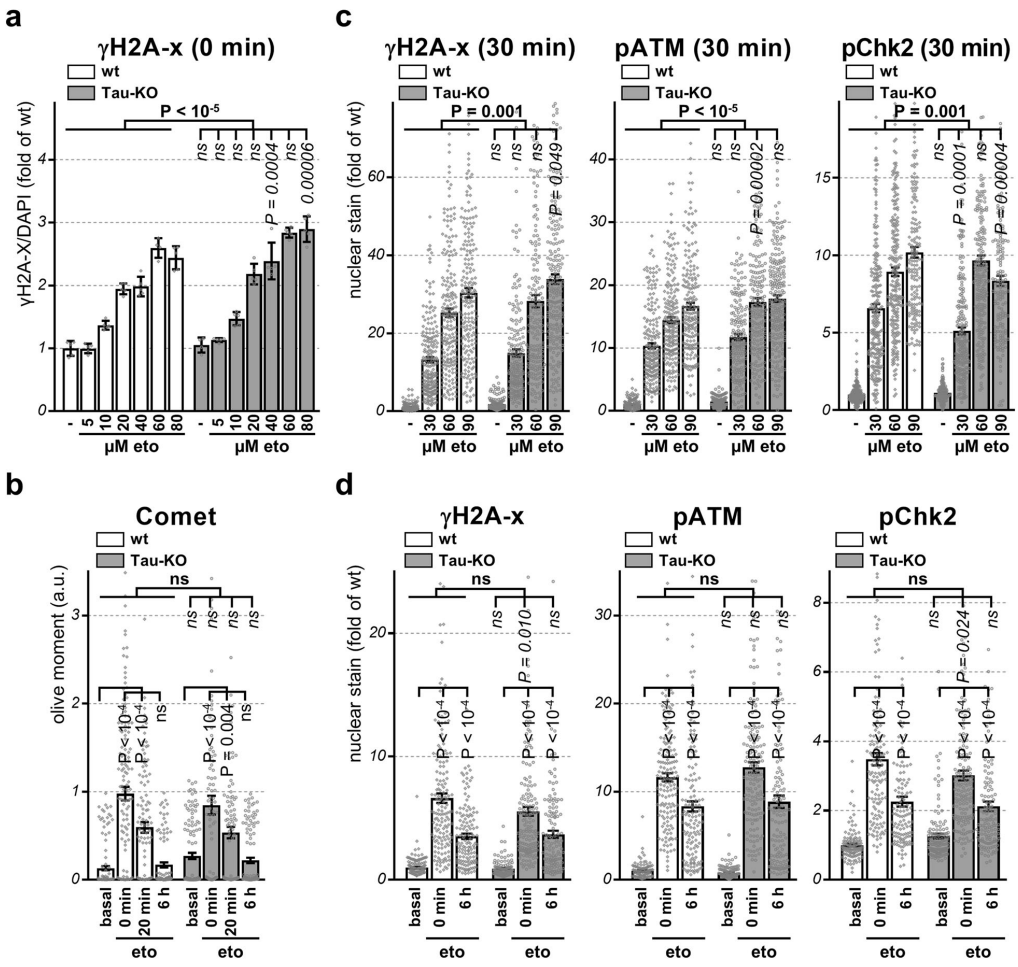

Fig. 4 Reduced P53 in Tau-KO cells is not caused by DDR activation. For all panels, parental (wt) or 232P (Tau-KO) cells were treated 30 min with the indicated etoposide concentrations and recovery times. **a** Mean intensity ± SD of γH2A-X staining normalized for DAPI staining by in-cell western is shown as fold of wt cells at basal conditions, $n = 5$ of biological replicates in a 96-well plate. Non-parametric independent Mann–Whitney U test between lines (in bold), or for each dose between lines (in italics). **b** Olive moment in the Comet assay is shown as mean ± sem, $n = 84$–146 cells/condition. **c**, **d** Mean intensity ± sem of single-cell nuclear γH2A-X, pATM or pChk2 staining (DAPI mask, ImageJ) is shown as fold of wt cells at basal conditions, $n > 100$ cells/condition distributed over five images. Statistical analysis by independent measures ordinary two-way ANOVA, source of variation for cell lines (in bold), multiple Bonferroni pairwise comparisons of each condition between lines (in italics) and of time points for each line (**b**, **d**, in vertical).

when compared to that detected in empty plasmid-transfected Tau-KO cells (Supplementary Fig. 3e).

Tau-KD-cells with reduced Tau-expression corresponding to 71 ± 1% for the 3127 shRNA and 64 ± 2% for the 2112 shRNA (Fig. 5c) when exposed to etoposide also showed reduced P53 activation (Fig. 5d) and apoptosis (Fig. 5e) in a Tau-dose-dependent manner. On the other hand, 60 ± 1% reduced Tau in 1881 shRNA cells did not affect P53 protein level and apoptosis (Fig. 5c–e). Single-cell analysis of the whole Tau-KO or Tau-KD cell population revealed that when we applied a threshold just above background to count P53-positive cells, etoposide-dependent P53 stabilization was better described by a change in the relative number of P53-positive cells rather than by a gradual correlation between Tau and P53 expression (Fig. 5f).

Reduced P53 and apoptosis occurs in other neuroblastomas. In order to validate the observation made in SH-SY5Y cells, we tested the effect of Tau down-regulation in IMR5 and IMR32 human neuroblastoma cell lines. Similar to SH-SY5Y cells, these two cell lines express a wild-type functional P53[26,27]. Several other neuroblastoma cell lines were disregarded because P53 mutations were causing either constitutive activation or expression loss of P53[27]. Tau expression in IMR5 cells was down-regulated ~4-fold in the presence of the 2112 shRNA (Supplementary Fig. 4a). Under these conditions, we observed lower etoposide-induced P53 stabilization in Tau-KD when compared to mock-transduced IMR5 cells as determined by western blot and immune staining analysis (Supplementary Fig. 4b). Similar to what observed in SH-SY5Y cells, etoposide-induced clCasp3 was

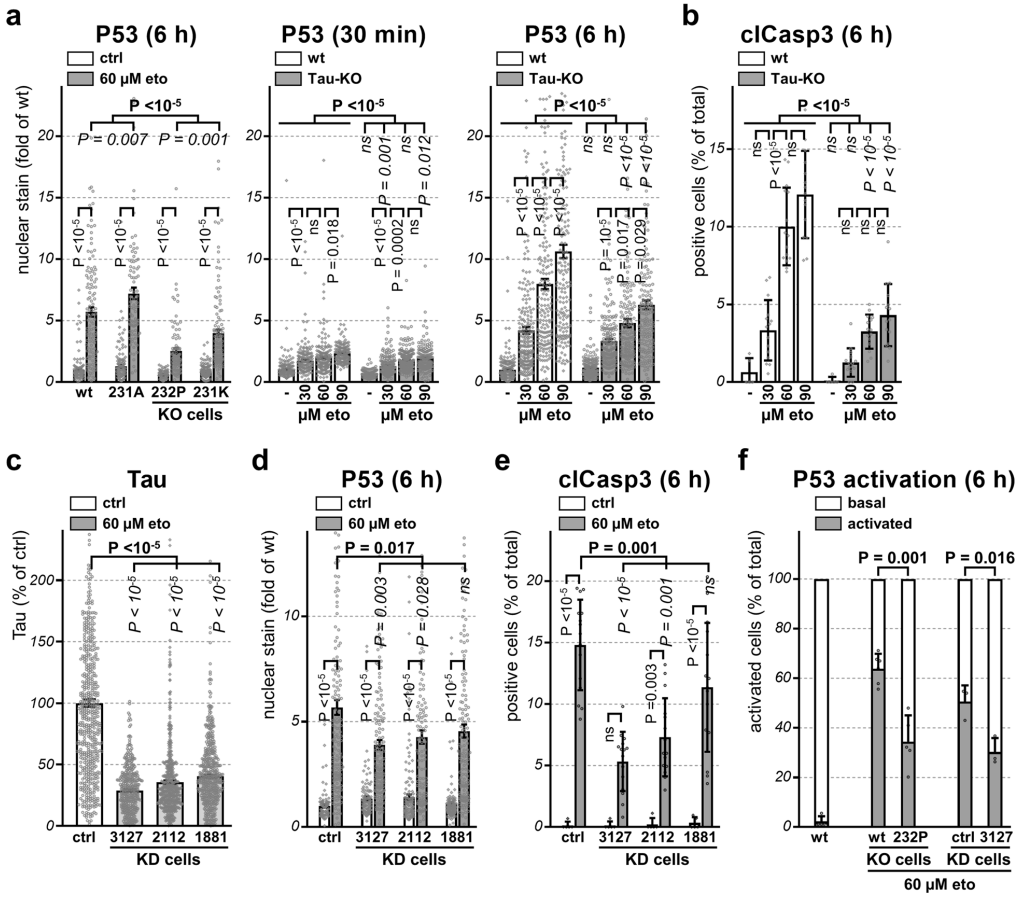

Fig. 5 Tau depletion decreases P53 level and apoptosis. For all panels the indicated cell lines (Tau-KO are 232P cells) were treated 30 min with the indicated etoposide concentrations and recovery times. **a** Mean intensity ± sem of single-cell nuclear P53 staining (DAPI mask, ImageJ) is shown as fold of wt cells at basal conditions, $n > 100$ cells/condition distributed over five images. **b** Percent clCasp3-positive cells are shown as mean ± SD of five images for the untreated cells and of 15 images for etoposide-treated cells, $n > 500$ cells/condition. **c** Mean intensity ± sem of single-cell Tau staining (tubulin mask, ImageJ) for the indicated cell lines is shown as percent of mock shRNA cells (ctrl), $n > 160$ cells/condition distributed over five images. **d** Mean intensity of single-cell nuclear P53 staining quantified as in **a**, $n > 380$ cell/condition distributed over 15 images from $n = 3$ biological replicates. **e** Percent clCasp3-positive cells quantified as in **b**, $n > 500$ cell/condition. **f** An arbitrary threshold was applied in order to count P53-positive cells as percentage ± SD of total DAPI-positive cell number, $n > 100$ cells/conditions. For the comparison between the four cell lines (**a**), non-parametric independent Mann–Whitney U test for genotype (in bold) and Kruskal–Wallis pairwise comparison of treatment for cell lines with same genotype (in italics) or for each line (in vertical). For the dose-dependency (**a**, **b**), non-parametric independent Mann–Whitney U test between cell lines (in bold), Kruskal–Wallis pairwise comparison for each dose (in italics) and between doses (in vertical). Non-parametric independent Mann–Whitney U test (**c**–**e**) between control and the three Tau-KD lines (in bold) and Kruskal–Wallis pairwise comparison for each Tau-KD line (in italic) and for each treatment (in vertical). Unpaired two-tailed t test with Welch's correction (**f**).

also reduced in Tau-depleted IMR5 cells (Supplementary Fig. 4c). The presence of the 3127 shRNA in IMR32 cells lowered Tau expression by ~40%, which resulted in reduced P53 stabilization and caspase-3 activation in cells exposed to the etoposide treatment (Supplementary Fig. 4d–f).

Tau regulates P53 expression post-translationally. To assess whether lower P53 protein level observed in Tau-KO cells was occurring by transcriptional or post-translational mechanism, we first determined by quantitative RT-PCR the amount of the P53 mRNA in wt and Tau-KO cells before or 6 h after the acute etoposide treatment. At basal conditions Tau-KO and Tau-KD cells showed a significant but modest increase in *TP53* transcription when compared to Tau-expressing cells. Etoposide exposure slightly increased the P53 transcript in all cell lines, but there was no difference when comparing treated Tau-expressing and treated Tau-KO cells (Fig. 6a, b). Overall, these data essentially dismissed the premise that the effect of Tau depletion on P53 stabilization occurred at the transcriptional level, rather suggesting a translational or post-translational control. On the other hand, etoposide treatment resulted in the expected

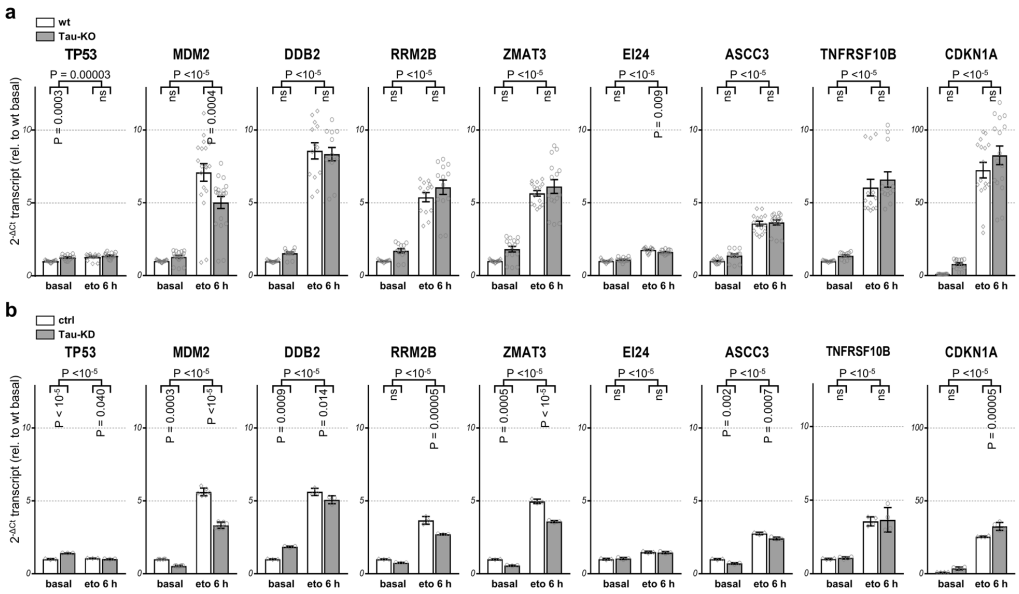

Fig. 6 Differential regulation of P53 transcription targets. Extracted RNA from parental (wt) and 232P (Tau-KO) cells in **a** or from control shRNA plasmid (ctrl) and 3127 (Tau-KD) cells in **b** at basal conditions or after 30 min 60 µM etoposide and 6 h recovery, was subjected to reverse-transcription and qPCR with primers specific for the indicated transcripts. Mean ± SD of relative mRNA levels ($n = 3$) shown as fold of the respective basal conditions for parental or control cells. Statistical analysis by independent measures ordinary two-way ANOVA, source of variation for cell lines (horizontal), multiple Sidak pairwise comparisons for treatment for each line (in vertical).

P53-dependent upregulation of *HDM2* transcription, but this was markedly reduced in Tau-KO and in Tau-KD cells (Fig. 6a, b), a result that was confirmed also at the MDM2 protein level (Supplementary Fig. 5). Analysis of additional direct targets of P53[28,29] showed a differential transcriptional response to etoposide in Tau-depleted cells. Whilst, transcription of the *EI24* gene was reduced in etoposide-treated Tau-KO cells, that of *RRM2B*, *TNFRSF10B*, *DDB2*, *ZMAT3, ASCC3* and *CDKN1A* was not affected in Tau-KO cells (Fig. 6a). Dysregulation of transcription of the P53 targets was more evident in Tau-KD cells, which showed reduced etoposide-induction for the *MDM2*, *DDB2*, *RRM2B*, *ZMAT3*, *ASCC3* transcripts, and no effect on the *EI24* and *TNFRSF10B* transcripts (Fig. 6b). Interestingly, as observed for the *CDKN1A* protein product p21 (Fig. 3c), also the *CDKN1A* transcript was increased in Tau-KD cells after etoposide treatment (Fig. 6b), whereas this did not reach significance in Tau-KO cells (Fig. 6a). A different regulation of direct P53-dependent genes after etoposide exposure, conveyed by a positive or negative difference in the degree of transcription activation between cells with normal or reduced Tau expression, substantiated a Tau-dependent modulation of P53 function at a post-translational level. Also, the heterogeneous response observed among the different P53 targets cannot be explained solely by a change in P53 protein stability but implied a more complex modulation of P53 activity.

Tau affects P53 and MDM2 modification. A post-translational clearance mechanism keeps P53 protein at low levels in the absence of a cellular stress[30]. This occurs mainly, but not exclusively, by the activity of the E3 ubiquitin ligase MDM2 (also known as HDM2) that associates with P53 to favor its degradation and interfere with its function[30,31]. We determined the amount of nuclear MDM2 and found that induction of MDM2 was lower in Tau-KO cells when compared to Tau-expressing cells, possibly explained by reduced gene transcription (see above, Fig. 6), whereas MDM2 expression in untreated cells was not modulated by Tau (Supplementary Fig. 5). Post-translational modification of P53 through the action of DDR transducing kinases causes the dissociation of the P53-MDM2 complex and induces stress-dependent P53 stabilization. In the presence of DSBs, this occurs mainly by N-terminal phosphorylation of the P53 transcription-activation domain by the ATM-Chk2 axis[22]. We tested two small molecules interfering with this process. KU-55933 is an ATM inhibitor blocking ATM-dependent P53 phosphorylation thus preserving the P53-MDM2 complex and its degradation. Nutlin-3 binds to the P53-binding pocket of MDM2 thus inhibiting their association and degradation. KU-55933 had no effect on P53 and MDM2 expression when tested alone (Fig. 7a). As expected, adding the drug after etoposide treatment severely impaired DSB-induced P53 and MDM2 stabilization and also blocked apoptosis activation (Fig. 7a, b). Consistent with its mode of action, the presence of nutlin-3 led to a strong increase in P53 and MDM2, which was higher to that caused by etoposide but, notably, did not induce apoptosis (Fig. 7a, b). Nutlin-3 potentiated the effect of etoposide in terms of P53-MDM2 stabilization in wt cells. In Tau-KO cells exposed to etoposide, nutlin-3 eliminated the drop in MDM2 and partly also that in P53 (Fig. 7a, b). Determination of P53 phosphorylation at S_{15} when normalized for total P53 protein showed a similar etoposide-dependent relative occupancy in Tau-KO cells when compared to Tau-expressing cells (Supplementary Fig. 6a). This was an unexpected result because amino-terminal P53 phosphorylation should stabilize P53 by interfering with the binding to MDM2, and thus increased P53 destabilization in Tau-KO cells should be reflected by a reduction in P53 phosphorylation. A

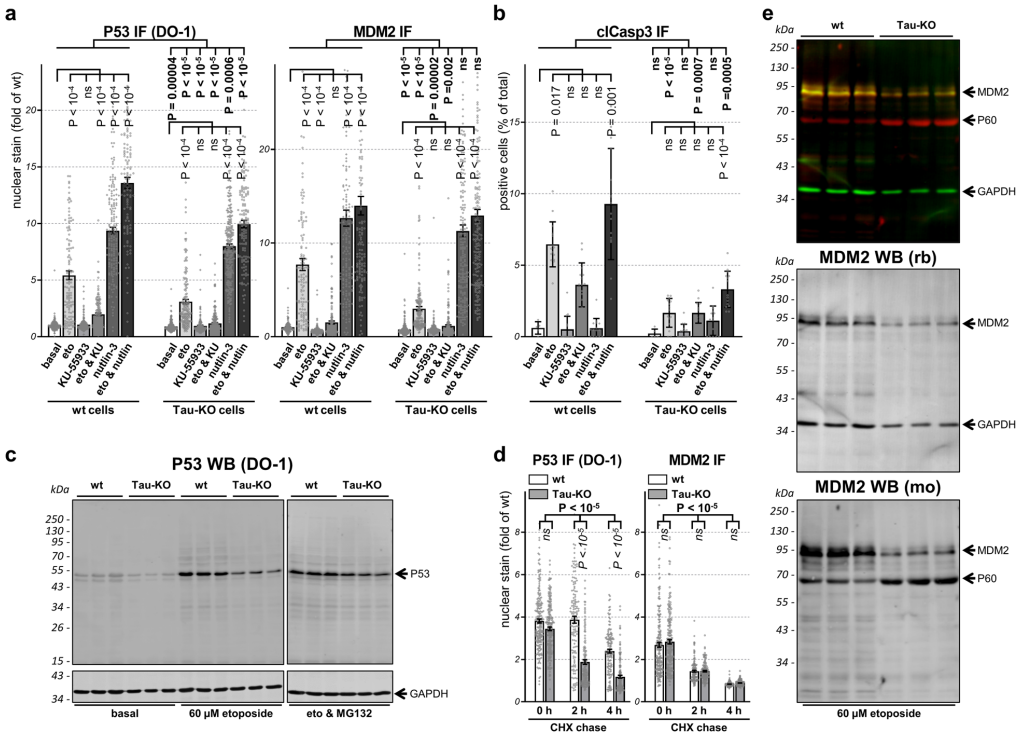

Fig. 7 Role of P53 and MDM2 modifications for P53 function and stability. a, **b** Parental (wt) or 232P (Tau-KO) cells treated 30 min without (basal) or with 60 µM etoposide and recovered for 6 h in the absence (eto) or presence of 10 µg/mL KU-55933 and/or 5 µg/mL nutlin-3. **a** Mean intensity ± sem of single-cell nuclear P53 or MDM2 (DAPI mask, ImageJ) shown as fold of basal conditions, $n > 100$ cells/condition distributed over five images. **b** Percent clCasp3-positive cells shown as mean ± SD of five images (basal) or 15 images (treatments), $n > 500$ cells/condition. Non-parametric independent samples test and Kruskal–Wallis pairwise comparison between cell lines (in bold) or for treatment for each cell line (in vertical). **c** Western bot analysis of P53 in parental (wt) or 232 P (Tau-KO) cells at basal conditions, after 30 min 60 µM etoposide and 4 h recovery without or with 10 µM MG132. GAPDH served as loading control. **d** Parental (wt) or 232P (Tau-KO) cells pre-treated for 30 min with 60 µM etoposide followed by 4 h with 10 µM MG132, were incubated with 25 µM of cycloheximide (CHX) for the indicated chase times. Single-cell nuclear P53 or nuclear MDM2 (DAPI mask, ImageJ) shown as fold of wt cells at basal conditions. Mean intensity ± sem of $n > 100$ cells/condition distributed over five images. Independent measures ordinary two-way ANOVA, source of variation for cell lines (bold), multiple Bonferroni pairwise comparisons of treatment for each line (in italic). **e** Parental (wt) or (Tau-KO) 232P cells treated for 30 min with 60 µM etoposide and 6 h recovery analyzed with a 90 kDa MDM2 rabbit antibody (green and middle panel with GAPDH as loading control) or a 60 and 90 kDa MDM2 mouse antibody (red and bottom panel).

possible explanation is that reduced DSB-dependent stabilization of P53 caused by the absence of Tau might be compensated by a change in P53 phosphorylation. Etoposide-induced P53 phosphorylation at S_{15} was severely impaired by the ATM inhibitor KU-55933 (Supplementary Fig. 6b), but this only partially blocked apoptosis induction in wt cells and had no effect in Tau-KO cells when compared to etoposide-exposure alone (Fig. 7b). In addition, P53 stabilization by nutlin-3 did not involve S_{15} phosphorylation (Supplementary Fig. 6b) and poorly induced apoptosis (Fig. 7b). Our attempts to analyze pS_{46}-P53 phosphorylation was unsuccessful as no signal was detected also under conditions of prolonged etoposide treatment both in Tau-expressing and Tau-KO cells. We concluded that in SH-SY5Y cells, DSB-induced apoptosis was at least in part dependent on P53 modification.

Tau-depletion increases P53 degradation rate. To address if Tau-KO cells displayed faster P53 degradation possibly accounting for the lower detection of P53 protein, we first inhibited the ubiquitin-proteasome system by treating the cells with MG132. The presence of MG132 during the recovery phase from etoposide exposure restored P53 stabilization in Tau-KO cells but had no effect in wt cells, suggesting that the absence of Tau favored P53 degradation (Fig. 7c and Supplementary Fig. 9c).

Taking advantage of the fact that MG132 was able to restore similar P53 protein levels in wt and Tau-KO cells exposed to etoposide, we then analyzed the rate of degradation of P53 and MDM2 by removing MG132 and adding the translation inhibitor cycloheximide. Under these conditions we observed a faster P53 degradation rate at 2 and 4 h wash-out in Tau-KO cells when compared to wt cells (Fig. 7d). In contrast, no difference was observed in terms of MDM2 degradation (Fig. 7d).

Western blot analysis of MDM2 with the same rabbit antibody used for immune staining of the cells confirmed reduced MDM2 expression in Tau-KO cells exposed to etoposide when compared to wt cells (Fig.7e and Supplementary Fig. 9e). Interestingly, when using a mouse antibody for MDM2, we also detected a 60 kDa MDM2 form (Fig.7e and Supplementary Fig. 9e), likely representing the amino-terminal caspase-2 cleavage product of

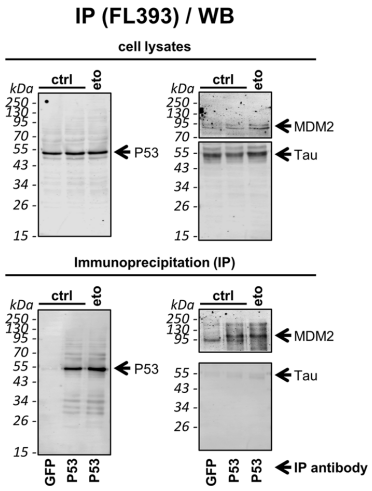

Fig. 8 Tau does not directly interact with P53. Cell lysates of SH-SY5Y treated with 10 μM of MG132 to stabilize P53 expression, without (ctrl) or with (eto) a 30 min pre-treatment with 60 μM etoposide, were subjected to immune precipitation of endogenous P53 with a rabbit antibody (P53) or with a rabbit GFP antibody as negative IP control (GFP). Western blot analysis for co-precipitation of MDM2 or Tau with the respective mouse antibodies as indicated. The blots on the top show the analysis of the starting material (cell lysates), those on the bottom the immunoprecipitation (IP). The P53 blots are entirely shown, whereas for MDM2 and Tau, the blots were cut between the 55 kDa and the 95 kDa protein size markers and analyzed separately.

full-length 90 kDa MDM2[32,33]. An opposite effect of etoposide-exposure was obtained for these two forms of MDM2 in Tau-KO cells when compared to wt cells. Although reduced 90 kDa MDM2 detection was confirmed in Tau-KO cells, in the same cells we found that etoposide markedly increased 60 kDa MDM2 (Fig.7e and Supplementary Fig. 9e).

Tau does not interact with P53. In the presence of the proteasome inhibitor, the interaction between P53 and MDM2 was confirmed by a co-precipitation experiment both in the presence and in the absence of etoposide treatment (Fig. 8 and Supplementary Fig. 10). However, although etoposide increased the amount of MDM2 detected in cell lysates when compared to the control, for both conditions a similar amount of MDM2 was co-precipitated by P53; a result consistent with decreased P53-MDM2 interaction as a consequence of DNA damage. In contrast, we did not detect any interaction between P53 and Tau in the presence or absence of DNA damage (Fig. 8 and Supplementary Fig. 10), suggesting that the modulatory function of Tau on P53 stabilization may not occur by a direct interaction between the two proteins in SH-SY5Y cells.

The data obtained implied that in neuroblastoma cells Tau modulated P53 in a manner that went beyond a simple regulation of its stabilization, but accounted also for a deregulation of P53 and MDM2 post-translational modification ultimately affecting the activity and function of P53 in cell fate decisions dependent on DNA damage.

Discussion

We report a new function of Tau as a regulator of DSB-induced cell fate and describe that this occurred by a deregulation of P53 activity. Our data support a role for Tau as a P53 modifier in neurodegeneration. Uncontrolled P53 activity in the presence of P53 or MDM2 mutations is one of the main pathomechanism of cancer[34]. Not surprisingly, the P53-MDM2 axis includes a variety of factors regulating their modification and localization[35]. Based on our data, Tau should now be listed as a modifier of wild-type P53 function, with possible implications in cancer biology.

The involvement of apoptosis in neurodegeneration is documented[36], but whether this is modulated by Tau remains questionable[37,38]. We show now that a brief DNA damaging insult positively associates Tau to programmed cell death and negatively to cellular senescence. Positive association to cell loss was already shown in Bloom's syndrome cells under continuous DNA damage for three days, although a distinction between cell death and senescence was not clear[39]. Age-dependent increase in senescent cells promotes tissue deterioration and neuronal dysfunction[40,41]. Moreover, increased senescent glia cells were found in a tauopathy model characterized by reduced soluble Tau and, remarkably, senescent cell removal prevented functional neuronal decline[42]. Nevertheless, direct evidence that Tau loss-of-function may promote senescence was not yet reported.

In the adult human brain, post-mitotic neurons express Tau in multiple alternative spliced isoforms that differ depending on the presence of up to two N-terminal inserts (0N, 1N, 2N) and on the presence of three or four microtubule-binding repeats (3R, 4R). In early development, 3R-Tau isoforms are predominant whereas in the adult brain the 3R and 4R isoforms are detected at a similar level, although they ratio is substantially altered in a peculiar manner for distinct tauopathies[43]. The cell lines used in our study (SH-SY5Y, IMR-32 and its subclone IMR-5) express predominantly the embryonic isoform 3R-Tau when actively dividing[44–46]. Our results showing that the effect of endogenous Tau deletion was reversed by ectopic expression of either 4R-Tau_{441} or 3R-Tau_{410} suggest that the modulatory role of Tau on P53 is possibly shared by all Tau isoforms. Tau phosphorylation in undifferentiated SH-SY5Y is increased[46], so at this time we cannot exclude that the modulatory effect of Tau on P53 may require modification of Tau by phosphorylation.

The balance between apoptosis and senescence is regulated by an intricate mechanism, which varies in response to distinct stressors[47]. In terms of DNA damage, crucial determinants are the nature and intensity of the stress. Since P53 drives both the induction of apoptosis and senescence, cell fate is finely tuned by changes in P53 kinetics and transcriptional activity under post-translational modification control[48]. The inference that Tau modifies P53 protein expression and the balance between cell death and senescence, suggests Tau as a modifier of P53 post-translation modification by acting on P53 modulators. P53 is modified by most types of substituents, which dictate the complex response to a wide range of cellular conditions[49]. Ubiquitination and phosphorylation control P53 stability, subcellular localization and transcriptional versus non-transcriptional activity, as well as cellular senescence[50] and apoptosis[51]. P53 acetylation may govern transcriptional-regulation of gene targets involved in growth arrest, and the choice to enter senescence or apoptosis[52]. In our cellular model, treatment with nutlin-3 restored P53 stabilization without involving P53 phosphorylation in Tau-depleted cells exposed to etoposide, but poorly reversed reduced activation of the apoptotic pathway. Nutlin-3 restored also the expression of the P53 negative regulator MDM2, which targets P53 for degradation, regulates its nuclear localization, and the interaction of P53 with transcriptional co-factors[35]. Therefore, considering only the protein amount of P53 or MDM2 inadequately explains the role of Tau as an effector balancing apoptosis and senescence. Additional P53-interacting protein such as WW domain-containing oxidoreductase (WWOX), which modulate Tau phosphorylation, may be involved in Tau-dependent regulation of P53[53,54].

Table 1 Argeted gRNA sequences for human *MAPT* gene.

Oligo	Sequence
231	CACGCTGGGACGTACGGGTTGGG
232	CCGCCAGGAGTTCGAAGTGATGGG

Tau has been described recently to be part of a complex containing P53, PARN and Pin1 involved in the regulation of mRNA stability through regulation of polyadenylation[9]. In this report, in HCT-116 colon cells Tau expression modulated the level of the P53 transcript and P53 that of Tau. In our cellular model, we also observed that Tau was able to modulate P53 expression, but we excluded that this occurred at the level of gene transcription and instead showed a post-translational mechanism. Nevertheless, the action of Tau on P53 degradation, on P53 activity as transcription factor and on P53 function as cell fate mediator reported herein for SH-SY5Y cells may well be regulated by a Tau complex similar to that described for HCT-116 cells. However, HCT-116 and other colon cancer cell lines modify Tau to an hyperphosphorylated form resembling the one deposited in tauopathy brains[55], suggesting a difference in function between pathogenic and physiological Tau.

Increased DNA damage has been reported as a consequence of Tau deletion and heat stress, indicating a protective role of Tau against DNA damage, which may require nuclear Tau translocation[10,11,35]. We reported that also etoposide exposure increased nuclear Tau and reduced its phosphorylation[12]. In the present study, determination of DNA integrity assessed by the Comet and γH2A-X assays confirmed the protective role of Tau, but rebuffed the possibility that decreased DNA damage in the absence of Tau may be the reason for decreased DSB-induced cell death. Moreover, we did not observe an overt effect on the ATM-Chk2 axis, implying that a downstream pathway was affected in Tau-KO cells.

P53 stabilization and apoptosis induction depended on the activity of the ATM-Chk2 axis, because they were stopped by the ATM inhibitor KU-55933. An alternative reading is that Tau may intervene on P53 modification or on its functional modulators. Whether this occurs in the cytosol, possibly based on its activity on microtubules, or following its nuclear translocation is yet to be examined. P53 has been shown to associate to and be regulated by microtubules[56,57]. Therefore, Tau may affect P53 interaction with the cytoskeleton by modulating microtubule dynamics. However, Tau is also present in the nucleus in normal and stress conditions and some functions associated to nuclear Tau were suggested[10,11,58–60].

The implication of the neurodegeneration-associated Tau protein in the biology of P53, the "guardian of the genome", is a thrilling finding that may explain the role of P53 and DDR dysfunction in neurodegeneration and the link between Tau and cancer. Abnormal P53 species are potential biomarkers of AD[61–63], the most common tauopathy with an high incidence of P53 mutations[64] and P53 deregulation[65]. Genetic manipulation of P53 family members in mice affects aging, cognitive decline, and Tau phosphorylation[66,67]. Cell cycle activators are upregulated in post-mitotic neurons by stress conditions and tauopathies, possibly representing a cause for neurodegeneration[68,69]. Increased DNA damage is found in AD[15,16] and persistent DDR causes neuronal senescence and upregulation of pro-inflammatory factors[70]. Our finding that cellular senescence is increased by DSBs in Tau-KO cells is consistent with these observations.

Intriguingly, hyperphosphorylated and insoluble Tau is detected in some prostate cancer[71], FTDP-17 *MAPT* mutations increase the incidence of cancer[72], and higher levels of phosphoSer199/202-Tau have value as predictors of non-metastatic colon cancer[73]. More recently several reports described that high Tau expression improves survival in several types of cancers[74–77]. Intriguingly, Tau deficiency resulting in reduced P53 stabilization reported herein provides a mechanism to explain why reduced Tau represents a negative prognostic marker. Moreover, since our data show that Tau expression also modulates etoposide cytotoxicity, we would like to propose that Tau protein level may acquire value as a response marker of genotoxic therapy.

Cancer and neurodegenerative diseases may involve common signaling pathways balancing cell survival and death[78–80] and may be defined as diseases of inappropriate cell-cycle control as a consequence of accumulating DNA damage. Epidemiological studies show an inverse correlation between cancer and neurodegeneration[79], although not consistently[81,82], and chemotherapy is associated to a lower predisposition for AD[83,84]. The study of Tau as a modifier of P53 and, importantly, P53 control of cell death and senescence is crucial because of the implication that Tau may modulate cell death and senescence in neurodegenerative tauopathies and in cancer. Considering the unmet medical need with vast social implications caused by these—unfortunately frequent —disorders, our finding holds sizeable scientific importance and may lead to innovative approaches for disease-modifying therapeutic interventions.

Methods

Cell culture and DNA transfections. Human neuroblastoma IMR5, IMR32, and SK-N-AS were kindly provided by Dr. Chiara Brignole and Dr. Mirco Ponzoni from the IRCCS Istituto Giannina Gaslini in Genova. These cells and the human neuroblastoma SH-SY5Y cells (94030304, Sigma-Aldrich) were cultured in complete DMEM: Dulbecco's Modified Eagle Medium (61965–059, Gibco) supplemented with 1% non-essential amino acids (11140035, Gibco), 1% penicillin-streptomycin (15140122, Gibco) and 10% fetal bovine serum (10270106, Gibco). Cells were grown at 37 °C with saturated humidity and 5% CO_2, and maintained in culture for <1 month. Cells grown on poly-D-lysine (P6407, Sigma-Aldrich) were transfected with jetPRIME (114–15, Polyplus) or Lipofectamine 3000 (L3000008, Invitrogen) according to the manufacturer's instructions or with the calcium phosphate method[85].

Targeted disruption of Tau expression. For disruption of the *MAPT* gene encoding for Tau by the CRISPR-Cas9 method, the two gRNAs 231 and 232 (Table 1) targeted exon 2 containing the initiating ATG (ENST00000344290.9). Cells in six-well plates were transfected with the plasmid kindly provided by Dr. Zhang[86] (52961, Addgene) driving expression of one of the two gRNA, Cas9 nuclease and puromycin resistance. One day post-transfection, cells were transferred to 10 cm plates and incubated for 2 days with 20 μg/mL puromycin (P8833, Sigma-Aldrich). Single colonies were isolated, amplified, and stored in liquid nitrogen. The cDNA encoding for human Tau isoform of 441 amino acids (Tau441) in the expression plasmid pcDNA3 and selection in 0.5 mg/mL Geneticin (11811031, Gibco) served to generate reconstituted Tau expression in the Tau-KO 232P cell line.

Sequencing of the targeted *MAPT* gene. Cell pellets were resuspended in 400 μL TNES buffer (0.6% SDS, 400 mM NaCl, 100 mM EDTA, 10 mM Tris pH 7.5) and 0.2 mg/mL proteinase-K (Abcam, ab64220) under continuous shaking 3–4 h at 50 °C, and then supplemented with 105 μL of 6 M NaCl. Genomic DNA was precipitated with one volume of ice-cold 100% ethanol, washed with 100% ethanol and with 70% ethanol, and air-dried. The genomic fragment containing the CRISPR-Cas9-targeted regions was amplified by PCR with primers containing BamHI or XhoI restriction sites (Table 2) with the AccuPrime™ Pfx SuperMix (12344–040, Invitrogen). PCR reactions were purified with the GeneJET PCR purification kit (K0701, ThermoFisher Scientific) and subcloned in pcDNA3. DNA from single bacterial colonies were analyzed by restriction mapping with NdeI and XhoI or Van91I, in order to verify the presence and the *MAPT* origin of the inserts. Inserts with different size were selected in order to increase the chance of sequencing both alleles (Microsynth).

Down-regulation of Tau or P53 expression. Short hairpin RNAs (shRNAs, Table 3) were inserted in the pGreenPuro vector (SI505A-1, System Biosciences). The design of shRNAs targeting Tau or P53 was done following the manufacturer's instructions or with the tool provided by Dr. Hannon at http://katahdin.cshl.org//siRNA/RNAi.cgi?type=shRNA. Pseudo-lentiviral particles were produced in

Table 2 PCR Primers (all specific for homo sapiens mRNAs).

Gene	Forward primer (5′–3′)	Reverse primer (5′–3′)
MAPT	GATCAGGATCCGTGAACTTTGAACCAGGATGGC	GATCAGGATCCGTGAACTTTGAACCAGGATGGC
MDM2	TGTTTGGCGTGCCAAGCTTCTC	CACAGATGTACCTGAGTCCGATG
TP53	CCTCAGCATCTTATCCGAGTGG	TGGATGGTGGTACAGTCAGAGC
CDKN1A	AGGTGGACCTGGAGACTCTCAG	TCCTCTTGGAGAAGATCAGCCG
DDB2	CCAGTTTTACGCCTCCTCAATGG	GGCTACTAGCAGACACATCCAG
ZMAT3	GCTCTGTGATGCCTCCTTCAGT	TTGACCCAGCTCTGAGGATTCC
RRM2B	ACTTCATCTCTCACATCTTAGCCT	AAACAGCGAGCCTCTGGAACCT
ASCC3	GATGGAAGCATCCATTCAGCCTA	CCACCAAGGTTCTCCTACTGTC
EI24	GCAAGTAGTGTCTTGGCACAGAG	CAGAACACTCCACCATTCCAAGC
GAPDH	TGCACCACCAACTGCTTAGC	GGCATGGACTGTGGTCATGAG
HPRT1	TGACACTGGCAAAACAATGCA	GGTCCTTTTCACCAGCAAGCT

Table 3 Oligonucleotide annealed for shRNA sequences.

P53	Sense	5′gatccgactccagtggtaatctaccttcctgtcagagtagattaccactggagtctttttg 3′
	Antisense	3′cgactccagtggtaatctaccttcctgtcagagtagattaccactggagtctttttgaatt 5′
Tau 1881	Sense	5′gatcctggtgaacctccaaaatcacttcctgtcagatgattttggaggttcaccatttttg 3′
	Antisense	3′ctggtgaacctccaaaatcacttcctgtcagatgattttggaggttcaccatttttgaatt 5′
Tau 2112	Sense	5′gatccaactgagaacctgaagcaccagcttcctgtcagactggtgcttcaggttctcagtgttttttg 3′
	Antisense	3′caactgagaacctgaagcaccagcttcctgtcagactggtgcttcaggttctcagtgtttttgaatt 5′
Tau 3127	Sense	5′gatccagcagacgatgtcaaccttgtgcttcctgtcagacacaaggttgacatcgtctgccttttttg 3′
	Antisense	3′cagcagacgatgtcaaccttgtgcttcctgtcagacacaaggttgacatcgtctgccttttttgaatt 5′

HEK-293 cells (HEK 293TN, System Biosciences) with the pPACKH1 kit (LV500A-1, System Biosciences) by the calcium phosphate transfection method[85]. Particles were harvested 48–72 h later, concentrated on a 30K MWCO Macrosep Advance Spin Filter (MAP030C37, Pall Corporation), aliquoted and stored at −80 °C until use. Particle titers were determined at 72 h post-transduction by calculating the percent of GFP-positive cells and the mean GFP intensity. Tau-KD and P53-KD cells were obtained upon transduction and selection in 5 µg/mL puromycin for one to 2 weeks.

Drug treatments. Etoposide (100 mM stock in DMSO; ab120227, Abcam) treatment was followed by three washes with complete DMEM and cells were allowed to recover for the indicated times. The concentration of etoposide was adapted depending on the cell line, most treatments of SH-SY5Y cells were performed at 60 or 100 µM etoposide, whereas 15 µM etoposide was used for IMR5 cells and 30 µM etoposide for IMR32 cells. When specified, recovery was done in the presence of 5 µg/mL nutlin-3 (5 mg/mL stock in DMSO; SC-45061, Santa Cruz), 10 µg/mL of KU-55933 (10 mg/mL stock in DMSO; SML1109, Sigma-Aldrich), 10 µM MG132 (10 mM stock in DMSO, M7449, Sigma-Aldrich) or 25 µM cycloheximide (10 mg/ml stock in H_2O, 01810, Sigma-Aldrich). Vehicle DMSO was added in the controls.

Immune assays. For immune staining, cells were grown on poly-D-lysine coated eight-well microscope slides (80826-IBI, Ibidi). Cells were fixed in paraformaldehyde and stained[12] with primary antibodies 1 µg/mL Tau13 (sc-21796, Santa Cruz), 0.5 µg/mL pS_{129}-H2A-X (sc-517348, Santa Cruz), 0.13 µg/mL pS_{1981}-ATM (#13050, Cell Signaling), 0.2 µg/mL pT_{68}-Chk2 (#2197, Cell Signaling), 0.4 µg/mL P53 DO-1 (sc-126, Santa Cruz,), 1 µg/mL pS_{15}-P53 (ab223868, Abcam), 0.2 µg/mL MDM2 (#86934, Cell Signaling), 0.05 µg/mL $clAsp_{175}$-Caspase3 (#9661, Cell Signaling), 0.5 µg/mL alpha-tubulin (ab18251, Abcam). Detection of endogenous Tau entailed the testing of a number of commercial antibodies so to find the human-specific Tau13 monoclonal antibody against an amino-terminal epitope as reagent providing the most reliable detection of endogenous Tau. Although determination of DSBs by γH2A-X is mostly performed by counting positive nuclear foci, we noticed that at the concentration of etoposide used here, single foci were poorly discernible, we nevertheless confirmed that mean intensity of nuclear γH2A-X staining correlated with foci counting and decided to apply the first method for our quantifications of DNA damage. Detection by fluorescent laser confocal microscopy (Nikon C2 microscope) was done with 2 µg/mL secondary antibodies anti-mouse IgG-Alexa594 or -Alexa 488 (A-11032, A-11001, ThermoFisher Scientific) or anti-rabbit IgG-Alexa594 or -Alexa488 (A-11037, A-11034, ThermoFisher Scientific). Nuclei were counterstained with 0.5 µg/mL DAPI (D9542, Sigma-Aldrich). Images were usually taken with a line by line scan with a sequence of excitations, i.e. 405 nm laser with 464/40–700/100 nm emission filter, 488 nm laser with 525/50 nm emission filter, and 561 nm laser with 561/LP nm emission filter. ImageJ was used for all image quantifications.

For biochemical analysis by western blot, cells plated in 6 well plates were directly lysed in 40 µL SDS PAGE sample buffer (1.5% SDS, 8.3% glycerol, 0.005% bromophenol blue, 1.6% β-mercaptoethanol and 62.5 mM Tris pH 6.8) and incubated 10 min at 100 °C.For immune precipitation, cells from 10 cm plates were rinsed with PBS and collected by scraping and low speed centrifugation. Cell lysates were prepared in 400 µL ice-cold RIPA buffer (R0278, Sigma-Aldrich), supplemented with protease and phosphatase inhibitor cocktails (S8820, 04906845001, Sigma-Aldrich) and treated with benzonase (707463, Novagen) 15 min at 37 °C.

Protein immune precipitation was performed by a batch procedure using Protein G-Sepharose® beads (101241, Invitrogen) overnight at 4 °C with 40 µL 30% slurry beads and 1 µg of HT7 antibody (MN1000, Invitrogen) or P53 antibody (FL-393, bs-8687R, Bioss Antibodies) antibody. The cell lysates for P53 immune precipitation were cleared by centrifugation at 20,000 g per 10 min. For immune blots[12], we used 0.2 µg/mL Tau13 (sc-21796, Santa Cruz), 0.18 µg/mL GAPDH (ab181602, Abcam), 0.4 µg/mL P53 DO-1 (sc-126, Santa Cruz), 4 µg/mL P53 Pab 1801 (sc-98, Santa Cruz), 0.5 µg/mL pS_{15}-P53 (ab223868, Abcam), 0.1 µg/mL rabbit D1V2Z MDM2 (#86934, Cell Signaling), 0.2 µg/mL mouse SMP14 MDM2 (sc965, Santa Cruz), 0.05 µg/mL $clAsp_{175}$-Caspase3 (#9661, Cell Signaling), or 0.2 µg/mL p21 (sc53870, Santa Cruz). Immune precipitated Tau protein was detected with 0.1 µg/mL biotinylated HT7 antibody (MN1000B, ThermoFisher Scientific) and 0.2 µg/mL streptavidin-IRDye (926–32230, Licor Biosciences). In the co-IP experiments, the antibodies used were 0.4 µg/mL P53 DO-1, 1 µg/mL Tau13 and 0.1 µg/mL D1V2Z MDM2.

For in cell western, cells plated on poly-D-lysine-coated 96-well microtiter plates were fixed with cold 4% paraformaldehyde in PBS 15 min at 4 °C, stained with 0.5 µg/mL pS_{129}-H2A.X (sc-517348, Santa Cruz), anti-mouse IgG-IRDye680 (926–68070, Licor), and analyzed on a dual fluorescent scanner (Odyssey CLx, LICOR). Determination of 0.5 µg/mL DAPI staining for normalization was performed with an absorbance reader (Infinite M Plex, Tecan).

Cell death and senescence assays. The LDH (Pierce LDH Cytotoxicity Assay Kit; 88954, ThermoFisher Scientific) and MTS assay (CellTiter 96® Aqueous Non-Radioactive Cell Proliferation Assay; G5421 Promega) were done following the manufacturer's instructions. For LDH, conditioned medium from cells plated in a 96-well microtiter plate was analyzed by measuring absorbance at 490 and 680 nm (Infinite M Plex, Tecan). Colorimetric measurement for MTS was performed at 490 nm (Infinite M Plex, Tecan).

Senescence-associated β-galactosidase staining was determined on cells plated in six-well plates, fixed with 2% paraformaldehyde 10 min at RT and washed twice with gentle shaking 5 min at RT. Then, cells were incubated with 1 mg/mL X-gal (20 mg/mL stock in DMF; B4252, Sigma-Aldrich,) diluted in pre-warmed 5 mM potassium ferricyanide crystalline (P-8131, Sigma-Aldrich), 5 mM potassium ferricyanide trihydrate (P-3289, Sigma-Aldrich), and 2 mM magnesium chloride (M-8266, Sigma-Aldrich) in PBS at pH 6.0. Acquisition and quantification of the

images for SA-βGal and cell area was done with an automated live cell imager (Lionheart FX, BioTek).

Comet assay. The assay was performed according to the manufacturer's instructions (STA-351, Cell Biolabs INC.). In short, cells were plated in 6 well plates for drug treatments, collected, counted, resuspended at 100,000 cells/mL and washed with PBS at 4 °C. Cells were mixed at 1:10 with low melting agarose at 37 °C, and poured on a glass microscope slide. After cell lysis, the slides were maintained at 4 °C in alkaline buffer (pH > 13) for 20 min. After electrophoresis, the slides were washed three times with a neutralizing buffer and stained with the Vista Green DNA Dye (#235003, Cell Biolabs). All manipulations were performed protected from direct light. Analysis was performed by capturing Z-stack images with a laser confocal microscopy and measurement of Olive tail moment with the CaspLab software.

RNA extraction and RT-qPCR. Total RNA extraction using the TRIzol™ Reagent (15596026, Invitrogen) and cDNA synthesis using the GoScript™ Reverse Transcription Mix, Random Primers (A2800, Promega) were done according to the manufacturer's instructions. Amplification was performed with SsoAdvanced™ Universal SYBR® Green Supermix (1725271, BioRad) with 43 cycles at 95 °C for 5 s, 60 °C for 30 s and 60 °C for 1 min (for the primers see Table 2). Relative RNA expression was calculated using the comparative Ct method and normalized to the geometric mean of the GAPDH and HPRT1 mRNAs.

Statistics and reproducibility. Statistical analysis was performed with the aid of GraphPad Prism version 8.4 using the method specified in the legend of each figure. Exact *p*-values are specified in the figures. All quantifications were performed based on at least three independent biological replicates, sample size, number of replicates and how they are defined is specified in the figure legends. When indicated, western blots and microscopic images are shown for representative data.

Reporting summary. Further information on research design is available in the Nature Research Reporting Summary linked to this article.

Data availability

The raw data for all the figures (Supplementary Data 1) and Supplementary Figures (Supplementary Material) are included as a Supplementary Data Files. All genomic sequencing data generated by the external provider (Microsynth AG, Balgach, Switzerland) for the CRISPR/Cas9 edited exon of *MAPT*, and all maps and sequences of the gene-editing plasmids and shRNA plasmids are included as supplementary material (Supplementary Data 2). All the data generated and/or analyzed, all plasmids and cell lines included in the current study are available from the corresponding authors on reasonable request.

Received: 18 November 2019; Accepted: 28 April 2020;
Published online: 19 May 2020

References

1. Hutton, M. et al. Association of missense and 5'-splice-site mutations in tau with the inherited dementia FTDP-17. *Nature* **393**, 702–705 (1998).
2. Spillantini, M. G. et al. Mutation in the tau gene in familial multiple system tauopathy with presenile dementia. *Proc. Natl Acad. Sci. USA* **95**, 7737–7741 (1998).
3. Jeganathan, S., von Bergen, M., Brutlach, H., Steinhoff, H. J. & Mandelkow, E. Global hairpin folding of tau in solution. *Biochemistry* **45**, 2283–2293 (2006).
4. Ludolph, A. C. et al. Tauopathies with parkinsonism: clinical spectrum, neuropathologic basis, biological markers, and treatment options. *Eur. J. Neurol.* **16**, 297–309 (2009).
5. Cross, D., Tapia, L., Garrido, J. & Maccioni, R. B. Tau-like proteins associated with centrosomes in cultured cells. *Exp. Cell Res.* **229**, 378–387 (1996).
6. Greenwood, J. A. & Johnson, G. V. Localization and in situ phosphorylation state of nuclear tau. *Exp. Cell Res.* **220**, 332–337 (1995).
7. Loomis, P. A., Howard, T. H., Castleberry, R. P. & Binder, L. I. Identification of nuclear tau isoforms in human neuroblastoma cells. *Proc. Natl Acad. Sci. USA* **87**, 8422–8426 (1990).
8. Thurston, V. C., Zinkowski, R. P. & Binder, L. I. Tau as a nucleolar protein in human nonneural cells in vitro and in vivo. *Chromosoma* **105**, 20–30 (1996).
9. Baquero, J. et al. Nuclear Tau, p53 and Pin1 regulate PARN-mediated deadenylation and gene expression. *Front. Mol. Neuroscie.* **12**, 242 (2019).
10. Sultan, A. et al. Nuclear tau, a key player in neuronal DNA protection. *J. Biol. Chem.* **286**, 4566–4575 (2011).
11. Violet, M. et al. A major role for Tau in neuronal DNA and RNA protection in vivo under physiological and hyperthermic conditions. *Front. Cell. Neurosci.* **8**, 84 (2014).
12. Ulrich, G. et al. Phosphorylation of nuclear Tau is modulated by distinct cellular pathways. *Sci. Rep.* **8**, 17702 (2018).
13. Iijima-Ando, K., Zhao, L., Gatt, A., Shenton, C. & Iijima, K. A DNA damage-activated checkpoint kinase phosphorylates tau and enhances tau-induced neurodegeneration. *Hum. Mol. Genet.* **19**, 1930–1938 (2010).
14. Rossi, G. et al. A new function of microtubule-associated protein tau: involvement in chromosome stability. *Cell Cycle* **7**, 1788–1794 (2008).
15. Lovell, M. A. & Markesbery, W. R. Oxidative DNA damage in mild cognitive impairment and late-stage Alzheimer's disease. *Nucleic Acids Res.* **35**, 7497–7504 (2007).
16. Mullaart, E., Boerrigter, M. E., Ravid, R., Swaab, D. F. & Vijg, J. Increased levels of DNA breaks in cerebral cortex of Alzheimer's disease patients. *Neurobiol. Aging* **11**, 169–173 (1990).
17. Reinhardt, H. C. & Schumacher, B. The p53 network: cellular and systemic DNA damage responses in aging and cancer. *Trends Genet.* **28**, 128–136 (2012).
18. Baldwin, E. L. & Osheroff, N. Etoposide, topoisomerase II and cancer. *Curr. Med. Chem. Anticancer Agents* **5**, 363–372 (2005).
19. Abbas, T. & Dutta, A. p21 in cancer: intricate networks and multiple activities. *Nat. Rev. Cancer* **9**, 400–414 (2009).
20. Hsu, C. H., Altschuler, S. J. & Wu, L. F. Patterns of early p21 dynamics determine proliferation-senescence cell fate after chemotherapy. *Cell* **178**, 361–373.e312 (2019).
21. Bradbury, J. M. & Jackson, S. P. ATM and A. T. R. *Curr. Biol.* **13**, R468 (2003).
22. Smith, J., Tho, L. M., Xu, N. & Gillespie, D. A. The ATM-Chk2 and ATR-Chk1 pathways in DNA damage signaling and cancer. *Adv. Cancer Res.* **108**, 73–112 (2010).
23. Offer, H. et al. The onset of p53-dependent DNA repair or apoptosis is determined by the level of accumulated damaged DNA. *Carcinogenesis* **23**, 1025–1032 (2002).
24. Roos, W. P. & Kaina, B. DNA damage-induced cell death by apoptosis. *Trends Mol. Med.* **12**, 440–450 (2006).
25. Bogen, D. et al. Aurora B kinase is a potent and selective target in MYCN-driven neuroblastoma. *Oncotarget* **6**, 35247–35262 (2015).
26. Van Maerken, T. et al. Functional analysis of the p53 pathway in neuroblastoma cells using the small-molecule MDM2 antagonist nutlin-3. *Mol. Cancer Therapeutics* **10**, 983–993 (2011).
27. Bouaoun, L. et al. TP53 variations in human cancers: new lessons from the IARC TP53 database and genomics data. *Hum. Mutat.* **37**, 865–876 (2016).
28. Andrysik, Z. et al. Identification of a core TP53 transcriptional program with highly distributed tumor suppressive activity. *Genome Res.* **27**, 1645–1657 (2017).
29. Fischer, M. Census and evaluation of p53 target genes. *Oncogene* **36**, 3943–3956 (2017).
30. Inuzuka, H., Fukushima, H., Shaik, S. & Wei, W. Novel insights into the molecular mechanisms governing Mdm2 ubiquitination and destruction. *Oncotarget* **1**, 685–690 (2010).
31. Pant, V. & Lozano, G. Limiting the power of p53 through the ubiquitin proteasome pathway. *Genes Dev.* **28**, 1739–1751 (2014).
32. Pochampally, R. et al. A 60 kd MDM2 isoform is produced by caspase cleavage in non-apoptotic tumor cells. *Oncogene* **17**, 2629–2636 (1998).
33. Pochampally, R., Fodera, B., Chen, L., Lu, W. & Chen, J. Activation of an MDM2-specific caspase by p53 in the absence of apoptosis. *J. Biol. Chem.* **274**, 15271–15277 (1999).
34. Vousden, K. H. & Prives, C. Blinded by the light: the growing complexity of p53. *Cell* **137**, 413–431 (2009).
35. Nag, S., Qin, J., Srivenugopal, K. S., Wang, M. & Zhang, R. The MDM2-p53 pathway revisited. *J. Biomed. Res.* **27**, 254–271 (2013).
36. Chi, H., Chang, H. Y. & Sang, T. K. Neuronal cell death mechanisms in major neurodegenerative diseases. *Int. J. Mol. Sci.* **19**, pii: E3082 (2018).
37. Li, H. L. et al. Phosphorylation of tau antagonizes apoptosis by stabilizing beta-catenin, a mechanism involved in Alzheimer's neurodegeneration. *Proc. Natl Acad. Sci. USA* **104**, 3591–3596 (2007).
38. Liu, X. A. et al. Tau dephosphorylation potentiates apoptosis by mechanisms involving a failed dephosphorylation/activation of Bcl-2. *J. Alzheimer's Dis.* **19**, 953–962 (2010).
39. Bou Samra, E. et al. A role for Tau protein in maintaining ribosomal DNA stability and cytidine deaminase-deficient cell survival. *Nat. Commun.* **8**, 693 (2017).
40. Baker, D. J. & Petersen, R. C. Cellular senescence in brain aging and neurodegenerative diseases: evidence and perspectives. *J. Clin. Investig.* **128**, 1208–1216 (2018).
41. Kritsilis, M. et al. Ageing, cellular senescence and neurodegenerative disease. *Int. J. Mol. Sci.* **19**, pii: E2937 (2018).

42. Bussian, T. J. et al. Clearance of senescent glial cells prevents tau-dependent pathology and cognitive decline. *Nature* **562**, 578–582 (2018).
43. Götz, J., Ittner, A. & Ittner, L. M. Tau-targeted treatment strategies in Alzheimer's disease. *Br. J. Pharm.* **165**, 1246–1259 (2012).
44. Sud, R., Geller, E. T. & Schellenberg, G. D. Antisense-mediated Exon skipping decreases Tau protein expression: a potential therapy for tauopathies. *Mol. Ther. Nucleic Acids* **3**, e180–e180 (2014).
45. Chen, S., Townsend, K., Goldberg, T. E., Davies, P. & Conejero-Goldberg, C. MAPT isoforms: differential transcriptional profiles related to 3R and 4R splice variants. *J. Alzheimer's Dis.* **22**, 1313–1329 (2010).
46. Smith, C. J., Anderton, B. H., Davis, D. R. & Gallo, J. M. Tau isoform expression and phosphorylation state during differentiation of cultured neuronal cells. *FEBS Lett.* **375**, 243–248 (1995).
47. Childs, B. G., Baker, D. J., Kirkland, J. L., Campisi, J. & van Deursen, J. M. Senescence and apoptosis: dueling or complementary cell fates? *EMBO Rep.* **15**, 1139–1153 (2014).
48. Bode, A. M. & Dong, Z. Post-translational modification of p53 in tumorigenesis. *Nat. Rev. Cancer* **4**, 793–805 (2004).
49. Kruse, J. P. & Gu, W. Modes of p53 regulation. *Cell* **137**, 609–622 (2009).
50. Webley, K. et al. Posttranslational modifications of p53 in replicative senescence overlapping but distinct from those induced by DNA damage. *Mol. Cell. Biol.* **20**, 2803–2808 (2000).
51. Feng, L., Hollstein, M. & Xu, Y. Ser46 phosphorylation regulates p53-dependent apoptosis and replicative senescence. *Cell Cycle* **5**, 2812–2819 (2006).
52. Reed, S. M. & Quelle, D. E. p53 acetylation: regulation and consequences. *Cancers* **7**, 30–69 (2014).
53. Chou, P. Y. et al. A p53/TIAF1/WWOX triad exerts cancer suppression but may cause brain protein aggregation due to p53/WWOX functional antagonism. *Cell Commun. Signal* **17**, 76 (2019).
54. Liu, C. C. et al. WWOX phosphorylation, signaling, and role in neurodegeneration. *Front Neurosci.* **12**, 563 (2018).
55. Huda, M. N. K., D. H.; Erdene-Ochir, E., Kim, Y. S. & Pan, C. H. Expression, phosphorylation, localization, and microtubule binding of tau in colorectal cell lines. *Appl. Biol. Chem.* **59**, 807–812 (2016).
56. Giannakakou, P. et al. Enhanced microtubule-dependent trafficking and p53 nuclear accumulation by suppression of microtubule dynamics. *Proc. Natl Acad. Sci. USA* **99**, 10855–10860 (2002).
57. Sablina, A. A., Chumakov, P. M., Levine, A. J. & Kopnin, B. P. p53 activation in response to microtubule disruption is mediated by integrin-Erk signaling. *Oncogene* **20**, 899–909 (2001).
58. Frost, B., Hemberg, M., Lewis, J. & Feany, M. B. Tau promotes neurodegeneration through global chromatin relaxation. *Nat. Neurosci.* **17**, 357–366 (2014).
59. Maina, M. B. et al. The involvement of tau in nucleolar transcription and the stress response. *Acta Neuropathologica Commun.* **6**, 70 (2018).
60. Siano, G. et al. Tau modulates VGluT1 expression. *J. Mol. Biol.* **431**, 873–884 (2019).
61. Buizza, L. et al. Conformational altered p53 as an early marker of oxidative stress in Alzheimer's disease. *PloS ONE* **7**, e29789 (2012).
62. Stanga, S., Lanni, C., Sinforiani, E., Mazzini, G. & Racchi, M. Searching for predictive blood biomarkers: misfolded p53 in mild cognitive impairment. *Curr. Alzheimer Res.* **9**, 1191–1197 (2012).
63. Tan, M., Wang, S., Song, J. & Jia, J. Combination of p53(ser15) and p21/p21 (thr145) in peripheral blood lymphocytes as potential Alzheimer's disease biomarkers. *Neurosci. Lett.* **516**, 226–231 (2012).
64. Dorszewska, J. et al. Mutations in the exon 7 of Trp53 gene and the level of p53 protein in double transgenic mouse model of Alzheimer's disease. *Folia Neuropathologica* **52**, 30–40 (2014).
65. Hooper, C. et al. p53 is upregulated in Alzheimer's disease and induces tau phosphorylation in HEK293a cells. *Neurosci. Lett.* **418**, 34–37 (2007).
66. Pehar, M., Ko, M. H., Li, M., Scrable, H. & Puglielli, L. P44, the 'longevity-assurance' isoform of P53, regulates tau phosphorylation and is activated in an age-dependent fashion. *Aging Cell* **13**, 449–456 (2014).
67. Cancino, G. I. et al. p63 regulates adult neural precursor and newly born neuron survival to control hippocampal-dependent behavior. *J. Neurosci.* **33**, 12569–12585 (2013).
68. Bonda, D. J. et al. Pathological implications of cell cycle re-entry in Alzheimer disease. *Expert Rev. Mol. Med.* **12**, e19 (2010).
69. Currais, A., Hortobagyi, T. & Soriano, S. The neuronal cell cycle as a mechanism of pathogenesis in Alzheimer's disease. *Aging* **1**, 363–371 (2009).
70. Fielder, E., von Zglinicki, T. & Jurk, D. The DNA damage response in neurons: die by apoptosis or survive in a senescence-like state? *J. Alzheimer's Dis.* **60**, S107–s131 (2017).
71. Souter, S. & Lee, G. Microtubule-associated protein tau in human prostate cancer cells: isoforms, phosphorylation, and interactions. *J. Cell. Biochem.* **108**, 555–564 (2009).
72. Rossi, G. et al. Tau mutations as a novel risk factor for cancer-response. *Cancer Res.* **78**, 6525 (2018).
73. Kit, O. I. et al. A proteomics analysis reveals 9 up-regulated proteins associated with altered cell signaling in colon cancer patients. *Protein J.* **36**, 513–522 (2017).
74. Zaman, S., Chobrutskiy, B. I. & Blanck, G. MAPT (Tau) expression is a biomarker for an increased rate of survival in pediatric neuroblastoma. *Cell Cycle* **17**, 2474–2483 (2018).
75. Zaman, S., Chobrutskiy, B. I., Sikaria, D. & Blanck, G. MAPT (Tau) expression is a biomarker for an increased rate of survival for lowgrade glioma. *Oncol. Rep.* **41**, 1359–1366 (2019).
76. Gargini, R., Segura-Collar, B. & Sanchez-Gomez, P. Novel Functions of the Neurodegenerative-Related Gene Tau in Cancer. *Front. Aging Neurosci.* **11**, 231 (2019).
77. Gargini, R. et al. The IDH-TAU-EGFR triad defines the neovascular landscape of diffuse gliomas. *Sci. Transl. Med.* **12**, pii: eaax1501 (2020).
78. de Strooper, B. Cancer and neurodegeneration meet. *EMBO Mol. Med.* **2**, 245–246 (2010).
79. Driver, J. A. Inverse association between cancer and neurodegenerative disease: review of the epidemiologic and biological evidence. *Biogerontology* **15**, 547–557 (2014).
80. Klus, P., Cirillo, D., Botta Orfila, T. & Gaetano Tartaglia, G. Neurodegeneration and cancer: where the disorder prevails. *Sci. Rep.* **5**, 15390 (2015).
81. Pan, T., Li, X. & Jankovic, J. The association between Parkinson's disease and melanoma. *Int. J. Cancer* **128**, 2251–2260 (2011).
82. Walter, U. et al. Frequency and profile of Parkinson's disease prodromi in patients with malignant melanoma. *J. Neurol. Neurosurg. Psychiatry* **87**, 302–310 (2016).
83. Frain, L. et al. Association of cancer and Alzheimer's disease risk in a national cohort of veterans. *Alzheimer's Dement.* **13**, 1364–1370 (2017).
84. Houck, A. L., Seddighi, S. & Driver, J. A. At the crossroads between neurodegeneration and cancer: a review of overlapping biology and its implications. *Curr. Aging Sci.* **11**, 77–89 (2018).
85. Foglieni, C. et al. Split GFP technologies to structurally characterize and quantify functional biomolecular interactions of FTD-related proteins. *Sci. Rep.* **7**, 14013 (2017).
86. Sanjana, N. E., Shalem, O. & Zhang, F. Improved vectors and genome-wide libraries for CRISPR screening. *Nat. Methods* **11**, 783–784 (2014).

Acknowledgements

We thank the whole laboratory for support and advice during this study. We express our gratitude and thanks to the generous funding from the Synapsis Foundation, the Gelu Foundation, the AILA/OIC Foundation, the Mecri Foundation and the Swiss National Science Foundation, grant #166612. We thank our hosting institutions Neurocenter of Southern Switzerland and Ente Ospedaliero Cantonale for financial support.

Author contributions

M.S. and C.M. designed, performed, analyzed and described most of the experiments; G.P. designed the strategy and established the knock-out cell lines; S.Pi. helped in implementing several analytical procedures; A.S. helped in creating, isolating and characterizing cell lines; S.Pa. supervised the whole study and wrote the first draft, P.P. finalized the paper; all authors revised the paper; S.Pa. and P.P. conceived and designed the study and provided the financial support for this study.

Competing interests

The authors declare no competing financial and non-financial interests. P.P. and S.Pa. owns stocks of AC Immune SA. No funding organizations was involved in the conceptualization, design, data collection, analysis, decision to publish, preparation of the paper, or may gain or lose financially through this publication. There are no patents, products in development, or marketed products to declare.

Additional information

Supplementary information is available for this paper at https://doi.org/10.1038/s42003-020-0975-4.

Correspondence and requests for materials should be addressed to P.P.

Reprints and permission information is available at http://www.nature.com/reprints

Publisher's note Springer Nature remains neutral with regard to jurisdictional claims in published maps and institutional affiliations.

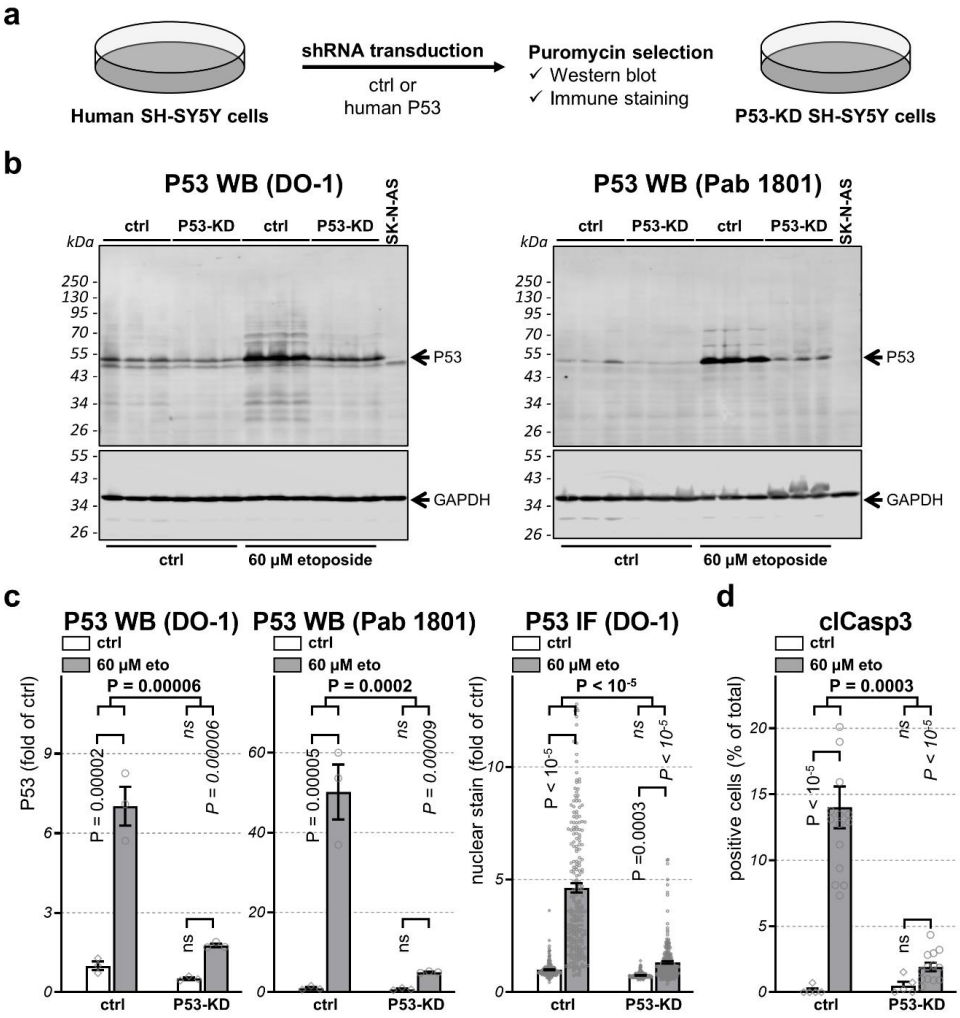

Supplementary Figure 1. DSBs-induced apoptosis is P53-dependent in SH-SY5Y cells. a. Scheme of procedure used to generate P53-KD cells and for their characterization by western blot and P53 immune staining when compared to cells transduced with the parental shRNA plasmid (ctrl). **b.** Cells at basal conditions (ctrl) or treated 30 min with 60 µM etoposide and recovered for 6 h before western blot analysis with the indicated P53 antibodies. GAPDH served as loading control. **c.** Western blot quantification of P53 signal intensity normalized for GAPDH shown as fold of control cells at basal conditions, mean +/- SD of n = 3 biological replicates. On the left is show the quantification of P53 immune staining as fold of control cells at basal conditions, mean

intensity +/- sem of single cell nuclear P53 staining (DAPI mask, ImageJ), n >219 cells/condition distributed over 5 images. **d**. Quantification of clCasp3 immune staining shown as percent of total DAPI-positive cells, mean ± SD of 5 images for the untreated cells (ctrl) and of 15 images for etoposide-treated cells (60 µM eto), n >500 cells/condition. Statistical analysis by independent measures ordinary 2way ANOVA, source of variation for cell lines (in bold), multiple Bonferroni pairwise comparisons among lines for each treatment (in italics), or among treatment for each line (in vertical).

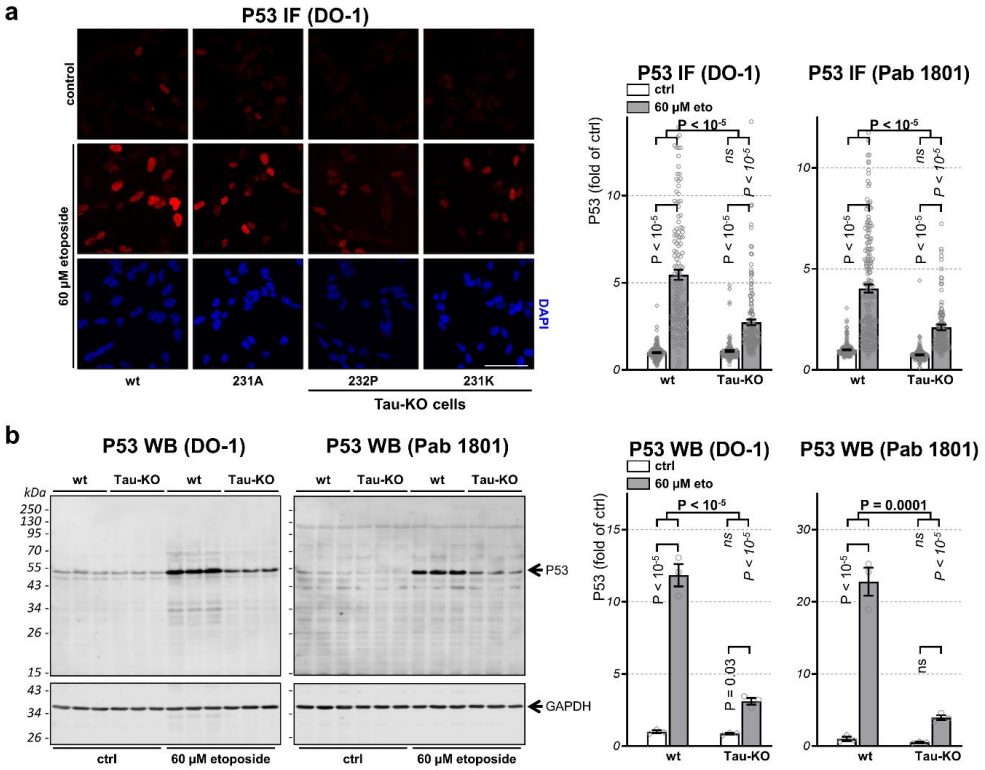

Supplementary Figure 2. Tau deficiency reduces cellular P53. a. Representative laser confocal microscopy images of P53 DO-1 antibody-immune stained parental cells (wt) and the indicated CRISPR-Cas9 cell lines at basal conditions (control) or treated for 30 min with 60 µM etoposide and recovered for 6 h. Shown are also the nuclear staining with DAPI. Scale bar 50 µm. Quantification of mean intensity +/- sem of single cell nuclear P53 staining (DAPI mask, ImageJ) shown as fold of wt cells at basal conditions using the indicated P53 antibodies, n >90 cells/condition distributed over 5 images. **b.** Parental (wt)

or 232P (Tau-KO) cells at basal conditions (ctrl) or treated for 30 min with 60 μM etoposide followed by 6 h recovery were analyzed for P53 by western blot with the indicated P53 antibodies, n = 3 biological replicates. GAPDH served as loading control. Quantification of P53 signal intensity normalized for GAPDH, mean +/- SD shown as fold of control (wt or ctrl cells at basal conditions). Statistical analysis by independent measures ordinary 2way ANOVA, source of variation for cell lines (in bold), multiple Bonferroni pairwise comparisons for each treatment among lines (in italics), or among treatment for each line (in vertical).

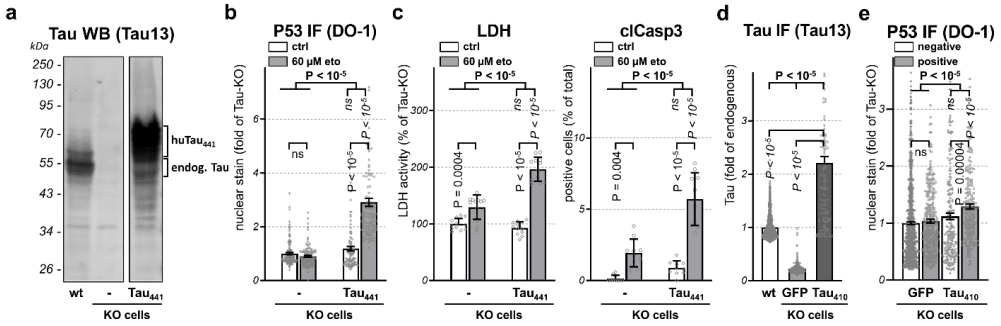

Supplementary Figure 3. Restoring Tau expression in Tau-KO cells rescues P53 and the apoptotic phenotype. a. Parental (wt), 232P (KO cells) or 232P cells stably re-expressing 4R-Tau (Tau_{441}) analyzed by western blot with the Tau13 antibody. **b.** Quantification of single cell nuclear P53 immune staining (DAPI mask, Image J) of 232P Tau-KO cells or 232P-Tau_{441} cells at basal conditions (ctrl) or treated 30 min with 60 μM etoposide and allowed to recover 6 h (60 μM eto), mean ± sem of n >100 cells/condition distributed over 5 images shown as fold of 232P cells at basal conditions. **c.** LDH release from the same cells treated as in **b.** (2 d recovery). Values are shown as percentage of Tau-KO cells at basal conditions, mean ± SD of 12 wells from three independent experiments. Cells were also analyzed by immune staining for clCasp3 at 6 h recovery. Percent clCasp3-positive cells, mean ± SD of 10 images, n >500 cells/condition. **d.** Quantification of Tau13 immune stained Tau in parental cells (endogenous Tau, wt), or in GFP-positive 232P cells (KO cells) transiently transfected with a 1:10 ratio of empty:GFP plasmids (GFP) or of 3R-Tau:GFP plasmids (Tau_{410}). Cells were stained 3 days after transfection (GFP mask, Image J). **e.** Immune staining quantification of nuclear P53 (DAPI mask, Image J) in GFP-positive 232 cells (KO cells) transiently transfected as in **d.** and treated for 30 min with 60 μM etoposide and recovered for 6 h, mean intensity ± sem

shown as fold of control-transfected 232P cells, n >100 cells/condition distributed over 5 images. Statistical analysis by independent measures ordinary 2way ANOVA, source of variation between non-transfected and Tau-transfected conditions (in bold), multiple Bonferroni pairwise comparisons among lines for each treatment (in italics), among treatment for each line (**b** and **c**, in vertical).

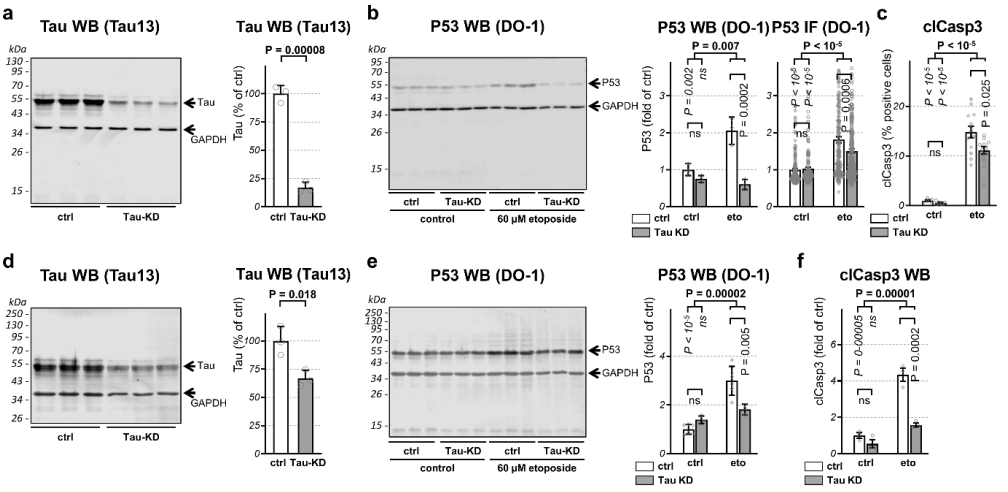

Supplementary Figure 4. Reduced etoposide-induced P53 protein in Tau-KD IMR5 and IMR32 cells. a. Cell lysates obtained from IMR5 cells transduced with the parental shRNA plasmid (ctrl) or with the Tau shRNA plasmid 2112 (Tau-KD) were analyzed by western blot for Tau expression. The Tau signal was normalized for GAPDH and reported as percent of the control, mean +/- SD, n = 3 biological replicates. Unpaired student t-test. **b.** The two IMR5 cell lines at basal conditions or treated 30 min with 15 μM etoposide and recovered for 6 h were analyzed by western blot with the P53 DO-1 antibody. The Tau signal was normalized for GAPDH and reported as fold of the control, mean +/- SD, n = 3 biological replicates. Same conditions were applied to quantify immune stained P53, mean intensity +/- sem of single cell nuclear P53 staining (DAPI mask, ImageJ) shown as fold of untreated control cells (ctrl), n >100 cells/condition distributed over 5 images. **c**. Apoptotic cells were determined by clCasp3 immune staining and reported as percent clCasp3-positive cells of total DAPI-positive cells, mean ± SD of 5 images for the untreated cells (ctrl) and of 15 images for etoposide-treated cells (15 μM eto), n >500 cells/condition. **d**. Same as in **a.** for IMR32 cells transduced with the parental shRNA plasmid (ctrl) or with Tau shRNA plasmid 3127 (Tau-KD). **e.** Same as in **b.** for the western blot analysis. **f**.

Same as in **c.** for 15 and 17 kDa clCasp3 fragments determined by western blot, mean +/- SD (n = 3 biological triplicates). Statistical analysis by independent measures ordinary 2way ANOVA, source of variation for cell lines (in bold), multiple Bonferroni pairwise comparisons for treatment between lines (in italics) or for each line (in vertical).

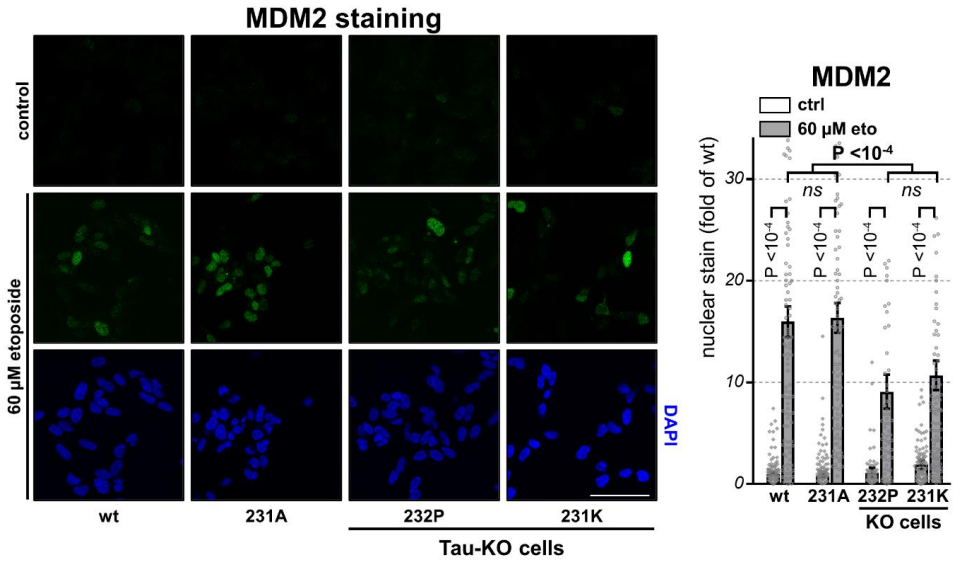

Supplementary Figure 5. Tau deficiency affects MDM2. a. Representative images by laser confocal microscopy of parental (wt) or CRISPR-Cas9 cell lines immune stained with the rabbit MDM2 antibody and counter-stained with DAPI. Cells at basal conditions (control) or after 30 min 60 µM etoposide and 6 h recovery, scale bar 50 µm. Mean intensity +/- sem of single cell nuclear MDM2 staining (DAPI mask, ImageJ) shown as fold of wt cells at basal conditions, n >90 cells/condition distributed over 5 images. Statistical analysis by independent measures ordinary 2way ANOVA, source of variation for genotype (in bold), multiple Bonferroni pairwise comparisons for etoposide treatment between lines with same genotype (in italics) or for the etoposide treatment for each line (in vertical).

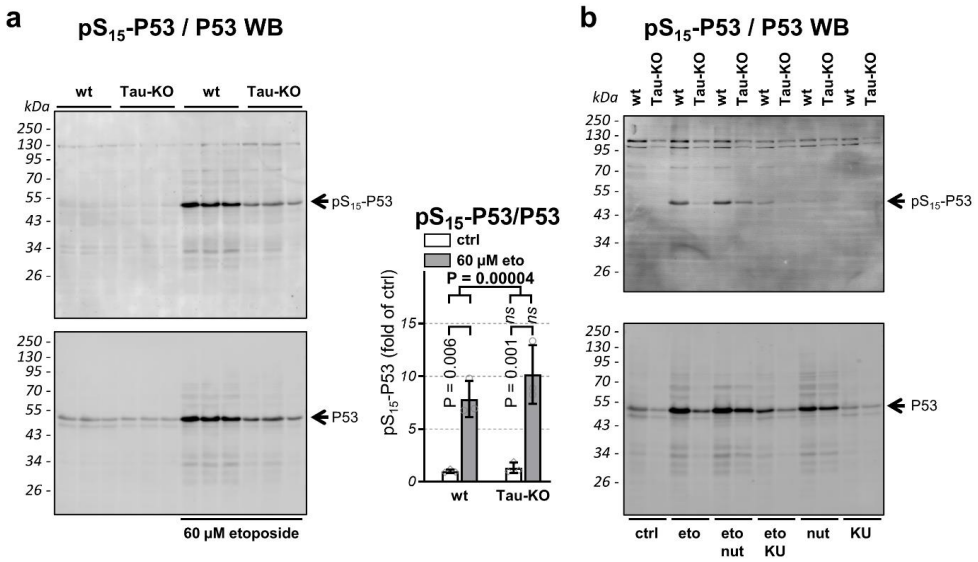

Supplementary Figure 6. Analysis of pS15-P53 phosphorylation. a. Parental (wt) or 232P (Tau-KO) cells at basal conditions or after 30 min 60 µM etoposide and 6 h recovery were analyzed for pS15-P53 or P53 by western blot, n = 3 biological triplicates. Quantification was performed by measuring the signal intensity of pS15-P53 normalized for the signal of total P53, mean +/- SD shown as percent of control (parental cells at basal conditions). Statistical analysis by independent measures ordinary 2way ANOVA, source of variation for cell lines (in bold), multiple Bonferroni pairwise comparisons among lines for each treatment (in italics), or of treatment for each line (in vertical). **b.** Parental (wt) or 232P (Tau-KO) cells at basal conditions (ctrl) or analyzed after 6 h recovery from a 30 min treatment in the absence or presence of 60 µM etoposide in the absence (eto), the recovery was performed in the absence or presence of 5 µg/mL nutlin-3 (eto nut) or 10 µg/mL KU-55933 (eto KU) as indicated. Analysis by western blot for pS15-P53 or P53, a representative experiment out of three experiments is shown.

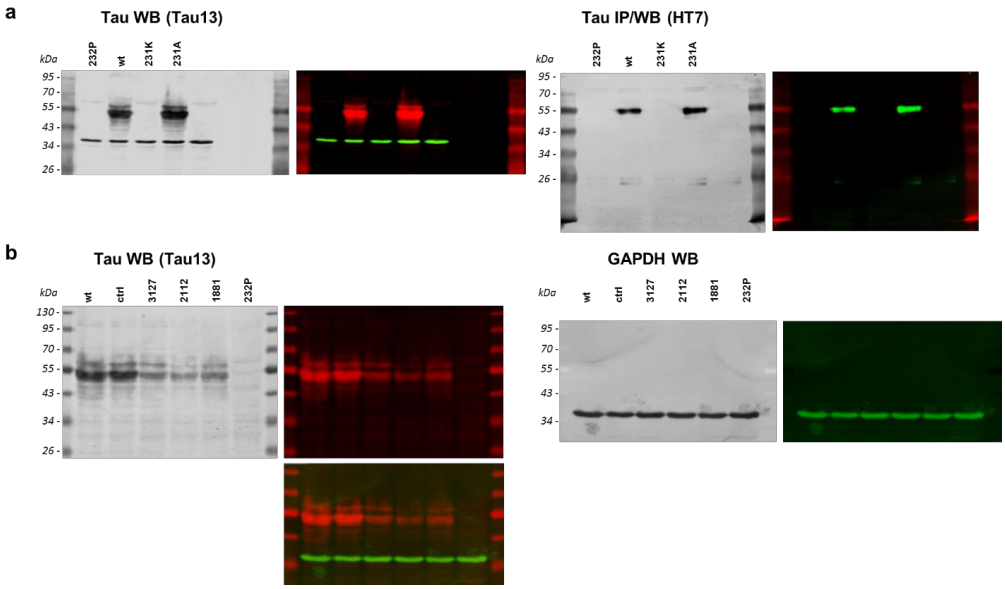

Supplementary Figure 7. Unprocessed western blot images (in grey tones) used for creating the corresponding panels in Fig.1a and 1b. Shown are also the original dual fluorescence images.

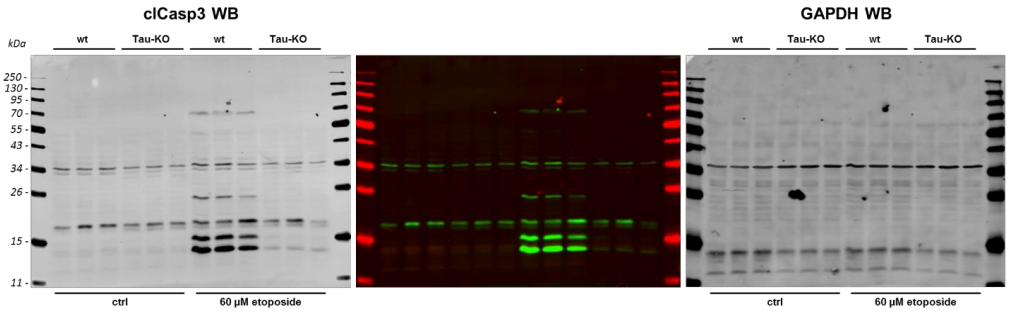

Supplementary Figure 8. Unprocessed western blot images (in grey tones) used for creating the corresponding panels in Fig.2. Shown are also the original dual fluorescence image.

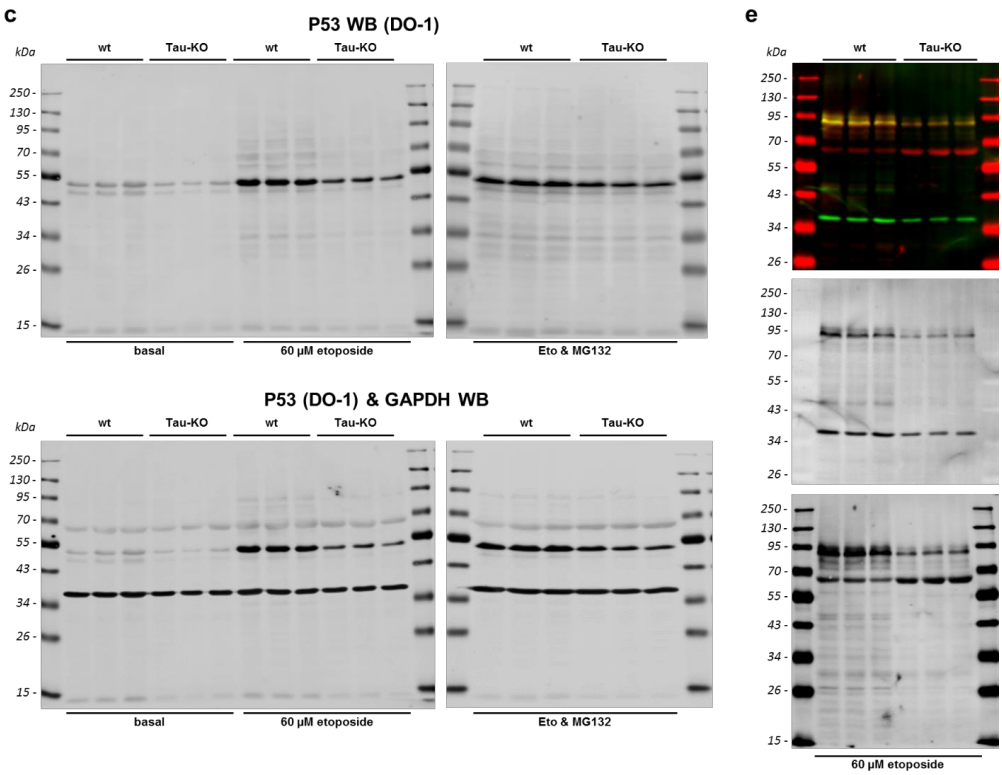

Supplementary Figure 9. Unprocessed western blot images used for creating the corresponding panels in Fig.7c and 7e.

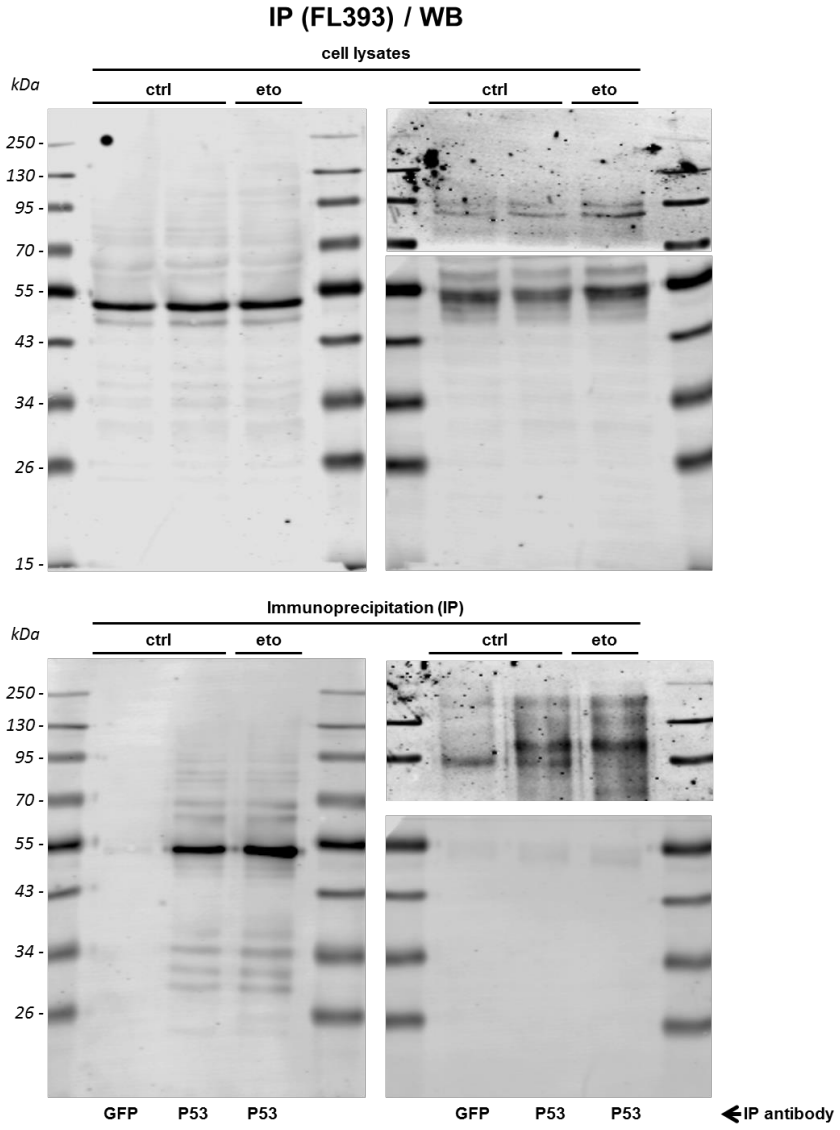

Supplementary Figure 10. Unprocessed western blot images used for creating the corresponding panels in Fig.8. The MDM2 and Tau blots shown on the left were cut between the 55 kDa and the 95 kDa protein size markers and analyzed separately.

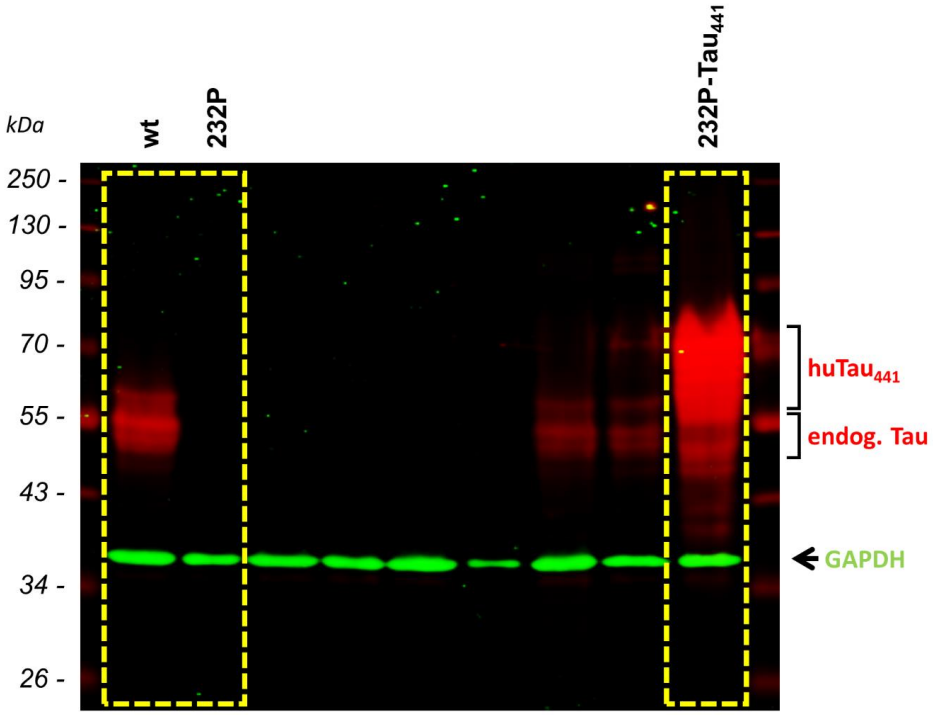

Supplementary Figure 11. Unprocessed gel image used for creating Supplementary Fig.3a.

Chapter 4

Tau Protein Modulates Epigenetic Mediated induction of Cellular Senescence

1. Introduction

1.1 Epigenetic machinery

Cell identity and cell fate are regulated by the epigenetic machinery during the development. Moreover, epigenetic is also important in different diseases such as neurodegenerative disorders and cancers[225,226]. The Polycomb Group (PcG) components are the most evolutionarily conserved proteins present both in animals and plants[227]. They were discovered seventy years ago in drosophila[228,229]. Specifically, PcG proteins are orchestrating the expression of genes, which are critical for developmental processes and cell differentiation[230]. PcG regulation is strongly conserved during evolution[231], whereas the mechanism of targeting chromatin is markedly different among species. In drosophila, the PcG complexes are targeted to chromatin through the Polycomb response elements (PREs), whereas in mammals, the PcG complexes are targeted by the hypomethylated CpG islands (CGIs)[231,232]. Recent studies demonstrated that PcG complexes regulate the expression of target genes through the modification of local chromatin structure and with the coordination of higher order chromatin[233].

1.2 Classification of Polycomb Repressive Complexes (PRC)

Polycomb proteins constitute two large multimeric complexes, which are the polycomb repressive complex 1 (PRC1) and 2 (PRC2)[234], which have distinct catalytic activities[235].
PRC1 presents an E3 ubiquitin ligase activity and its main function is to catalyze histone H2A lysine 119 mono-ubiquitination (H2AK119ub)[236,237]. The core of PRC1 comprises RING1B or its paralogue RING1A and one of six Polycomb group ring finger (PCGF) proteins[238]. PRC1 complex comprises eight different variant forms, which are categorized by the different interactors with the E3 ligase RING1A/B[239] and distinguish canonical PRC1 (cPRC1) and non-canonical PRC1 (ncPRC1)[240] **(Figure 5)**.
The main difference between cPRC1 and ncPRC1 is based on their function and the dependency on PRC2 methylase activity. Thus, the binding of the CBX protein of the cPRC1

to H3K27me3 is required to promote the chromatin occupancy of other cPRC1 variants. Although the functions of CBX proteins remain unclear, studies demonstrated that these CBX proteins have different functions possibly mediated by tissue-specific expression or abundance.[241] The chromatin occupancy of ncPRC1 variants is independent of PRC2 activity[242].

The ncPRC1 is composed by the RYBP or YAF2 subunits, which have an amino-terminal zinc finger domain that stimulates the E3 ubiquitin ligase activity of RING1A/B[243]. The ability of ncPRC1 to bind chromatin was demonstrated to be independent from PRC2 proteins or activity. Indeed, in PRC2-deficient mouse embryonic stem cells (mESCs) RYBP was retained on chromatin whereas RING1B and cPRC1 were depleted from chromatin[244]. Moreover, cPRC1 presents less ubiquitin ligase activity compared to ncPRC1 **(Figure 5)**.

The PRC2 has a unique molecular structure and it regulates the expression of more than 2000 genes distributed over 10 different chromosomes[245,246].

PRC2 is composed by a tetrameric core subunit, which comprises embryonic ectoderm development (EED) protein, suppressor of zeste 12 (SUZ12), enhancer of zeste homolog 2 or 1 (EZH2/1) and RBBP4 or RBBP7[247–249] **(Figure 5)**. Importantly, the activity of the complex is subordinated by the integrity and the presence of all the core components. Furthermore, PRC2 structure is based on two distinct lobes called the catalytic lobe and the regulatory lobe, which are responsible respectively for the methylation process and the stabilization and allosteric stimulation of PRC2[250]. These lobes are connected by SUZ12[251,252]. In addition, EZH2 presents a catalytic region composed of the SET and the SAL domains[253] and in particular SET is the most conserved region of EZH2[254]. Moreover, the activity of EZH2 is strictly related to SUZ12 and EED because they are important for the H3K27 methylation driven by EZH2.

It was demonstrated that mice lacking these PRC2 core proteins presented morphological defects and premature death because of the transcription of damaging proteins. These experiments demonstrated the relevance of the PRC2 complex in cell development and differentiation[255–257].

Moreover, other accessory proteins: Jumonji and AT-rich interaction domain 2 (JARID2), adipocyte enhancer-binding protein 2 (AEBP2), and Polycomb-like proteins (PCL1, PCL2, PCL3) are conserved during evolution. These proteins are essential for the modulation of the recruitment and the activity on chromatin of the core of PRC2[258–260] **(Figure 5)**.

The activity of PRC2 is based on mono, di or tri methylation of histone H3 at Lys27 (H3K27me1, H3K27me2 and H3K27me3).

The key function of PRC2 is to catalyze the methylation of H3 at the level of lysine 27, which leads to increased chromatin compaction[261,262]. As consequence, the increased chromatin compaction blocks the access of the transcriptional factors to the transcription start site of different genes. The silencing of specific genes plays an important role in epigenetics and PRC2 works to maintain the correct epigenetic regulation. In particular, each component of the PRC2 complex has a specific function that in general leads to the ultimate gene suppression.

Understanding the molecular function of the PcG complex is mandatory to understand its recruitment process. The first model proposed was based on the idea that the two complexes PRC1 and PRC2 are depending on each other for the recruitment. The idea is that the H3K27me3 mark is recognized by PRC1 and the H2AK119ub1 mark is recognized by PRC2[263]. It was demonstrated that the polycomb response elements (PREs) contribute for the recruitment of PcG complexes providing stability[264].

PRC2 complex is relatively stable and it is able to maintain its enzymatic activity. However, the proteins of the core complex are unstable individually[265,266].

The interactions of the three core components of PRC2 influence the binding of the complex with CG island and lead to the stability of the complex[267]. Therefore, the SET domain of EZH2/1 is not active when isolated from the complex demonstrating that these protein-protein interactions are essential for the stabilization and the activity of the complex. Moreover, the interaction of the PRC2 complex with the accessory proteins are essential for maintaining the stability of the complex. In particular, RBBP4/7 facilitates the maintenance of PRC2 position creating bonds between chromatin and the complex. Meanwhile, AEBP2 enhances the stabilization of the complex forming bonds between its DNA-binding motif and the nearby structures[268].

Providing optimal complex stabilization allows PRC2 to effectively complete trimethylation and thus spread its repressive marks along the genome.

Another important interactor of PRC2 is JARID2, which is involved in brain development and it is responsible for some human cerebral disabilities[269]. JARID2 does not have the potential to bind DNA it acts as an inhibitor or activator of the PRC2 complex. Therefore, JARID2 is also acting on the recruitment of PRC2[267,270].

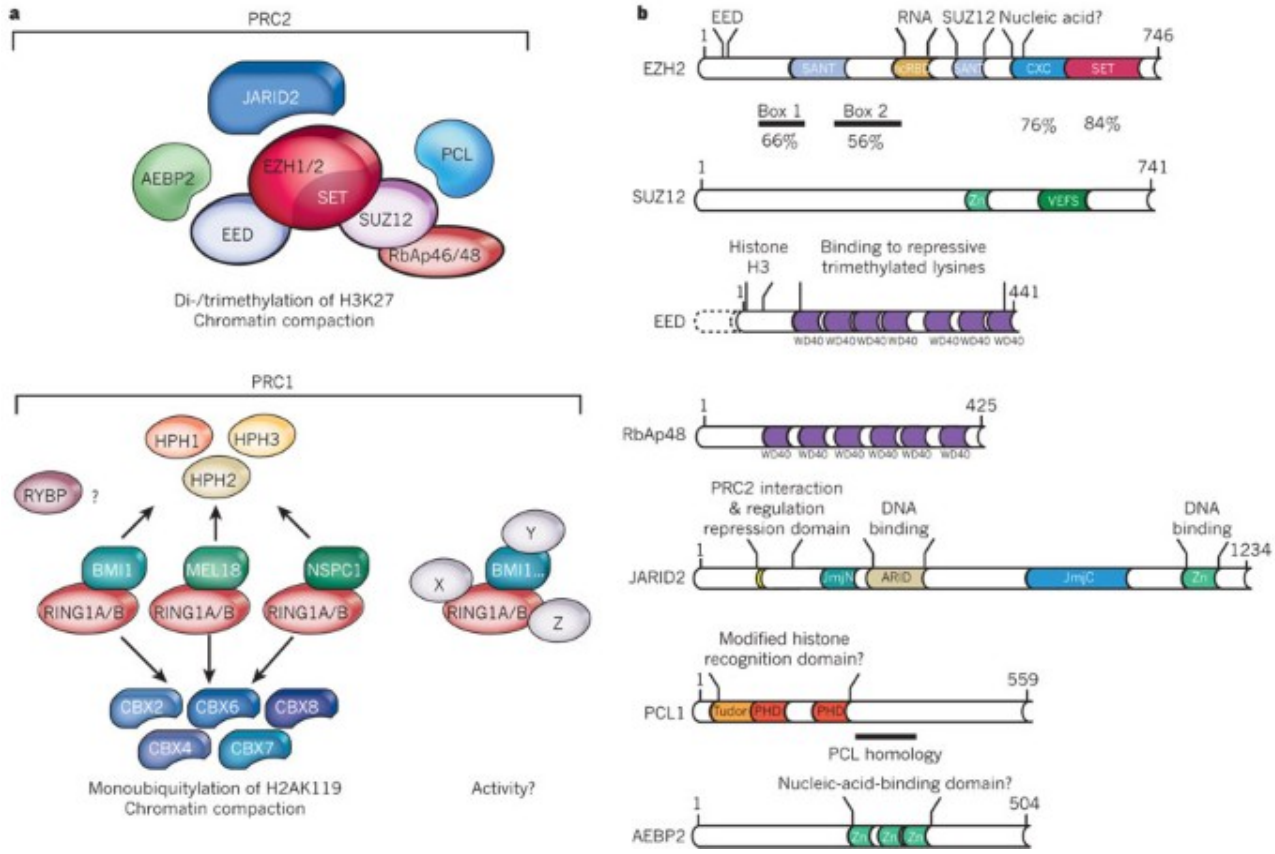

Figure 5. Detailed scheme representing the composition of PRC2 and PRC1 [271]

1.3 PRC2 and its disease-associated functions

1.3.1 PRC2 and cancer

It is known that the upregulation of PRC2 components is related to the development and the progression of different types of cancers such as lymphoma, melanoma, prostate and breast cancer.

Specifically, different studies demonstrated that EZH2 has cancerogenic effect and it is recognized as a marker of some aggressive stages of prostate and breast cancer[272,273]. In general, the PRC2 complex controls the methylation state of different tumor suppressor genes promoting the transformation from normal cells to malignant cancer cells[273] , and it is correlated with poor prognosis. The oncogenic role of EZH2 is also supported by recent findings showing that the heterozygous point mutations at tyrosine 641 (Y641) is present in germinal center B-cell (GCB) diffuse large cell B-cell lymphomas (DLBCL) and follicular lymphomas (FL). This mutation confers a gain-of-function of EZH2 leading to a massive conversion of H3K27 to H3K27me3 form[274].

For this reason, different EZH2 inhibitors are in pre-clinical studies or clinical trials as possible chemotherapeutic drugs[275–277]. The expression of PRC2 components is controlled by the pRB-E2F pathway, which is essential for cell proliferation[278] and it is highly dysregulated in cancer[279]. Moreover, the deregulation of miRNAs that control the EZH2 expression could be the rationale behind the role of EZH2 in cancer.

On the other hand, it has been reported that the loss-of-function mutations of PRC2 could confer a tumor-suppressive activity in different types of tumours[280,281]. For example, in malignant peripheral nerve sheath tumors (MPNSTs) PRC2 core components genes have a high frequency of deletion and the exogenous expression of the deleted PRC2 subunit leads to a tumor-suppressive function.

1.3.2 PRC2 and neurodegeneration

Following the initial neuron development and neuronal specification, the transcription programs have to be preserved during adulthood in order to maintain precise molecular functions. The main regulator of this process is the PRC2 complex, which represses detrimental transcriptional programs[282] in adult neurons and prevents the expression of non-neural genes in neurons[283].

Aging slows down the methylation processes and compromises the regulation of gene transcription[284]. This would explain why PRC2 complex is crucial not only during embryonic development but also in preserving the neuronal process constantly. Recently, the alteration of PRC2 activity and H3K27me3 levels have been associated with several human neurodegenerative diseases[285]. Different studies shown that PRC2 expression is reduced and it is not able to properly regulate genes, which are important for the progression of late-onset Alzheimer's disease (LOAD)[286]. Specifically, PRC2 is also acting in downregulating the expression of genes associated with AD through its methylation activity[287].

2. Results

frontiers

Tau Protein Modulates an Epigenetic Mechanism of Cellular Senescence

Claudia MAGRIN[1, 2], Martina Sola[1], Ester Piovesana[1, 2], Marco Bolis[3], Andrea Rinaldi[3], Stéphanie Papin[1], Paolo Paganetti[1, 2*]

[1]Ente Ospedaliero Cantonale (EOC), Switzerland, [2]University of Italian Switzerland, Switzerland, [3]Institute of Oncology Research (IOR), Switzerland

Submitted to Journal:
Frontiers in Cell and Developmental Biology

Specialty Section:
Molecular and Cellular Pathology

Article type:
Original Research Article

Manuscript ID:
1232963

Received on:
01 Jun 2023

Journal website link:
www.frontiersin.org

Conflict of interest statement

The authors declare that the research was conducted in the absence of any commercial or financial relationships that could be construed as a potential conflict of interest

Author contribution statement

Conceptualization: SP, PP
Methods and investigations: CM, MS, EP. MB, AR
Supervision: SP, PP
Writing (original draft): SP
Writing (review & editing): all co-authors

Keywords

tau, PRC2, transcription, IGFBP3, senescence, Aging, Disease

Abstract

Word count: 199

Progressive Tau deposition in neurofibrillary tangles and neuropil threads is the hallmark of tauopathies, a disorder group that includes Alzheimer's disease. Since Tau is a microtubule-associated protein, a prevalent concept to explain the pathogenesis of tauopathies is that abnormal Tau modification contributes to dissociation from microtubules, assembly into multimeric ß-sheets, proteotoxicity, neuronal dysfunction and cell loss. Tau also localizes in the cell nucleus and evidence supports an emerging function of Tau in DNA stability and epigenetic modulation. To better characterize the possible role of Tau in regulation of chromatin compaction and subsequent gene expression, we performed a bioinformatics analysis of transcriptome data obtained from Tau-depleted human neuroblastoma cells. Among the transcripts deregulated in a Tau-dependent manner, we found an enrichment of target genes for the polycomb repressive complex 2. We further describe decreased cellular amounts of the core components of the polycomb repressive complex 2 complex and a lower histone 3 trimethylation activity in Tau deficient cells. Among the de-repressed polycomb repressive complex 2 target gene products, IGFBP3 protein was found to be linked to increased senescence induction in Tau-deficient cells. Our findings propose a mechanism for Tau-dependent epigenetic modulation of cell senescence, a key event in pathologic aging.

Contribution to the field

We report an original study performed in our laboratory searching for a molecular mechanism that may explain the role of Tau protein in the induction of senescence (Sola et al. Commun Biol. 2020; 3: 245. doi: 10.1038/s42003-020-0975-4). Our data, based on an initial RNAseq analysis, point to the involvement of an epigenetic mechanism governed by PRC2 where IGFBP3 appears the critical inducer of senescence in our neuroblastoma cell model. Our data are supported by thorough validation with orthogonal assays. In view of the involvement of Tau in aging-associated processes such as neurodegeneration and cancer (Papin and Paganetti, Brain Sci. 2020; 10: 862. doi: 10.3390/brainsci10110862), we believe our work may open new avenues to better understand the relevance of Tau-dependent epigenetic modulation of cell senescence in pathologic aging.

Ethics statements

Studies involving animal subjects
Generated Statement: No animal studies are presented in this manuscript.

Studies involving human subjects
Generated Statement: No human studies are presented in this manuscript.

Inclusion of identifiable human data
Generated Statement: No potentially identifiable human images or data is presented in this study.

Data availability statement

Generated Statement: The datasets presented in this study can be found in online repositories. The names of the repository/repositories and accession number(s) can be found below:
https://www.ebi.ac.uk/metagenomics/, E-MTAB-8166 .

Tau Protein Modulates an Epigenetic Mechanism of Cellular Senescence

Claudia Magrin[1,2], Martina Sola[1,2], Ester Piovesana[1,2], Marco Bolis[3], Andrea Rinaldi[4], Stéphanie Papin[1,†], Paolo Paganetti[1, 2,†,*]

[1]Laboratory for Aging Disorders, Laboratories for Translational Research, Ente Cantonale Ospedaliero, Bellinzona, Switzerland.

[2]PhD Program in Neurosciences, Faculty of Biomedical Sciences, Università della Svizzera Italiana, Lugano, Switzerland.

[3]Functional Cancer Genomics Laboratory, Institute of Oncology Research, Bellinzona, Switzerland. Bioinformatics Core Unit, Swiss Institute of Bioinformatics, Bellinzona, Switzerland. Università della Svizzera Italiana, Lugano, Switzerland. Laboratory of Molecular Biology, Istituto di Ricerche Farmacologiche Mario Negri IRCCS, Milano, Italy.

[4]Lymphoma and Genomics Research Program, Institute of Oncology Research, Bellinzona, Switzerland

[†]These authors share last authorship

*** Correspondence:**

Prof. Paolo Paganetti, Laboratory for Aging Disorders, LRT EOC, Via Chiesa 5, 6500 Bellinzona, Switzerland. Phone +4158 666 7103.
paolo.paganetti@eoc.ch

Keywords: Tau, PRC2, transcription, IGFBP3, senescence, aging, disease

Abstract

Progressive Tau deposition in neurofibrillary tangles and neuropil threads is the hallmark of tauopathies, a disorder group that includes Alzheimer's disease. Since Tau is a microtubule-associated protein, a prevalent concept to explain the pathogenesis of tauopathies is that abnormal Tau modification contributes to dissociation from microtubules, assembly into multimeric β-sheets, proteotoxicity, neuronal dysfunction and cell loss. Tau also localizes in the cell nucleus and evidence supports an emerging function of Tau in DNA stability and epigenetic modulation. To better characterize the possible role of Tau in regulation of chromatin compaction and subsequent gene expression, we performed a bioinformatics analysis of transcriptome data obtained from Tau-depleted human neuroblastoma cells. Among the transcripts deregulated in a Tau-dependent manner, we found an enrichment of target genes for the polycomb repressive complex 2. We further describe decreased cellular amounts of the core components of the polycomb repressive complex 2 complex and a lower histone 3 trimethylation activity in Tau deficient cells. Among the de-repressed polycomb repressive complex 2 target gene products, IGFBP3 protein was found to be linked to increased senescence induction in Tau-deficient cells. Our findings propose a mechanism for Tau-dependent epigenetic modulation of cell senescence, a key event in pathologic aging.

1 Introduction

Tau pathology is the hallmark of tauopathies, a neurodegenerative disorder group that includes Alzheimer's disease (AD), where progressive Tau deposition in neurofibrillary tangles and neuropil threads correlates with a deteriorating clinical course (Long and Holtzman, 2019). Autosomal dominant mutations in the *MAPT* gene encoding for Tau lead to a relatively small group of frontotemporal lobar degenerations (FTLD-Tau), which are classified among frontotemporal dementia (Josephs, 2018) diagnosed mostly at 45-65 years of age (Hutton et al., 1998, Spillantini et al., 1998). With Tau being a microtubule-binding protein, a prevalent concept to explain the pathogenesis of tauopathies is that abnormal Tau modification e.g., phosphorylation and folding, contributes to Tau dissociation from microtubules, assembly into multimeric β-sheets, proteotoxicity, neuronal dysfunction and cell loss (Jeganathan et al., 2006, Ludolph et al., 2009). In addition to its well-characterized role in neurodegeneration, studies reporting a correlation between *MAPT* gene products and survival in various types of tumors endorse an implication of Tau in cancer (Papin and Paganetti, 2020, Gargini et al., 2020, Gargini et al., 2019, Cimini et al., 2022, Rossi et al., 2018). The mechanisms underlying these findings may involve microtubule-unrelated Tau functions.

Tau exerts non canonical functions e.g., it localizes in the cell nucleus and binds DNA (Cross et al., 1996, Greenwood and Johnson, 1995, Loomis et al., 1990, Thurston et al., 1996). Heat or oxidative stress cause nuclear translocation of Tau, which may favor its role in DNA protection (Sultan et al., 2011). Neurons knocked-out for *MAPT* display enhanced DNA damage (Violet et al., 2014), and induced DNA damage correlates with nuclear translocation and dephosphorylation of Tau (Ulrich et al., 2018). Chromosomal abnormalities in AD fibroblasts (Rossi et al., 2008) and frequent DNA damage in AD brains (Lovell and Markesbery, 2007, Mullaart et al., 1990), both reinforce the emerging function of Tau in DNA stability. Tau depletion also modulates the induction of apoptosis and cell senescence in response to DNA damage by a mechanism involving P53, the guardian of the genome (Sola et al., 2020). Additional functions of Tau in epigenetic modulation were also reported (Rico et al., 2021). Upon binding to histones, Tau stabilizes chromatin compaction (Montalbano et al., 2021, Frost et al., 2014, Rico et al., 2021, Montalbano et al., 2020) and affects global gene expression during the neurodegenerative process (Frost et al., 2014, Klein et al., 2019). A meta-analysis of dysregulated DNA methylation in AD identified over hundreds genomic sites in cortical regions (Shireby et al., 2022); growing to thousands when looking at the dentate gyrus of oldest old patients (Lang et al., 2022).

DNA and histone modification is an effective mechanism to regulate gene activity. Hence, with the aim to investigate a possible participation of Tau in gene expression, we performed a bioinformatics analysis of transcriptome data obtained from Tau-depleted human neuroblastoma cells. Among the transcripts deregulated in a Tau-dependent manner, we found an enrichment of target genes for the Polycomb Repressive Complex 2 (PRC2), a result confirmed by decreased PRC2 protein and histone 3 (H3) methylation in Tau deficient cells. Notably, among the de-repressed gene products, Insulin Growth Factor Binding Protein 3 (IGFBP3) was linked to senescence induction. Our findings propose a Tau-driven mechanism for epigenetic modulation of cell senescence, a key event in pathologic aging.

2 Materials and methods

2.1 Cell culture

Human neuroblastoma SH-SY5Y cells (94030304, Sigma-Aldrich) were cultured in complete Dulbecco's Modified Eagle Medium (61965–059, Gibco) supplemented with 1% non-essential amino acids (11140035, Gibco), 1% penicillin-streptomycin (15140122, Gibco) and 10% fetal bovine serum (FBS; 10270106, Gibco). Cells were grown at 37°C with saturated humidity and 5% CO_2 and maintained in culture for less than one month. *MAPT* knock-out cells were described previously (Sola et al., 2020).

2.2 RNAseq

Total RNA extraction with the TRIzol™ Reagent (15596026, Invitrogen) was done according to the instructions of the manufacturer. Extracted RNA was processed with the NEBNext Ultra Directional II RNA library preparation kit for Illumina and sequenced on the Illumina NextSeq500 with single-end, 75 base pair long reads. The overall quality of sequencing reads was evaluated using a variety of tools, namely FastQC (Wingett and Andrews, 2018), RSeQC (Wang et al., 2012), AfterQC (Chen et al., 2017) and Qualimap (García-Alcalde et al., 2012). Sequence alignments to the reference human genome (GRCh38) was performed using STAR (v.2.5.2a) (Dobin et al., 2013). Transcript expression was quantified at gene level with the comprehensive annotations v27 release of the Gene Transfer File (GTF) made available by Gencode (Harrow et al., 2012). Raw-counts were further processed in the R Statistical environment and downstream differential expression analysis was performed using the DESeq2 pipeline (Love et al., 2014). Transcripts characterized by low mean normalized counts were filtered out by the Independent Filtering feature embedded in DESeq2 (alpha = 0.05). The RNA-Seq data have the accession no. E-MTAB-8166 and were uploaded on https://www.ebi.ac.uk/biostudies/arrayexpress/studies/E-MTAB-8166?key=64a67428-adb9-4681-99c9-98910b78ed4c. The genes differentially expressed between WT and Tau-KO cells (734) were used to interrogate a possible gene-set enrichment utilizing the transcription tool of the EnrichR portal (Chen et al., 2013, Kuleshov et al., 2016, Xie et al., 2021).

2.3 Pseudoviral particle production and transduction

Pseudolentiviral particles were produced by transient transfection of HEK293FT cells with 2 µg of the pSIF-H1-puro-IGFBP3 shRNA-2 or of the control plasmid pSIF-H1-puro-luciferase shRNA and 8 µg of the feline immunodeficiency virus (FIV) packaging plasmid mix (pFIV-34N & pVSV-G); all plasmids were kindly provided by Prof. Yuzuru Shiio (Greehey Children's Cancer Research Institute, University of Texas). Cell conditioned medium was collected 2 days after transfection and cleared by centrifugation at 300 g for 5 min, 4°C. Pseudo-lentiviruses were 20-fold concentrated with centrifugal filters (MWCO 30 kDa, UFC903024, Amicon) at 3'000 g for 30-45 min, 4°C, aliquoted and stored at -80°C.

Human neuroblastoma SH-SY5Y cells (1 x10^5) were seeded into a 24-well plate coated with poly-D-lysine (p6407, Sigma-Aldrich) one day before pseudo-lentiviral particle transduction. One day after transduction, cells were supplemented with fresh complete medium and selected in the presence of 2.5 µg/mL puromycin (P8833, Sigma-Aldrich) for two weeks.

2.4 Drugs and cell treatments

Treatment of SH-SY5Y cells with Tazemetostat (CAS No. 1403254-99-8, S7128, Selleckchem) was performed at 10 µM for four days staring from a 10 mM stock solution in DMSO; vehicle 0.1% DMSO was added to the controls.

2.5 Western blot and immune precipitation

For direct analysis by western blot, total lysates from cells cultured in 6-well plates were prepared in 50 µL of SDS-PAGE sample buffer (1.5% SDS, 8.3% glycerol, 0.005% bromophenol blue, 1.6% β-mercaptoethanol and 62.5 mM Tris pH 6.8) and incubated for 10 min at 100°C. 15 µL per lane of the sample was loaded on SDS-polyacrylamide gels (SDS-PAGE).

For immune isolation, the cells were rinsed with PBS and lysed on ice in 100 µL of AlphaLisa Lysis Buffer (AL003, PerkinElmer) supplemented with protease and phosphatase inhibitor cocktails (S8820 & 04906845001, Sigma-Aldrich). Cell lysates were treated with benzonase (707463, Novagen) for 15 min at 37°C, centrifuged at 20'000 g for 10 min at 4°C and supernatants were collected as cell extracts. These latter were diluted in HiBlock buffer (10205589, PerkinElmer) and incubated overnight at 4°C with 0.5 µg of primary antibodies against SUZ12 (3737, Cell Signaling Technology), or EZH2 (5246, Cell Signaling Technology). Protein G-Sepharose beads (101241, Invitrogen) were added for 1 h at room temperature (RT) and the beads were washed three times in PBS with 0.1% Tween-20. Bead-bound proteins were eluted in SDS-PAGE sample buffer by boiling for 10 min at 100°C.

After SDS-PAGE, PVDF membranes with transferred proteins were incubated with primary antibodies: 0.084 µg/mL SUZ12, 0.421 µg/mL EZH2, 0.18 µg/mL GAPDH (ab181602, Abcam), 0.1 µg/mL H3K27me3 (C15410069, Diagenode), 0.02 µg/mL H3 (ab176842, Abcam), or 0.4 µg/mL IGFBP3 (sc365936, Santa Cruz Biotechnology). Primary antibodies were revealed with anti-mouse IgG coupled to IRDye RD 680 or anti-rabbit IgG coupled to IRDye 800CW (Licor Biosciences, 926–68070 & 926–32211) on a dual infrared imaging scanner (Licor Biosciences, Odyssey CLx 9140) and quantified with the software provided (Licor Biosciences, Image Studio V5.0.21, 9140–500).

2.6 Immune staining

For immune staining, cells were grown on poly-D-lysine coated 8-well microscope slides (80826-IBI, Ibidi). Cells were fixed in 4% paraformaldehyde and stained (Ulrich et al., 2018) with primary antibodies: 0.168 µg/mL SUZ12, 0.842 µg/mL EZH2, 1.6 µg/mL H3K27me3 or 1.5 µg/mL p16 (ab108349, Abcam). Detection by fluorescent laser confocal microscopy (Nikon C2 microscope) was done with 2 µg/mL secondary antibodies anti-mouse IgG Alexa594, anti-rabbit IgG -Alexa 488 or anti-rabbit IgG-Alexa 647 (A-11032, A-11034, A21245, Thermo Fisher Scientific). Nuclei were counterstained with 0.5 µg/mL DAPI (D9542, Sigma-Aldrich). Images were acquired by sequential excitations (line-by-line scan) with the 405 nm laser (464/40 emission filter), the 488 nm laser (525/50 nm filter), the 561 nm laser (561/LP nm filter) and the 650 nm laser (594/633 emission filter). ImageJ was used for all image quantifications.

2.7 RNA extraction and RT-qPCR

Total RNA extraction using the TRIzol™ Reagent (15596026, Invitrogen) and cDNA synthesis using the GoScript Reverse Transcription Mix Random Primers (A2800, Promega) were done according to the instructions of the manufacturer. Amplification was performed with SsoAdvanced Universal SYBR Green Supermix (1725271, BioRad) with 43 cycles at 95°C for 5 sec, 60°C for 30 sec and 60°C for 1 min using specific primers for *EZH2*, *SUZ12*, *IGFBP3*, *GPR37*, *ITGA3*, *MRC2* and *IRF6* gene transcripts **(Supplementary Table IV)**. Relative RNA expression was calculated using the comparative Ct method and normalized to the geometric mean of the GAPDH and HPRT1 mRNAs.

2.8 SA-βGal assay

Senescence-associated β-galactosidase (SA-βGal) staining was determined on cells grown in 6-well plates, fixed with 2% paraformaldehyde for 10 min at RT and washed twice with gentle shaking for 5 min at RT. Cells were then incubated with 1 mg/mL X-gal (20 mg/mL stock in DMF; B4252, Sigma-Aldrich,) diluted in pre-warmed 5 mM $K_3[Fe(CN)_6]$ (P-8131, Sigma-Aldrich), 5 mM $K_4[Fe(CN)_6]\cdot 3H_2O$ (P-3289, Sigma-Aldrich), and 2 mM $MgCl_2$ (M-8266, Sigma-Aldrich) in PBS at pH 6.0. Acquisition and quantification of the images for SA-βGal activity and cell area were done with an automated live cell imager (Lionheart FX, BioTek).

2.9 LysoTracker

For LysoTracker staining, cells were seeded in poly-D-lysine coated 8-well microscope slides, incubated for 10 min at 37°C with 0.25 µM Lysotracker Red (L7528, Thermo Fischer Scientific). Nuclei were counterstained with 2.5 µg/mL Hoechst (H3570, Invitrogen) for 10 min at 37°C, afterwards cells were washed with complete medium. Images of living cells were acquired on a fluorescent laser confocal microscope (C2, Nikon) by sequential excitations (line-by-line scan) with the 405 nm laser (464/40 nm emission filter), and the 561 nm laser (561/LP nm filter). ImageJ was used for all image quantifications. Both the lysosomes area and the mean number of lysosomes per cells and per images were determined.

3 Results

3.1 Transcriptomics analysis of Tau-KO cells

We performed a next-generation transcription (RNAseq) analysis of human SH-SY5Y neuroblastoma cells knocked-out for Tau when compared to normal Tau-expressing cells (**Fig 1A**). The sequences obtained from the six samples analyzed (three Tau expressing cell lines, three Tau-KO cell lines) mapped reliably to ~16'000 genes. Additional 14'000 transcripts were expressed at low levels and were not included in the differential expression analysis. The primary data were stored at https://www.ebi.ac.uk/biostudies/ with open access (E-MTAB-8166). When filtering for differentially expressed transcripts in Tau-KO cells, 1388 RNAs displayed a significant change (Adj P <.05), of which 723 RNAs were up-regulated in the log2(FC) range between 0.31 and 11.05 (between 1.24 and ~2000 fold higher than in control Tau expressing cells) (**Supplementary Table I**).

We selected these 723 differentially expressed genes to interrogate a possible gene-set enrichment utilizing the transcription tool of the EnrichR portal (Chen et al., 2013, Kuleshov et al., 2016, Xie et al., 2021). The CHIP-sequencing datasets (ChEA 2016) identified an overrepresentation of Polycomb Repressive Complex-associated proteins among the 68 datasets showing a significant (Adj P <.01) difference. Indeed, almost half of the enriched CHIP-sequencing datasets were obtained from core components or known regulators of PRC2 (32%) or of PRC1 (16%) (**Fig 1B**; **Supplementary Table II).** PRC2 actively catalyzes the trimethylation of histone 3 (H3) at lysin 27 (H3K27me3) (Laugesen et al., 2016, Moritz and Trievel, 2018). In agreement with the identification of PRC2 in the CHIP-sequencing datasets, mining of the epigenomics roadmap (HM ChIP-seq) resulted in a 73% enrichment of the H3K27me3 signature (Adj P <.01) in 45 datasets (**Fig 1C**; **Supplementary Table III**). Altogether, analysis of the RNAseq data suggested that up-regulation of transcription of a specific set of genes in Tau-depleted neuroblastoma SH-SY5Y cells might ensue from a relief of gene activity decline controlled by PRC2.

3.2 Reduced expression and activity of PRC2 in Tau-depleted cell

We subsequently analyzed the amount of two PRC2 core components in Tau-KO cells by western blot. In agreement with what suggested by the transcriptomics data, we observed reduced amounts of the catalytic subunit EZH2 and the scaffold subunit SUZ12 of PRC2 in Tau-KO cells when compared to Tau-expressing cells (**Fig 2A**). Reduced proteins were found also by quantitative immune staining of the cells utilizing specific antibodies (**Fig 2B**). RT-qPCR analysis excluded that the effect on PRC2 protein resulted from reduced transcription since no difference was found for the EZH2 and SUZ12 mRNAs (**Fig 2C**), data that suggested a Tau-dependent effect on PRC2 protein stability. Nonetheless, co-immune isolation revealed the presence of the EZH2-SUZ2 core complex of PRC2 in Tau-KO cells, albeit at reduced levels when compared to controls (**Fig 2D**).

PRC2 enzymatic activity was determined by western blot and quantitative immune staining of H3K27me3, an epigenetic mark produced by the histone methyl transferase activity of PRC2 (Guo et al., 2021). Confirming the lower amounts of the PRC2 complex, we found that Tau-KO cells display reduced H3K27me3 (**Fig 3A-B**). Among the upregulated transcripts found by RNA-seq in Tau-KO cells, we selected five known PRC2 targets displaying close to average signals (**Supplementary Table I**): *IGFBP3* (19.0x of WT, adjP .004), *GPR37* (9.3x, .015), *ITGA3* (6.3x, .017.3x), *MRC2* (5.1x, .016), and *IRF6* (3.2x, .0498). Determination of mRNA expression by RT-qPCR validated their up-regulation (**Fig 3C**); indicating again that Tau-depletion relieved repression of transcription caused by reduced PRC2 activity in Tau-depleted cells.

3.3 PRC2-dependent overproduction of IGFBP3 in Tau-KO cells

IGFBP3 protein is a component of the senescence-associated secreted phenotype (SASP) (Basisty et al., 2020). Having previously reported that Tau-depletion favored cellular senescence (Sola et al., 2020), we interrogated the role of IGFBP3 in this process. As anticipated from the mRNA data, a strong overproduction of endogenous IGFBP3 was present in Tau-KO cells (**Fig 4A**). Reinforcing the link between PRC2 and IGFBP3, treatment of SH-SY5Y cells with Tazemetostat, a specific blocker of the histone methyl transferase activity of EZH2 (Straining and Eighmy, 2022), reduced H3K27me3 and increased IGFBP3 (**Fig 4B**). Lower EZH2 and SUZ12 and higher IGFBP3 was confirmed in an independent Tau-KO cell line (**Supplementary Fig 1**).

3.4 Tau/PRC2/IGFBP3 triad in senescence

Increased cellular expression of IGFBP3 is associated with autocrine and paracrine senescence induction (Elzi et al., 2012), and reduced PRC2 is also linked to increased cellular senescence (Ito et al., 2018). Furthermore, increased senescence is observed in Tau-KO cells (Sola et al., 2020). Thus, we postulated that PRC2-dependent de-repression of IGFBP3 in Tau-depleted cells may explain the induction of cellular senescence. We observed first that Tau depletion as well as PRC2 inhibition both increased the percentage of SH-SY5Y cells entering in senescence, as assessed by three independent markers: P16, senescence-associated β-galactosidase (SA-βgal), and the number and size of lysosomes labelled with the acidotrophic LysoTracker dye (**Fig 5A**). Next, we reduced IGFBP3 expression in Tau-KO cells by a shRNA-based approach **(Fig 5B)** and found that this reduced senescence induction in Tau-KO cells **(Fig 5C)**. Thus, we validated our hypothesis that increased senescence in Tau-KO SH-SY5Y cells was likely the consequence of decreased PRC2-dependent repression of IGFBP3 expression.

4 Discussion

We report data demonstrating a non-canonical role of Tau as a modulator of the epigenetic activity of PRC2 inducing cellular senescence in neuroblastoma SH-SY5Y cells. In our study we identified a prevalent PRC2 signature for shared modulation of upregulated transcripts in Tau-depleted cells. PRC1 and PRC2 are multi-subunit transcriptional repressors that crucially modulate chromatin structure and gene expression by distinct enzymatic activities (Vijayanathan et al., 2022). PRC1 is an E3 ubiquitin ligase that catalyzes H2A ubiquitination at lysine119, whereas PRC2 acts as a methyltransferase that generates H3K27me3 with some cross-talk between the two complexes (Guerard-Millet et al., 2021). Confirming the bioinformatics results, Tau depletion caused reduced cellular amounts of PRC2 and its product H3K27me3. Increased senescence status upon Tau-depletion was reproduced through pharmacological inhibition of PRC2 in Tau-expressing cells. Finally, we report that reversing the up-regulation of the PRC2-target IGFBP3, impaired senescence induction in Tau-depleted cells.

Evidence exists for the implication of Tau in chromatin remodeling. A pioneering study investigated chromatin conformation in mouse and drosophila models of AD as well as in human diseased brain, whereby a general loss of heterochromatin was associated with aberrant gene expression in all three paradigms (Frost et al., 2014). More recently, binding of Tau to histones was linked to the maintenance of condensed chromatin (Rico et al., 2021). Thus, Tau may favor chromatin compaction for preventing aberrant gene transcription. Misfolding, hyperphosphorylation or sequestration of Tau in oligomers and fibrils, typical hallmarks of tauopathies, could all result in a negative regulation of this non-canonical function of Tau. In our study, we show that in addition to the direct interaction between Tau and histones (Rico et al., 2021), an indirect mechanism involving PRC2 is an additional instrument for modulating chromatin compaction.

The role of PRC2 in senescence was shown by findings indicating that impairment of its catalytic activity induces a delayed decrease in H3K27me3 at the CDKN2A locus, which upregulates p16, the SASP phenotype, and senescence (Ito et al., 2018). This function of PRC2 represents a target for anticancer therapies e.g., through EED inhibition associated to de-repression of SASP-encoding genes and entry of proliferative cancer cells in a senescent state (Chu et al., 2022). Beside the paradoxical implication in cancer (Yang et al., 2021), senescence contributes to neurodegenerative diseases. Senescent neurons, microglia, astrocytes and neuronal stem cells were found during the pathogenic process (Si et al., 2021). A recent study in a tauopathy mouse model supported a causal link between cell senescence and cognitive decline linked to neuronal loss. Indeed, p16INK4A-positive senescent glial cells were found associated to Tau lesions, and, strikingly, the clearance of these cells prevented Tau hyperphosphorylation, Tau fibril deposition, whilst preserving neuronal survival and cognitive functions (Bussian et al., 2018). We describe now a conceivable mechanism linking depletion of functional Tau in tauopathies and senescence induction.

Among the PRC2 targets, we identified IGFBP3 as a main driver of senescence resulting from Tau-depletion. Ectopic expression of the SASP component IGFBP3 or its administration to MCF7 or IMR-90 cells is sufficient to induce senescence, whereas IGFBP3 knock-down impairs doxorubicin-induced senescence (Elzi et al., 2012). Although the role of PRC2 and IGFBP3 were established independently, to our knowledge our study is the first one showing IGFBP3 as a main executor of PRC2-dependent senescence induction and its modulation by Tau protein levels.

PRC2 has numerous functions in the developing central nervous system, with many neurogenesis-linked genes regulated by the PRC2/H3K27 axis (Liu et al., 2017). PRC2 is essential in preserving neural progenitor cell identity and neuroepithelial integrity (Akizu et al., 2016). PRC2 deficiency in mice leads to aberrant gastrulation and lack of neural tissue (Schumacher et al., 1996). Later in development, a transcription pattern with a PRC2 signature drives neuronal migration and is essential

for the organization of neural circuits (Zhao et al., 2015). The rare Weaver syndrome linked to developmental cognitive deficits is caused by autosomal dominant mutations in any one of the three PRC2 core components EZH2, EED and SUZ12 (Deevy and Bracken, 2019). However, PRC2 is also involved in neurodegeneration. PRC2 deficiency in striatal neurons of mice reactivates the deleterious expression of transcripts that are normally suppressed in these cells, ultimately causing premature lethality (Von Schimmelmann et al., 2016). Additional studies implicated PRC2 in ataxia-telangiectasia (Li et al., 2013), Parkinson's disease, Huntington's disease and AD (Kuehner and Yao, 2019). A meta-analysis of differentially methylated regions in prefrontal neocortex at different disease stages has identified in AD several hypermethylated regions, which were significantly enriched in polycomb repressed regions (Zhang et al., 2020). These data also link PCR2-dependent methylation of H3 with that of CpG islands of the genome, another epigenetic mechanism of gene repression (Phillips, 2008).

PRC2 lacks sequence-specific DNA-binding ability and therefore relies on accessory proteins for targeting specific loci. Factors contributing to selective PRC2 recruitment to chromatin are the interaction with sequence-specific transcription factors or RNAs, and or discerning chromatin features (Blackledge and Klose, 2021). In the fly, PRC2 activity is regulated through the interaction with transcription factors binding to polycomb response elements often located in proximal promoter regions of developmental genes (Kassis and Brown, 2013). However, the orthologue system was not found in mammals (Bauer et al., 2016). Rather, it is maybe replaced by the evolution of a mechanism based on non-methylated CpG islands (Ku et al., 2008) and the action of DNA-binding proteins binding to them. Proteins with such features are the PRC1.1 complex member KDM2B, or the PRC2-members PHF1, MTF2 and PHF19 (Owen and Davidovich, 2022).

PRC histone modifications are heritable over mitotic cell division providing an epigenetic memory for stable cell identity and adequate response to stress (Reinig et al., 2020). Thus, PRC2 dysfunction is frequently associated with neoplastic progression and is a target for anticancer therapy (Comet et al., 2016). Expression of its catalytic subunit EZH2 correlates with cell proliferation, and its aberrant overexpression is frequent in many types of cancer cells (Liu and Liu, 2022). However, in line with a role in tumor suppression, loss-of-function of PRC2 is also involved in cancer (Liu et al., 2017). PRC2 modulation by Tau implicates this latter in the pathogenesis of cancer, supporting the observation that the Tau mRNA correlates with survival in several tumors (Gargini et al., 2019, Papin and Paganetti, 2020). The mechanism explaining this correlation is unknown but may involve the non-canonical role of Tau in modulating chromatin compaction and senescence induction. This may open new therapeutic opportunities for neurodegenerative diseases and cancer.

Figures Legends

Figure 1. Deregulation of the PRC2 pathway in human Tau-KO SH-SY5Y neuroblastoma cells. (**A**). Scheme of the procedure for the RNAseq and EnrichR analyses in Tau-expressing (WT) and Tau-knock-out (Tau-KO) cells. (**B-C**). The EnrichR analysis based on 723 upregulated genes in Tau-KO cells resulted in the enrichment of the PRC2 pathway with the ChIP datasets (**B**) and of H3K27me3 with the epigenomics datasets (**C**).

Figure 2. Reduced PRC2 complex in Tau-KO SH-SY5Y cells.
(**A**). Shown are matched protein amounts of parental (WT) or Tau-KO cell lysates analyzed by western blot (biological triplicates on a single gel) with EZH2, SUZ12 or GAPDH primary antibodies and anti-rabbit IgG IRDye 800CW secondary antibody. The EZH2 and SUZ12 signals were normalized on the respective GAPDH signals and reported as fold of WT; mean ± SD of 9 biological replicates, unpaired Mann-Whitney test. (**B**). Determination of nuclear EZH2 or SUZ12 mean fluorescent intensity analyzed by immune fluorescence staining and laser confocal microscopy with EZH2 or SUZ12 antibodies revealed with an anti-rabbit AlexaFluor 488 antibody. Data obtained with a DAPI nuclear mask (ImageJ) are reported as fold of WT; mean ± SEM of 292-475 nuclei from two (EZH2) or three (SUZ12) independent experiments, unpaired Mann-Whitney test. (**C**). Shown are RT-PCR determination of mRNA with specific primers for EZH2 or SUZ12. Normalization was performed on the geometric mean of the GAPDH and HPRT1 mRNA values and reported as fold of WT; mean ± SD of 12 biological replicates, unpaired Mann-Whitney test. (**D**). Shown are matched protein amounts of cell lysates subjected to immune isolation (IP) with EZH2 or SUZ12 antibodies or matched amounts of control antibodies (ctrl IP). Samples were resolved on a single same gel and analyzed by western blot with EZH2 or SUZ12 antibodies and secondary anti-rabbit IgG IRDye 800CW antibody.

Figure 3. Reduced PRC2 activity in Tau-KO SH-SY5Y cells.
(**A**). Shown are matched protein amounts of parental (WT) or Tau-KO cell lysates analyzed by western blot (biological triplicates on a single gel) with H3K27me3, H3 or GAPDH primary antibodies and anti-rabbit IgG IRDye 800CW secondary antibody. The H3K27me3 and H3 signals were normalized for GAPDH and reported as fold of WT for the H3K27me3/H3 ratios; mean ± SD of 8-9 biological replicates, unpaired Mann-Whitney test. (**B**). Nuclear H3K27me3 mean fluorescent intensity was determined by immune fluorescence staining and laser confocal microscopy. Data obtained with a DAPI nuclear mask (ImageJ) are reported as fold of WT; mean ± SEM of 695-716 nuclei from five independent experiments, unpaired Mann-Whitney test. (**C**). Shown are RT-PCR determination of mRNA with specific primers as indicated. Normalization was performed on the geometric mean of the GAPDH and HPRT1 mRNA values and reported as fold of WT; mean ± SD of 3-12 biological replicates, unpaired Mann-Whitney test.

Figure 4. Increased IGFBP3 in SH-SY5Y cells after Tau-KO or PRC2 inhibition.
(**A**). Shown are matched protein amounts of parental (WT) or Tau-KO cell lysates analyzed by western blot (biological triplicates on a single gel) with IGFBP3 or GAPDH primary antibodies and anti-mouse IgG IRDye 680RD or anti-rabbit IgG IRDye 800CW secondary antibodies. The IGFBP3 signals were normalized for GAPDH and reported as fold of WT; mean ± SD of 8-9 biological replicates, unpaired Mann-Whitney test. (**B-C**). Shown is a western blot of matched protein amounts of SH-SY5Y cells treated for 4 days in the absence (WT) or presence of 10 µM Tazemetostat (EZH2i). Biological triplicates on a single gel were probed (**B**) with H3K27me3, H3 or GAPDH primary antibodies and anti-rabbit IgG IRDye 800CW secondary antibody or (**C**) with IGFBP3 or

GAPDH antibodies. Protein signals were normalized for GAPDH and reported as fold of WT; mean ± SD of 6 biological replicates, unpaired Mann-Whitney test.

Figure 5. Increased IGFBP3-induced senescence in cells.
(**A**). Senescence markers were analyzed in parental (WT), Tau-KO or 10 μM Tazemetostat-treated parental (EZH2i) cells. The nuclear P16 fluorescent intensity (P16 IF) was determined with a DAPI nuclear mask (ImageJ) by immune fluorescence staining and laser confocal microscopy and reported as fold of WT; mean ± sem of 1991-3153 nuclei. The percent of senescence-associated βGal positive cells (βGal) was determined by automated cell imaging; mean ± SD of 7-14 fields. Living cells labeled with the acidotrophic dye LysoTracker (DOs) were imaged on a laser confocal microscope and analyzed for the size (area of 643-3429 DOs) and mean number per cell (13-18 fields) of LysoTracker-positive organelles (ImageJ). Values are reported as fold of WT; mean ± sem (area) or ± SD (number), non-parametric Krustal-Wallis and Dunn's multiple comparison test. (**B**). Matched protein amounts of SH-SY5Y cells transduced with mock (ctrl) or IGFBP3 shRNA (IGFBP3-KD) pseudo lentiviral particles were analyzed by western blot (biological triplicates on a single gel) with IGFBP3 or GAPDH primary antibodies and anti-mouse IgG IRDye 680RD or anti-rabbit IgG IRDye 800CW secondary antibodies. The IGFBP3 signals were normalized for GAPDH and reported as fold of WT; mean ± SD of 9 biological replicates, unpaired Mann-Whitney test. (**C**). As in (**A**) for SH-SY5Y cells transduced with mock (ctrl) or IGFBP3 shRNA (IGFBP3-KD) pseudo lentiviral particles. P16 IF: mean ± sem of 669-881 nuclei; βGal: mean ± SD of 6 fields. DOs; area of 456-551 DOs, mean number per cell (5 fields) of LysoTracker-positive organelles (ImageJ). Values are reported as fold of WT; mean ± sem (area) or ± SD (number); unpaired Mann-Whitney test.

Supplementary Figure 1. Reduced EZH2/SUZ12 and increased IGFBP3 in an independent Tau-KO SH-SY5Y cell line.
(**A**). Nuclear EZH2 or SUZ12 mean fluorescent intensity was analyzed by immune fluorescence staining and laser confocal microscopy with EZH2 or SUZ12 antibodies revealed with an anti-rabbit AlexaFluor 488 antibody. Data obtained with a DAPI nuclear mask (ImageJ) are reported as fold of WT; mean ± sem of 202-208 nuclei (EZH2) or 182-184 nuclei (SUZ12), unpaired Mann-Whitney test. (**B**). IGFBP3 was determined by western blot for matched protein amounts of parental (WT) or Tau-KO (2) cell lysates (biological triplicates on a single gel). Data are reported as fold of WT, mean ± SD of 9 biological replicates, unpaired Mann-Whitney test.

5 Conflict of Interest

The authors declare that the research was conducted in the absence of any commercial or financial relationships that could be construed as a potential conflict of interest.

6 Author Contributions

Conceptualization: SP, PP
Methods and investigations: CM, MS, EP. MB, AR
Supervision: SP, PP
Writing (original draft): SP
Writing (review & editing): all co-authors

7 Funding

The Paganetti's lab is founded by the Gelu Foundation, the Mecri Foundation and The Charitable Gabriele Foundation.

8 Acknowledgments

We thank the whole laboratory for support and advice during this study.

9 Data Availability Statement

The RNA-Seq data have the accession no. E-MTAB-8166 and were uploaded on https://www.ebi.ac.uk/biostudies/arrayexpress/studies/E-MTAB-8166?key=64a67428-adb9-4681-99c9-98910b78ed4c.

Akizu, N., García, M. A., Estarás, C., Fueyo, R., Badosa, C., De La Cruz, X. & Martínez-Balbás, M. A. 2016. EZH2 regulates neuroepithelium structure and neuroblast proliferation by repressing p21. *Open Biol,* 6**,** 150227.

Basisty, N., Kale, A., Patel, S., Campisi, J. & Schilling, B. 2020. The power of proteomics to monitor senescence-associated secretory phenotypes and beyond: toward clinical applications. *Expert Rev Proteomics,* 17**,** 297-308.

Bauer, M., Trupke, J. & Ringrose, L. 2016. The quest for mammalian Polycomb response elements: are we there yet? *Chromosoma,* 125**,** 471-96.

Blackledge, N. P. & Klose, R. J. 2021. The molecular principles of gene regulation by Polycomb repressive complexes. *Nat Rev Mol Cell Biol,* 22**,** 815-833.

Bussian, T. J., Aziz, A., Meyer, C. F., Swenson, B. L., Van Deursen, J. M. & Baker, D. J. 2018. Clearance of senescent glial cells prevents tau-dependent pathology and cognitive decline. *Nature,* 562**,** 578-582.

Chen, E. Y., Tan, C. M., Kou, Y., Duan, Q., Wang, Z., Meirelles, G. V., Clark, N. R. & Ma'ayan, A. 2013. Enrichr: interactive and collaborative HTML5 gene list enrichment analysis tool. *BMC Bioinformatics,* 14**,** 128.

Chen, S., Huang, T., Zhou, Y., Han, Y., Xu, M. & Gu, J. 2017. AfterQC: automatic filtering, trimming, error removing and quality control for fastq data. *BMC Bioinformatics,* 18**,** 80.

Chu, L., Qu, Y., An, Y., Hou, L., Li, J., Li, W., Fan, G., Song, B.-L., Li, E., Zhang, L. & Qi, W. 2022. Induction of senescence-associated secretory phenotype underlies the therapeutic efficacy of PRC2 inhibition in cancer. *Cell Death & Disease,* 13**,** 155.

Cimini, S., Giaccone, G., Tagliavini, F., Costantino, M., Perego, P. & Rossi, G. 2022. P301L tau mutation leads to alterations of cell cycle, DNA damage response and apoptosis: Evidence for a role of tau in cancer. *Biochem Pharmacol,* 200**,** 115043.

Comet, I., Riising, E. M., Leblanc, B. & Helin, K. 2016. Maintaining cell identity: PRC2-mediated regulation of transcription and cancer. *Nature Reviews Cancer,* 16**,** 803-810.

Cross, D., Tapia, L., Garrido, J. & Maccioni, R. B. 1996. Tau-like proteins associated with centrosomes in cultured cells. *Exp Cell Res,* 229**,** 378-87.

Deevy, O. & Bracken, A. P. 2019. PRC2 functions in development and congenital disorders. *Development,* 146.

Dobin, A., Davis, C. A., Schlesinger, F., Drenkow, J., Zaleski, C., Jha, S., Batut, P., Chaisson, M. & Gingeras, T. R. 2013. STAR: ultrafast universal RNA-seq aligner. *Bioinformatics,* 29**,** 15-21.

Elzi, D. J., Lai, Y., Song, M., Hakala, K., Weintraub, S. T. & Shiio, Y. 2012. Plasminogen activator inhibitor 1 - insulin-like growth factor binding protein 3 cascade regulates stress-induced senescence. *Proceedings of the National Academy of Sciences,* 109**,** 12052-12057.

Frost, B., Hemberg, M., Lewis, J. & Feany, M. B. 2014. Tau promotes neurodegeneration through global chromatin relaxation. *Nat Neurosci,* 17**,** 357-66.

García-Alcalde, F., Okonechnikov, K., Carbonell, J., Cruz, L. M., Götz, S., Tarazona, S., Dopazo, J., Meyer, T. F. & Conesa, A. 2012. Qualimap: evaluating next-generation sequencing alignment data. *Bioinformatics,* 28**,** 2678-9.

Gargini, R., Segura-Collar, B., Herránz, B., García-Escudero, V., Romero-Bravo, A., Núñez, F. J., García-Pérez, D., Gutiérrez-Guamán, J., Ayuso-Sacido, A., Seoane, J., Pérez-Núñez, A., Sepúlveda-Sánchez, J. M., Hernández-Laín, A., Castro, M. G., García-Escudero, R., Ávila, J. & Sánchez-Gómez, P. 2020. The IDH-TAU-EGFR triad defines the neovascular landscape of diffuse gliomas. *Sci Transl Med,* 12.

Gargini, R., Segura-Collar, B. & Sánchez-Gómez, P. 2019. Novel Functions of the Neurodegenerative-Related Gene Tau in Cancer. *Front Aging Neurosci,* 11**,** 231.

Greenwood, J. A. & Johnson, G. V. 1995. Localization and in situ phosphorylation state of nuclear tau. *Exp Cell Res,* 220**,** 332-7.

Guerard-Millet, F., Gentile, C., Paul, R., Mayran, A. & Kmita, M. 2021. Polycomb Repressive Complexes occupancy reveals PRC2-independent PRC1 critical role in the control of limb development. *bioRxiv*, 2021.10.28.466236.
Guo, Y., Zhao, S. & Wang, G. G. 2021. Polycomb Gene Silencing Mechanisms: PRC2 Chromatin Targeting, H3K27me3 'Readout', and Phase Separation-Based Compaction. *Trends in Genetics,* 37, 547-565.
Harrow, J., Frankish, A., Gonzalez, J. M., Tapanari, E., Diekhans, M., Kokocinski, F., Aken, B. L., Barrell, D., Zadissa, A., Searle, S., Barnes, I., Bignell, A., Boychenko, V., Hunt, T., Kay, M., Mukherjee, G., Rajan, J., Despacio-Reyes, G., Saunders, G., Steward, C., Harte, R., Lin, M., Howald, C., Tanzer, A., Derrien, T., Chrast, J., Walters, N., Balasubramanian, S., Pei, B., Tress, M., Rodriguez, J. M., Ezkurdia, I., Van Baren, J., Brent, M., Haussler, D., Kellis, M., Valencia, A., Reymond, A., Gerstein, M., Guigo, R. & Hubbard, T. J. 2012. GENCODE: the reference human genome annotation for The ENCODE Project. *Genome Res,* 22, 1760-74.
Hutton, M., Lendon, C. L., Rizzu, P., Baker, M., Froelich, S., Houlden, H., Pickering-Brown, S., Chakraverty, S., Isaacs, A., Grover, A., Hackett, J., Adamson, J., Lincoln, S., Dickson, D., Davies, P., Petersen, R. C., Stevens, M., De Graaff, E., Wauters, E., Van Baren, J., Hillebrand, M., Joosse, M., Kwon, J. M., Nowotny, P., Che, L. K., Norton, J., Morris, J. C., Reed, L. A., Trojanowski, J., Basun, H., Lannfelt, L., Neystat, M., Fahn, S., Dark, F., Tannenberg, T., Dodd, P. R., Hayward, N., Kwok, J. B., Schofield, P. R., Andreadis, A., Snowden, J., Craufurd, D., Neary, D., Owen, F., Oostra, B. A., Hardy, J., Goate, A., Van Swieten, J., Mann, D., Lynch, T. & Heutink, P. 1998. Association of missense and 5'-splice-site mutations in tau with the inherited dementia FTDP-17. *Nature,* 393, 702-5.
Ito, T., Teo, Y. V., Evans, S. A., Neretti, N. & Sedivy, J. M. 2018. Regulation of Cellular Senescence by Polycomb Chromatin Modifiers through Distinct DNA Damage- and Histone Methylation-Dependent Pathways. *Cell Rep,* 22, 3480-3492.
Jeganathan, S., Von Bergen, M., Brutlach, H., Steinhoff, H. J. & Mandelkow, E. 2006. Global hairpin folding of tau in solution. *Biochemistry,* 45, 2283-93.
Josephs, K. A. 2018. Rest in peace FTDP-17. *Brain,* 141, 324-331.
Kassis, J. A. & Brown, J. L. 2013. Polycomb group response elements in Drosophila and vertebrates. *Adv Genet,* 81, 83-118.
Klein, H.-U., Mccabe, C., Gjoneska, E., Sullivan, S. E., Kaskow, B. J., Tang, A., Smith, R. V., Xu, J., Pfenning, A. R., Bernstein, B. E., Meissner, A., Schneider, J. A., Mostafavi, S., Tsai, L.-H., Young-Pearse, T. L., Bennett, D. A. & De Jager, P. L. 2019. Epigenome-wide study uncovers large-scale changes in histone acetylation driven by tau pathology in aging and Alzheimer's human brains. *Nature Neuroscience,* 22, 37-46.
Ku, M., Koche, R. P., Rheinbay, E., Mendenhall, E. M., Endoh, M., Mikkelsen, T. S., Presser, A., Nusbaum, C., Xie, X., Chi, A. S., Adli, M., Kasif, S., Ptaszek, L. M., Cowan, C. A., Lander, E. S., Koseki, H. & Bernstein, B. E. 2008. Genomewide analysis of PRC1 and PRC2 occupancy identifies two classes of bivalent domains. *PLoS Genet,* 4, e1000242.
Kuehner, J. N. & Yao, B. 2019. The Dynamic Partnership of Polycomb and Trithorax in Brain Development and Diseases. *Epigenomes,* 3, 17-24.
Kuleshov, M. V., Jones, M. R., Rouillard, A. D., Fernandez, N. F., Duan, Q., Wang, Z., Koplev, S., Jenkins, S. L., Jagodnik, K. M., Lachmann, A., Mcdermott, M. G., Monteiro, C. D., Gundersen, G. W. & Ma'ayan, A. 2016. Enrichr: a comprehensive gene set enrichment analysis web server 2016 update. *Nucleic Acids Res,* 44, W90-7.
Lang, A.-L., Eulalio, T., Fox, E., Yakabi, K., Bukhari, S. A., Kawas, C. H., Corrada, M. M., Montgomery, S. B., Heppner, F. L., Capper, D., Nachun, D. & Montine, T. J. 2022. Methylation differences in Alzheimer's disease neuropathologic change in the aged human brain. *Acta Neuropathologica Communications,* 10, 174.

512 Laugesen, A., Højfeldt, J. W. & Helin, K. 2016. Role of the Polycomb Repressive Complex 2
513 (PRC2) in Transcriptional Regulation and Cancer. *Cold Spring Harbor Perspectives in*
514 *Medicine,* 6.
515 Li, J., Hart, R. P., Mallimo, E. M., Swerdel, M. R., Kusnecov, A. W. & Herrup, K. 2013. EZH2-
516 mediated H3K27 trimethylation mediates neurodegeneration in ataxia-telangiectasia. *Nat*
517 *Neurosci,* 16**,** 1745-53.
518 Liu, P.-P., Xu, Y.-J., Teng, Z.-Q. & Liu, C.-M. 2017. Polycomb Repressive Complex 2: Emerging
519 Roles in the Central Nervous System. *The Neuroscientist,* 24**,** 208-220.
520 Liu, X. & Liu, X. 2022. PRC2, Chromatin Regulation, and Human Disease: Insights From Molecular
521 Structure and Function. *Front Oncol,* 12**,** 894585.
522 Long, J. M. & Holtzman, D. M. 2019. Alzheimer Disease: An Update on Pathobiology and
523 Treatment Strategies. *Cell,* 179**,** 312-339.
524 Loomis, P. A., Howard, T. H., Castleberry, R. P. & Binder, L. I. 1990. Identification of nuclear tau
525 isoforms in human neuroblastoma cells. *Proc Natl Acad Sci U S A,* 87**,** 8422-6.
526 Love, M. I., Huber, W. & Anders, S. 2014. Moderated estimation of fold change and dispersion for
527 RNA-seq data with DESeq2. *Genome Biol,* 15**,** 550.
528 Lovell, M. A. & Markesbery, W. R. 2007. Oxidative DNA damage in mild cognitive impairment and
529 late-stage Alzheimer's disease. *Nucleic Acids Res,* 35**,** 7497-504.
530 Ludolph, A. C., Kassubek, J., Landwehrmeyer, B. G., Mandelkow, E., Mandelkow, E. M., Burn, D.
531 J., Caparros-Lefebvre, D., Frey, K. A., De Yebenes, J. G., Gasser, T., Heutink, P., Hoglinger,
532 G., Jamrozik, Z., Jellinger, K. A., Kazantsev, A., Kretzschmar, H., Lang, A. E., Litvan, I.,
533 Lucas, J. J., Mcgeer, P. L., Melquist, S., Oertel, W., Otto, M., Paviour, D., Reum, T., Saint-
534 Raymond, A., Steele, J. C., Tolnay, M., Tumani, H., Van Swieten, J. C., Vanier, M. T.,
535 Vonsattel, J. P., Wagner, S. & Wszolek, Z. K. 2009. Tauopathies with parkinsonism: clinical
536 spectrum, neuropathologic basis, biological markers, and treatment options. *Eur J Neurol,* 16**,**
537 297-309.
538 Montalbano, M., Jaworski, E., Garcia, S., Ellsworth, A., Mcallen, S., Routh, A. & Kayed, R. 2021.
539 Tau Modulates mRNA Transcription, Alternative Polyadenylation Profiles of hnRNPs,
540 Chromatin Remodeling and Spliceosome Complexes. *Front Mol Neurosci,* 14**,** 742790.
541 Montalbano, M., Mcallen, S., Puangmalai, N., Sengupta, U., Bhatt, N., Johnson, O. D., Kharas, M.
542 G. & Kayed, R. 2020. RNA-binding proteins Musashi and tau soluble aggregates initiate
543 nuclear dysfunction. *Nat Commun,* 11**,** 4305.
544 Moritz, L. E. & Trievel, R. C. 2018. Structure, mechanism, and regulation of polycomb-repressive
545 complex 2. *J Biol Chem,* 293**,** 13805-13814.
546 Mullaart, E., Boerrigter, M. E., Ravid, R., Swaab, D. F. & Vijg, J. 1990. Increased levels of DNA
547 breaks in cerebral cortex of Alzheimer's disease patients. *Neurobiol Aging,* 11**,** 169-73.
548 Owen, B. M. & Davidovich, C. 2022. DNA binding by polycomb-group proteins: searching for the
549 link to CpG islands. *Nucleic Acids Res,* 50**,** 4813-4839.
550 Papin, S. & Paganetti, P. 2020. Emerging Evidences for an Implication of the Neurodegeneration-
551 Associated Protein TAU in Cancer. *Brain Sci,* 10.
552 Phillips, T. 2008. The Role of Methylation in Gene Expression. *Nature Education,* 1.
553 Reinig, J., Ruge, F., Howard, M. & Ringrose, L. 2020. A theoretical model of Polycomb/Trithorax
554 action unites stable epigenetic memory and dynamic regulation. *Nature Communications,* 11**,**
555 4782.
556 Rico, T., Gilles, M., Chauderlier, A., Comptdaer, T., Magnez, R., Chwastyniak, M., Drobecq, H.,
557 Pinet, F., Thuru, X., Buée, L., Galas, M. C. & Lefebvre, B. 2021. Tau Stabilizes Chromatin
558 Compaction. *Front Cell Dev Biol,* 9**,** 740550.

559 Rossi, G., Dalpra, L., Crosti, F., Lissoni, S., Sciacca, F. L., Catania, M., Di Fede, G., Mangieri, M.,
560 Giaccone, G., Croci, D. & Tagliavini, F. 2008. A new function of microtubule-associated
561 protein tau: involvement in chromosome stability. *Cell Cycle,* 7**,** 1788-94.
562 Rossi, G., Redaelli, V., Contiero, P., Fabiano, S., Tagliabue, G., Perego, P., Benussi, L., Bruni, A. C.,
563 Filippini, G., Farinotti, M., Giaccone, G., Buiatiotis, S., Manzoni, C., Ferrari, R. & Tagliavini,
564 F. 2018. Tau Mutations Serve as a Novel Risk Factor for Cancer. *Cancer Res,* 78**,** 3731-3739.
565 Schumacher, A., Faust, C. & Magnuson, T. 1996. Positional cloning of a global regulator of anterior–
566 posterior patterning in mice. *Nature,* 383**,** 250-253.
567 Shireby, G., Dempster, E. L., Policicchio, S., Smith, R. G., Pishva, E., Chioza, B., Davies, J. P.,
568 Burrage, J., Lunnon, K., Seiler Vellame, D., Love, S., Thomas, A., Brookes, K., Morgan, K.,
569 Francis, P., Hannon, E. & Mill, J. 2022. DNA methylation signatures of Alzheimer's disease
570 neuropathology in the cortex are primarily driven by variation in non-neuronal cell-types.
571 *Nature Communications,* 13**,** 5620.
572 Si, Z., Sun, L. & Wang, X. 2021. Evidence and perspectives of cell senescence in neurodegenerative
573 diseases. *Biomedicine & Pharmacotherapy,* 137**,** 111327.
574 Sola, M., Magrin, C., Pedrioli, G., Pinton, S., Salvadè, A., Papin, S. & Paganetti, P. 2020. Tau affects
575 P53 function and cell fate during the DNA damage response. *Commun Biol,* 3**,** 245.
576 Spillantini, M. G., Murrell, J. R., Goedert, M., Farlow, M. R., Klug, A. & Ghetti, B. 1998. Mutation
577 in the tau gene in familial multiple system tauopathy with presenile dementia. *Proc Natl Acad*
578 *Sci U S A,* 95**,** 7737-41.
579 Straining, R. & Eighmy, W. 2022. Tazemetostat: EZH2 Inhibitor. *J Adv Pract Oncol,* 13**,** 158-163.
580 Sultan, A., Nesslany, F., Violet, M., Begard, S., Loyens, A., Talahari, S., Mansuroglu, Z., Marzin, D.,
581 Sergeant, N., Humez, S., Colin, M., Bonnefoy, E., Buee, L. & Galas, M. C. 2011. Nuclear
582 tau, a key player in neuronal DNA protection. *J Biol Chem,* 286**,** 4566-75.
583 Thurston, V. C., Zinkowski, R. P. & Binder, L. I. 1996. Tau as a nucleolar protein in human
584 nonneural cells in vitro and in vivo. *Chromosoma,* 105**,** 20-30.
585 Ulrich, G., Salvade, A., Boersema, P., Cali, T., Foglieni, C., Sola, M., Picotti, P., Papin, S. &
586 Paganetti, P. 2018. Phosphorylation of nuclear Tau is modulated by distinct cellular
587 pathways. *Sci Rep,* 8**,** 17702.
588 Vijayanathan, M., Trejo-Arellano, M. G. & Mozgová, I. 2022. Polycomb Repressive Complex 2 in
589 Eukaryotes-An Evolutionary Perspective. *Epigenomes,* 6.
590 Violet, M., Delattre, L., Tardivel, M., Sultan, A., Chauderlier, A., Caillierez, R., Talahari, S.,
591 Nesslany, F., Lefebvre, B., Bonnefoy, E., Buee, L. & Galas, M. C. 2014. A major role for Tau
592 in neuronal DNA and RNA protection in vivo under physiological and hyperthermic
593 conditions. *Front Cell Neurosci,* 8**,** 84.
594 Von Schimmelmann, M., Feinberg, P. A., Sullivan, J. M., Ku, S. M., Badimon, A., Duff, M. K.,
595 Wang, Z., Lachmann, A., Dewell, S., Ma'ayan, A., Han, M. H., Tarakhovsky, A. & Schaefer,
596 A. 2016. Polycomb repressive complex 2 (PRC2) silences genes responsible for
597 neurodegeneration. *Nat Neurosci,* 19**,** 1321-30.
598 Wang, L., Wang, S. & Li, W. 2012. RSeQC: quality control of RNA-seq experiments.
599 *Bioinformatics,* 28**,** 2184-5.
600 Wingett, S. W. & Andrews, S. 2018. FastQ Screen: A tool for multi-genome mapping and quality
601 control. *F1000Res,* 7**,** 1338.
602 Xie, Z., Bailey, A., Kuleshov, M. V., Clarke, D. J. B., Evangelista, J. E., Jenkins, S. L., Lachmann,
603 A., Wojciechowicz, M. L., Kropiwnicki, E., Jagodnik, K. M., Jeon, M. & Ma'ayan, A. 2021.
604 Gene Set Knowledge Discovery with Enrichr. *Current Protocols,* 1**,** e90.
605 Yang, J., Liu, M., Hong, D., Zeng, M. & Zhang, X. 2021. The Paradoxical Role of Cellular
606 Senescence in Cancer. *Front Cell Dev Biol,* 9**,** 722205.

607 Zhang, L., Silva, T. C., Young, J. I., Gomez, L., Schmidt, M. A., Hamilton-Nelson, K. L., Kunkle, B.
608 W., Chen, X., Martin, E. R. & Wang, L. 2020. Epigenome-wide meta-analysis of DNA
609 methylation differences in prefrontal cortex implicates the immune processes in Alzheimer's
610 disease. *Nat Commun,* 11**,** 6114.
611 Zhao, L., Li, J., Ma, Y., Wang, J., Pan, W., Gao, K., Zhang, Z., Lu, T., Ruan, Y., Yue, W., Zhao, S.,
612 Wang, L. & Zhang, D. 2015. Ezh2 is involved in radial neuronal migration through regulating
613 Reelin expression in cerebral cortex. *Sci Rep,* 5**,** 15484.

614

Figure 1.JPEG

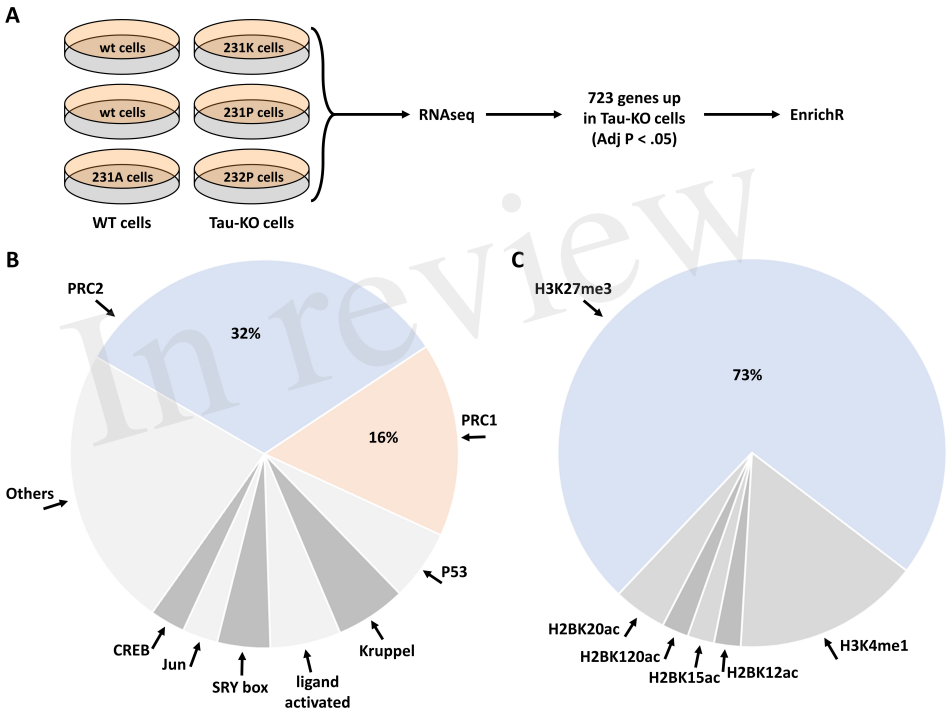

Figure 2.JPEG

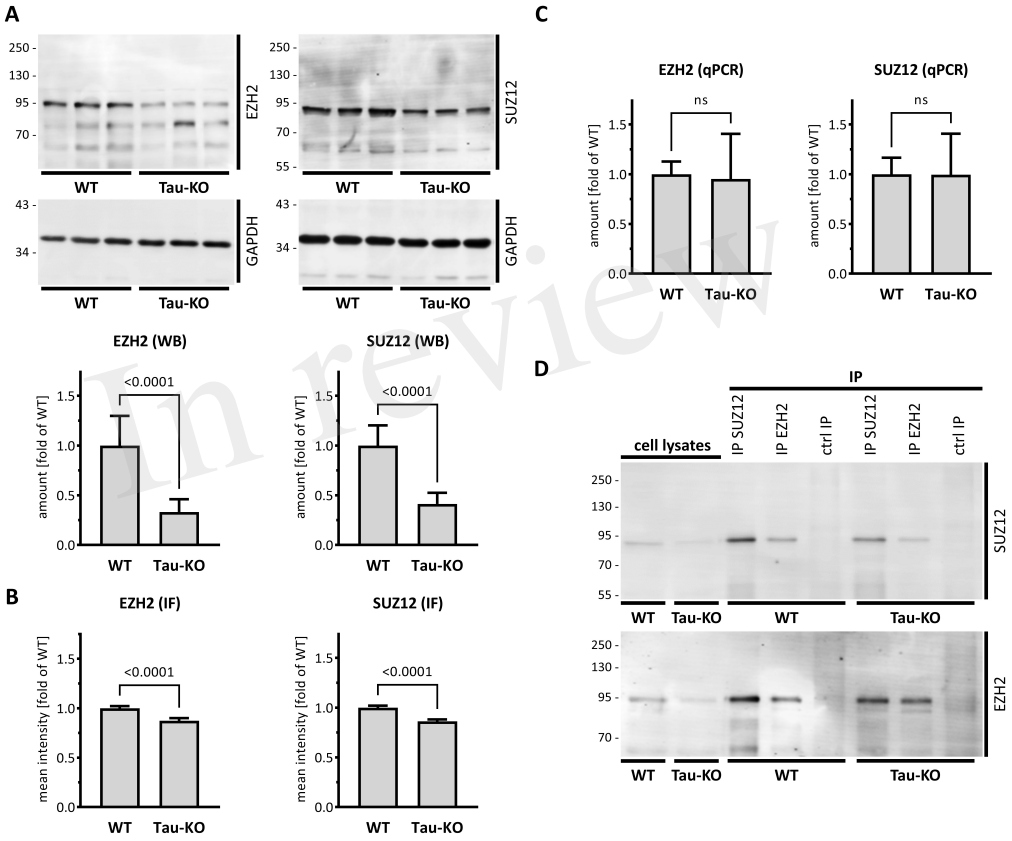

Figure 3.JPEG

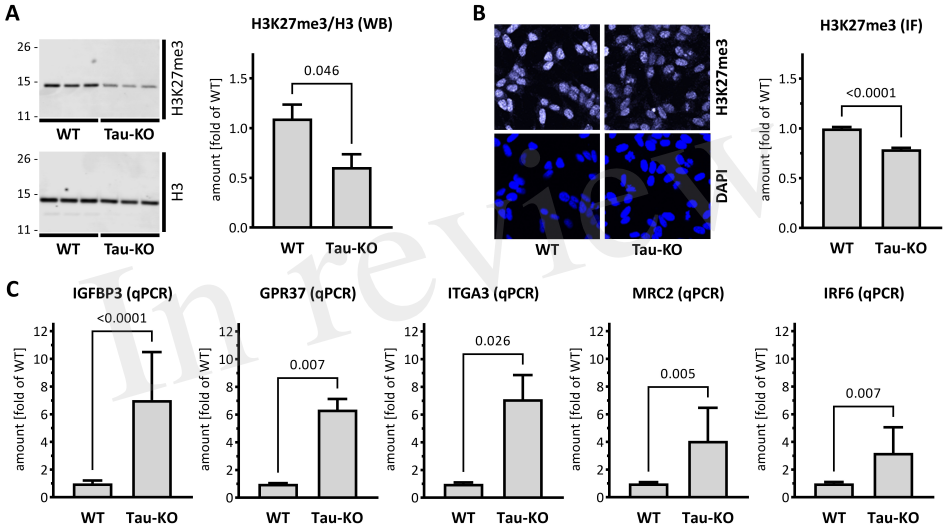

Figure 4.JPEG

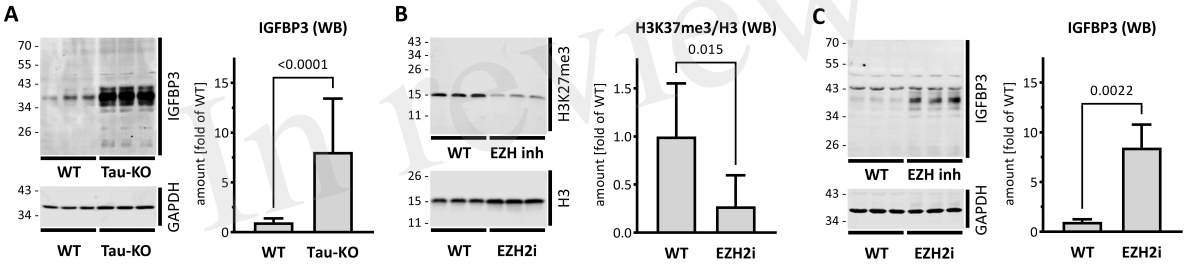

Supplementary Table I. Transcripts upregulated in human Tau-KO SH-SY5Y cells (Adj P <.05) listed in order of decreasing significance

Symbol	log2FC	Symbol	log2FC	Symbol	log2FC	Symbol	log2FC
CDKN1A	2.24	TMEM63A	2.19	WWC3	1.39	PACSIN2	0.39
C22orf34	8.85	PDGFA	4.48	RELB	1.75	AGA	1.82
SLC12A7	2.93	ASB9	3.14	LGR5	2.09	PRCP	0.58
EVC2	7.23	ZFP36L2	0.76	GPX7	0.86	NTRK2	3.13
DCN	10.43	CILP	2.70	SLC10A3	1.17	SSPO	2.79
TNFRSF1A	11.05	LOC100507156	2.69	ARHGEF40	0.99	XYLT1	2.74
HMCN2	2.05	CAVIN2	4.65	CXCL16	4.90	APLP2	0.77
APOBEC3C	3.27	HAS2	6.02	SPATA20	1.04	CBR3	1.69
COL3A1	8.26	TGFB1I1	1.04	TBX2	0.91	ABCA7	0.85
MGP	6.99	CDC42EP1	2.48	IGFBP2	1.21	PDLIM7	1.00
RGS11	1.70	PSMB10	2.44	IL11RA	1.40	MEST	4.65
CFLAR	1.38	OBP2A	5.69	NFKBIE	1.27	EDN3	5.11
RHBDF1	4.25	TRIL	1.74	LRP1B	5.68	ZBTB46	1.51
KCNG1	1.90	DDR1	1.48	PDE4A	1.27	BTG2	0.57
SEL1L3	6.30	SSH3	1.33	RBPMS2	0.72	TCTN3	0.50
S100A11	6.39	CRACR2B	1.93	AVIL	2.59	ABLIM3	1.62
CSF1	1.95	CLU	4.18	BHLHE40	5.44	TESK1	0.76
CCDC80	7.90	VCAN	5.01	HSD3B7	2.55	TNFRSF9	3.24
CD9	3.13	TNS2	1.97	TPBG	2.67	PXDC1	2.20
TIMP1	7.39	S100A10	7.90	ZNF425	0.73	LRP10	1.27
PTGS1	6.25	NT5E	4.88	MCAM	1.92	SERTAD1	1.10
RBPMS	6.08	RDH10	2.62	KIAA0040	1.38	SLC26A11	0.82
LTBP2	1.56	GNG11	1.04	FOXI3	3.60	FMN1	2.87
EVA1A	7.27	MTUS2	5.11	C1QTNF1-AS1	1.16	FSTL1	2.17
S100A16	7.04	LAT2	3.32	PGGHG	1.12	FAM46C	3.27
GNG3	2.71	ST6GAL1	2.61	ORMDL2	0.85	POP5	0.64
TRIM17	1.53	HLX	2.95	KRT17	4.14	NUAK1	3.11
GLIS2	1.32	LUM	4.89	CERCAM	1.17	ZDHHC1	0.84
MAB21L2	9.87	PEAR1	0.78	POLD4	1.71	IRF2BPL	0.84
MR1	5.41	S1PR3	1.65	PLK2	2.05	SEMA3B	1.63
ARHGAP36	3.04	GPX3	1.59	ANTXR1	2.22	RAB3IL1	0.96
TUBB6	1.31	RBM47	6.48	VIM	1.83	BMP1	1.13
A2M	9.55	NQO1	1.89	ZC3H12A	1.50	NOTCH4	1.41
PHLDA3	1.23	ARSA	1.29	RBM24	4.66	LOC101927752	1.11
SYT9	4.48	SPSB2	1.29	PANX2	1.75	STAC	1.11
INSRR	0.79	PTN	3.99	SERPINE1	3.14	COCH	1.22
HGF	10.53	TMEM254	0.86	HECW1	2.42	CRLF1	3.75
ABCC3	6.27	CCL2	4.38	CDH2	2.33	METTL7A	0.78
MOCOS	3.48	ITPKB	2.24	AAED1	1.72	TMEM150C	2.10
C7	2.90	TP53I13	1.31	ANXA7	0.73	TMEM253	1.84
LCAT	1.19	GPNMB	4.78	EPS8L2	1.48	SIRPA	2.87
ITGA5	5.60	ID4	3.92	SERPINB8	2.17	CYTH3	0.49
IDUA	1.64	KIRREL	8.84	SAMD14	1.06	ATXN1	2.37
PRR16	1.84	TRIM5	5.31	CYSTM1	2.26	GJC2	1.61
HS3ST3B1	6.17	KLHL36	1.20	PPCS	0.49	TMED1	0.81
OSGIN1	1.67	SDC4	2.74	SLC7A4	2.57	SLC39A11	0.51

NACC2	1.42	ABI3BP	5.64	RAB26	1.28	RTL5	0.99
CELSR1	5.30	ITM2A	4.28	PLEKHG5	0.76	FOXD1	2.76
GPRC5C	3.49	KCNH2	0.84	FAM110B	0.74	LRRC29	1.27
KCNMB4	1.25	CORIN	7.09	CHRNA9	4.51	WIPI1	1.22
CAVIN1	5.39	GALNT6	2.81	RUSC1	0.72	ADAMTS2	2.13
CHRD	5.54	THSD4	2.39	ROM1	0.78	FBLIM1	1.58
LOXL2	3.68	IER5L	1.47	FEZ1	0.92	SIK2	1.73
ERVMER34-1	3.40	LDLRAP1	1.47	KIF26A	1.00	ZNF467	2.73
TRIOBP	1.19	PLEKHA4	1.34	NPC2	1.71	PTCH2	1.38
MSX2	1.10	ACADS	1.12	METRNL	1.77	NRBP2	0.59
NOTCH1	1.59	DHRS1	0.91	AGRN	1.20	MYO15B	1.06
SPHK1	4.05	AP1G2	0.67	HYI	1.14	CXCL12	3.16
GBP2	6.29	SP5	6.48	SMIM3	3.00	CMTM3	1.20
LAMB3	4.06	HEG1	3.46	FN1	2.99	SLC27A3	1.07
APLNR	2.94	CPVL	1.43	C1orf204	2.44	ARSB	0.82
FAM129A	3.95	COL1A2	2.84	BOK	1.29	LINC00890	7.03
MMP15	2.44	GAD1	4.94	SIX1	6.68	HES1	1.39
TFEB	2.32	ARSD	1.46	SPOCK2	2.08	PPM1M	0.73
IL13RA1	5.07	ORAI3	1.69	FAM124A	1.32	HBEGF	2.73
SLC12A4	1.35	ARID3A	0.63	IGF2BP2	8.80	COL4A1	1.16
FBXL7	0.60	ITGA6	4.65	NRIP2	3.93	PPL	1.31
TGFBI	6.17	NRP1	4.96	CARNS1	3.78	PCOLCE	1.01
VTN	4.11	FOXC1	2.15	EYA4	3.23	C12orf75	1.42
PGF	2.43	SHROOM1	1.40	IL10RB	1.10	CHGB	1.34
VWA5B2	3.59	ACPP	6.17	DNALI1	0.60	POPDC2	1.29
SP110	4.59	ARSJ	4.43	HEXIM1	0.72	GPRC5A	3.64
FGFRL1	5.65	COL27A1	2.11	TGFBR2	2.89	ANXA4	0.74
ACHE	1.92	CA12	5.72	BOC	0.74	NFKB2	1.13
JDP2	1.88	ACADVL	1.17	SNTB1	7.16	MAP3K12	0.51
IGSF11	4.11	NTNG2	1.37	SIX2	4.04	SLC27A1	0.92
LGALS3	1.36	IFITM2	5.59	FGFR2	2.79	HS3ST5	3.81
SPRN	4.16	SERPINF1	2.90	C1QTNF1	2.14	WHRN	1.47
LHFP	2.96	SIX5	2.27	FAM114A1	1.54	ZNF582-AS1	1.37
TGM2	2.51	NTNG1	3.74	ENDOD1	1.20	GNAI2	1.12
ASL	1.33	TGFB3	4.20	CTDSPL	1.10	NPY	1.04
LAYN	3.12	CRYM	4.02	TRADD	1.02	SLIT2	2.86
HSPB7	3.51	RRAS	2.37	PDGFRL	2.76	DUSP3	0.86
NEDD9	4.45	MB21D2	3.10	GALNT2	0.67	LMF2	0.88
MST1	1.09	TMBIM1	3.99	BDKRB2	1.96	NCK2	0.45
HTRA1	5.98	HTR4	7.33	MYO3B	4.59	MCHR1	3.23
SH2D2A	5.79	TAPBP	1.30	CDH11	1.80	FNDC5	2.27
PTGER2	5.63	CTSS	4.36	IFT43	0.89	CST3	1.06
MAP3K6	1.26	RAMP1	1.22	LRPAP1	0.73	TSPAN9	0.78
TNFRSF12A	4.22	COL6A2	1.79	IAH1	0.69	GNB5	0.41
PTPN14	3.56	PGAP3	0.96	S100A2	2.09	UBA7	2.28
PAQR6	0.97	PPIC	2.63	EFEMP2	1.79	ZFP36	1.81
SLC6A9	2.24	TPST1	1.15	HLA-C	2.16	RBM3	0.44
PLA2G4C	3.06	LRRC4C	5.91	PLXDC2	5.96	GBP3	4.67
NOL3	1.08	GLIPR2	1.19	SRPX	2.62	SNX21	0.57
SPON2	3.88	FECH	0.45	SLC9A1	1.38	HPCA	1.66
LTBP1	3.18	CASP4	4.53	ACCS	0.59	LRP1	1.00

3

ATP8A2	6.49	SDK2	2.94	SVIL	2.37	CHPF2	0.72
SLC16A4	5.40	PLAU	3.08	KIAA1217	2.06	RNH1	0.93
KCNAB1	5.26	MIR100HG	5.42	MTCL1	0.95	CD59	1.69
CORO2B	3.38	OSBPL5	2.68	DHRS12	0.67	SHISA4	1.16
PIEZO1	3.24	SLC22A18	1.61	AFAP1L1	1.70	KCNJ2	3.81
KIF1C	2.03	CYBA	1.16	SHISA5	1.81	TLR2	2.98
INPP1	0.80	GADD45A	0.59	ELMO1	1.06	CD274	3.08
RGS3	2.54	LMNA	0.93	RAB7A	0.31	EVC	1.05
RNASET2	1.04	SCUBE2	2.86	COL6A3	2.51	CEP170B	0.90
PLAT	3.14	RELN	4.74	MARCH2	0.84	CHST14	0.69
COL7A1	2.37	PTPN3	3.75	RABEP2	0.84	HGSNAT	0.80
C10orf10	6.27	ARPIN	0.99	TIRAP	0.59	FZD7	2.12
PLPP4	5.73	COL13A1	6.17	SELENOM	1.15	MYO1D	1.41
AGT	5.19	C1QTNF2	2.27	CYBRD1	2.96	CNTNAP1	1.07
IGFBP3	4.25	IL4R	5.70	IGSF1	1.13	TPM2	1.25
MELTF	1.12	SLC31A2	2.09	RAB38	2.34	HOMER3	1.07
EHBP1L1	1.80	TAP1	3.16	VPS9D1	1.01	LOC339803	0.59
SYT12	7.06	PRSS23	3.16	SFXN5	0.73	SFRP1	1.65
CYTOR	7.48	SIPA1	0.93	TRABD2B	5.52	GDF15	1.39
TFPI2	2.36	IL32	3.61	ADORA2A	2.14	BOLA3	0.64
TNC	5.01	ZNF185	2.03	BAALC	2.28	GAP43	1.98
NLRC5	3.23	PAPPA	6.17	B4GALT1	1.57	ARHGAP6	2.71
ANXA2	2.03	FAM19A5	3.34	DKK1	1.25	DYNC1I1	3.00
ADAMTS15	4.93	SYTL4	2.99	MARVELD1	0.81	AHNAK	2.52
SYK	1.39	EDN1	4.66	GBX2	6.09	FAM131B	4.24
SOX9	4.19	SYNGR3	1.10	C6orf1	0.81	IFI6	1.03
COL5A1	4.66	DGKQ	1.15	IL33	5.88	TGFB1	2.76
GPC3	5.16	DEPTOR	4.82	TMEFF2	1.82	IL11	1.75
FAM89A	5.33	GLI1	4.44	PDLIM1	1.75	RARB	2.70
LOC101927809	3.62	EPDR1	0.73	FBXL8	1.16	CMKLR1	3.78
GJA1	8.42	TRAF1	3.60	TMEM8A	0.89	ZYX	1.22
OLFML3	4.44	ASTN1	0.66	OSMR	6.51	SIAE	1.13
DRAM1	2.79	EPS8L1	1.20	FBN1	2.85	RPN2	0.53
MMP11	1.97	FSTL3	2.82	SLC39A13	0.76	LOC645166	1.28
METRN	1.60	FKRP	0.59	STARD8	1.71	KLF2	2.54
SCN4B	1.30	DGKA	1.22	LOC101927204	3.44	SPARCL1	6.88
EWSAT1	4.66	KIAA1211L	2.37	SPOCD1	4.23	NTAN1	0.64
SGPP2	3.40	TBX18	6.79	DEGS1	0.58	ANO10	0.51
SH3TC1	1.70	PID1	3.47	PNPLA3	4.00	HHAT	0.75
ZFYVE21	0.80	B3GNT9	1.06	ISYNA1	0.96	CREB3L2	1.28
MIR4435-2HG	5.83	TNFRSF19	1.60	IFITM3	4.94	C19orf66	1.17
ANGPTL4	5.80	GPR37	3.22	PLTP	0.86	PLXNB1	0.48
SH3RF3	2.56	PTHLH	4.93	KDELR3	2.27	SCN9A	3.17
CD82	1.91	DNAJC22	2.70	CASP8	4.29	SPATA2L	1.12
DKK2	4.40	CD151	1.45	CEL	1.40	ATG16L2	0.73
NTRK1	1.27	GAL3ST1	1.48	NOTCH3	1.28	NUAK2	2.39
ECM1	5.15	LOXL4	1.15	SPRY4	1.16	SPEG	0.66
B3GNT4	2.91	PMP22	0.93	COLEC11	0.80	CEMIP	5.15
SERPINE2	7.09	SVEP1	4.68	PHYKPL	0.50	GFRA1	3.04
TXNDC11	0.65	LSR	1.98	MUM1	0.48	UXS1	1.07
TCF7L1	2.16	DOCK2	4.75	RAB20	1.93	DNASE1L2	1.75

PPP1R13B	1.32	PXDN	0.95	AJUBA	1.25	B3GAT3	0.81
CLCF1	5.16	DUSP10	2.50	CPXM1	1.04	POLR2L	0.90
TRIM21	2.73	MRC2	2.35	NPAS3	4.29	MAN2B2	0.66
YAP1	5.61	DUSP6	1.02	KREMEN1	1.21	CTTN	0.31
KRT18	5.21	ABTB1	1.03	BDKRB1	2.90	SORBS3	0.74
GABARAPL1	1.91	ABHD15	1.19	LGALS1	1.15	BATF3	2.42
GRIN2C	4.75	TRPM4	1.26	LTBP3	0.93	SEMA3D	4.22
RHOC	1.79	EPN3	4.24	LOC100506258	3.75	B4GALNT3	0.94
LRP4	1.91	MAN1A1	3.33	TRIB2	1.95	ADAM19	1.85
EVA1B	2.66	TMEM108-AS1	3.36	SGSH	0.80	EFHD1	1.77
ICAM1	4.82	SCARF2	1.30	IL17RA	2.84	AK5	1.40
TAGLN	1.82	PTPRR	2.22	FAM120AOS	0.48	FMNL1	1.19
PLPPR3	1.26	MIPEP	0.69	PTGR1	2.65	ALKAL2	3.24
SSC5D	4.72	MVP	2.02	ITGA7	2.23	MSRB3	2.38
ADAMTSL4	3.43	CORO2A	2.43	VIPR2	2.17	SH2B3	0.86
PTPRB	2.84	OLFML2A	1.95	TMSB4X	1.66	GFRA2	2.31
RET	0.49	ITGA3	2.65	SUMF1	0.81	CYB5R2	4.47
PTPRE	4.26	CPNE2	1.00	XYLT2	0.76	TMEM59L	0.81
THBS2	9.60	PQLC3	1.46	TMEM100	3.47	DSTNP2	0.94
AQP3	3.09	RPS6KA4	0.88	COL11A2	1.94	BRINP1	2.33
FAM20C	6.85	C1QTNF6	1.51	ITPR3	1.45	SPON1	4.72
BCL3	2.89	SHISA2	5.42	CDC42BPG	2.45	LOC101926941	0.91
RENBP	1.88	MPP4	5.47	SRD5A3	0.47	ID1	0.82
ALS2CL	1.85	GPC4	4.09	HSPB8	3.13	SH3BGRL3	0.92
ECEL1	3.02	LPAR1	3.99	LTK	1.73	CRELD1	0.78
PHLDA1	3.70	NME3	1.43	FLI1	5.30	PSMB8	3.05
FAM111A	4.50	PBXIP1	2.07	LHX9	4.59	ADAMTS7	0.84
ACTA2	1.68	WTIP	3.04	TSPAN8	2.52	RBCK1	0.64
TPM1	1.89	SSBP2	2.20	SMAGP	2.37	IRF6	1.68
IL13RA2	4.48	CHST1	2.05	FAM196B	5.05	DRAXIN	1.28
MOV10L1	3.23	EMILIN1	1.28	SPRY1	1.64	NOD2	1.93
TMEM150A	1.15	CPT1A	0.76	ASIC3	0.87	CAPS	0.73
SPARC	2.82	C1R	2.74	TTLL3	0.81		

21

5

Tau Protein Modulates an Epigenetic Mechanism of Cellular Senescence

Claudia Magrin[1,2], Martina Sola[1,2], Ester Piovesana[1,2], Marco Bolis[3], Andrea Rinaldi[4], Stéphanie Papin[1,†], Paolo Paganetti[1, 2,†,*]

[1]Laboratory for Aging Disorders, Laboratories for Translational Research, Ente Cantonale Ospedaliero, Bellinzona, Switzerland.

[2]PhD Program in Neurosciences, Faculty of Biomedical Sciences, Università della Svizzera Italiana, Lugano, Switzerland.

[3]Functional Cancer Genomics Laboratory, Institute of Oncology Research, Bellinzona, Switzerland. Bioinformatics Core Unit, Swiss Institute of Bioinformatics, Bellinzona, Switzerland. Università della Svizzera Italiana, Lugano, Switzerland. Laboratory of Molecular Biology, Istituto di Ricerche Farmacologiche Mario Negri IRCCS, Milano, Italy.

[4]Lymphoma and Genomics Research Program, Institute of Oncology Research, Bellinzona, Switzerland

[†]These authors share last authorship

*** Correspondence:**

Prof. Paolo Paganetti, Laboratory for Aging Disorders, LRT EOC, Via Chiesa 5, 6500 Bellinzona, Switzerland. Phone +4158 666 7103.
paolo.paganetti@eoc.ch

Keywords: Tau, PRC2, transcription, IGFBP3, senescence, aging, disease

Supplementary Table II. CHiP datasets identified with 723 upregulated transcripts in human Tau-KO cells (Adj P<.01). Analysis performed August 4th 2022.

ChEA_2016 Term	Adj P	Comment
SUZ12 20075857 ChIP-Seq MESCs Mouse	1.22E-31	PRC2 core
MTF2 20144788 ChIP-Seq MESCs Mouse	3.73E-21	PRC2.1 facultative subunit
ELK3 25401928 ChIP-Seq HUVEC Human	1.83E-17	TX factor
RELA 24523406 ChIP-Seq FIBROSARCOMA Human	1.27E-12	TX factor - NFKB subunit - EZH2 interactor
SUZ12 18974828 ChIP-Seq MESCs Mouse	1.89E-12	PRC2 core
TCF21 26020271 ChIP-Seq SMOOTH MUSCLE Human	1.90E-12	TX factor - basic helix-loop-helix
RACK7 27058665 Chip-Seq MCF-7 Human	1.78E-11	TX regulator - RACK receptor - PRC2 regulator
SUZ12 27294783 Chip-Seq ESCs Mouse	3.39E-11	PRC2 core
EGR1 20690147 ChIP-Seq ERYTHROLEUKEMIA Human	4.40E-11	TX regulator - C2H2 zink finger
SUZ12 18692474 ChIP-Seq MEFs Mouse	9.20E-11	PRC2 core
KDM2B 26808549 Chip-Seq K562 Human	2.20E-10	PRC1 core
EZH2 27294783 Chip-Seq ESCs Mouse	2.20E-10	PRC2 core
JARID2 20075857 ChIP-Seq MESCs Mouse	6.20E-10	PRC2.2 facultative subunit
RNF2 18974828 ChIP-Seq MESCs Mouse	6.31E-10	PRC1 core
EZH2 18974828 ChIP-Seq MESCs Mouse	6.31E-10	PRC2 core
WT1 20215353 ChIP-ChIP NEPHRON PROGENITOR Mouse	6.31E-10	TX factor
RING1B 27294783 Chip-Seq ESCs Mouse	6.75E-10	PRC1 core
SUZ12 18692474 ChIP-Seq MESCs Mouse	1.05E-09	PRC2 core
SUZ12 18555785 ChIP-Seq MESCs Mouse	4.07E-09	PRC2 core
KDM2B 26808549 Chip-Seq SUP-B15 Human	4.83E-09	PRC1 core
SRY 25088423 ChIP-ChIP EMBRYONIC GONADS Mouse	7.06E-09	TX factor - SRY-Box
KLF4 26769127 Chip-Seq PDAC-Cell line Human	3.39E-08	TX - Kruppel
RNF2 27304074 Chip-Seq ESCs Mouse	5.77E-08	PRC1 core
WT1 25993318 ChIP-Seq PODOCYTE Human	7.32E-08	TX factor
JARID2 20064375 ChIP-Seq MESCs Mouse	9.08E-08	PRC2.2 facultative subunit
SOX2 20726797 ChIP-Seq SW620 Human	1.31E-07	TX factor - SRY-Box
RARG 19884340 ChIP-ChIP MEFs Mouse	2.46E-07	TX factor - ligand activated
UBF1/2 26484160 Chip-Seq HMEC-DERIVED Human	3.52E-07	TX factor - RNA transcription
RUNX2 24764292 ChIP-Seq MC3T3 Mouse	6.32E-07	TX factor
TP53 20018659 ChIP-ChIP R1E Mouse	9.40E-07	TX factor - P53 family
SMC1 22415368 ChIP-Seq MEFs Mouse	1.09E-06	cohesin subunit - PRC1 regulator
ZNF217 24962896 ChIP-Seq MCF-7 Human	2.05E-06	TX factor - repressor - PRC2 regulator
SA1 22415368 ChIP-Seq MEFs Mouse	3.08E-06	cohesin subunit
KDM2B 26808549 Chip-Seq JURKAT Human	3.08E-06	PRC1 core
RING1B 27294783 Chip-Seq NPCs Mouse	3.08E-06	PRC1 core
KLF5 25053715 ChIP-Seq YYC3 Human	3.08E-06	TX - Kruppel
ESR2 21235772 ChIP-Seq MCF-7 Human	4.87E-06	TX factor - hormone activated
KDM2B 26808549 Chip-Seq DND41 Human	9.18E-06	PRC1 core
EOMES 21245162 ChIP-Seq HESCs Human	1.05E-05	TX factor - T-box
P300 27058665 Chip-Seq ZR-75-30cells Human	1.49E-05	HAT
JUN 26020271 ChIP-Seq SMOOTH MUSCLE Human	1.49E-05	TX factor - proto-oncogene
KLF6 26769127 Chip-Seq PDAC-Cell line Human	2.39E-05	TX - Kruppel
CJUN 26792858 Chip-Seq BT549 Human	2.39E-05	TX factor - proto-oncogene
CTCF 27219007 Chip-Seq ERYTHROID Human	2.39E-05	TX regulator - zink finger - PRC2 regulator
ATF3 23680149 ChIP-Seq GBM1-GSC Human	2.70E-05	TX factor - CREB
BACH1 22875853 ChIP-PCR HELA AND SCP4 Human	3.63E-05	TX factor - CNC-bZip - PRC2 regulator

KDM2B 26808549 Chip-Seq SIL-ALL Human	6.35E-05	PRC1 core
ZFP281 27345836 Chip-Seq ESCs Mouse	6.35E-05	TX factor - repressor - PRC2 regulator
CEBPD 21427703 ChIP-Seq 3T3-L1 Mouse	7.41E-05	TX factor - bZIP
P63 26484246 Chip-Seq KERATINOCYTES Human	0.00010	TX factor - P53 family
TP63 17297297 ChIP-ChIP HaCaT Human	0.00013	TX factor - P53 family
EED 16625203 ChIP-ChIP MESCs Mouse	0.00014	PRC2 core
NFI 21473784 ChIP-Seq ESCs Mouse	0.00016	TX factor - CTF/NF-I family
EZH2 27304074 Chip-Seq ESCs Mouse	0.00021	PRC2 core
ELF3 26769127 Chip-Seq PDAC-Cell line Human	0.00025	TX factor
LXR 22292898 ChIP-Seq THP-1 Human	0.00025	TX factor - ligand activated
ESR1 21235772 ChIP-Seq MCF-7 Human	0.00033	TX factor - hormone activated
BRD4 25478319 ChIP-Seq HGPS Human	0.00037	TX factor - bromodomain
SMC3 22415368 ChIP-Seq MEFs Mouse	0.00037	cohesin subunit - PRC1 regulator
CLOCK 20551151 ChIP-Seq 293T Human	0.00037	TX factor - regulation of circadian rhythms
CTCF 27219007 Chip-Seq Bcells Human	0.00037	TX regulator - zink finger - PRC2 regulator
SUZ12 16625203 ChIP-ChIP MESCs Mouse	0.00057	PRC2 core
CREB1 26743006 Chip-Seq LNCaP-abl Human	0.00057	TX factor - CREB
CTCF 21964334 Chip-Seq Bcells Human	0.00057	TX regulator - zink finger - PRC2 regulator
TP53 23651856 ChIP-Seq MEFs Mouse	0.00071	TX factor - P53 family
KLF4 18358816 ChIP-ChIP MESCs Mouse	0.00091	TX - Kruppel
SOX9 24532713 ChIP-Seq HFSC Mouse	0.00097	TX factor - SRY-Box
NUCKS1 24931609 ChIP-Seq HEPATOCYTES Mouse	0.00097	TX regulator - dna repair

21

Tau Protein Modulates an Epigenetic Mechanism of Cellular Senescence

Claudia Magrin[1,2], Martina Sola[1,2], Ester Piovesana[1,2], Marco Bolis[3], Andrea Rinaldi[4], Stéphanie Papin[1,†], Paolo Paganetti[1, 2,†,*]

[1]Laboratory for Aging Disorders, Laboratories for Translational Research, Ente Cantonale Ospedaliero, Bellinzona, Switzerland.

[2]PhD Program in Neurosciences, Faculty of Biomedical Sciences, Università della Svizzera Italiana, Lugano, Switzerland.

[3]Functional Cancer Genomics Laboratory, Institute of Oncology Research, Bellinzona, Switzerland. Bioinformatics Core Unit, Swiss Institute of Bioinformatics, Bellinzona, Switzerland. Università della Svizzera Italiana, Lugano, Switzerland. Laboratory of Molecular Biology, Istituto di Ricerche Farmacologiche Mario Negri IRCCS, Milano, Italy.

[4]Lymphoma and Genomics Research Program, Institute of Oncology Research, Bellinzona, Switzerland

[†]These authors share last authorship

*** Correspondence:**

Prof. Paolo Paganetti, Laboratory for Aging Disorders, LRT EOC, Via Chiesa 5, 6500 Bellinzona, Switzerland. Phone +4158 666 7103.
paolo.paganetti@eoc.ch

Keywords: Tau, PRC2, transcription, IGFBP3, senescence, aging, disease

Supplementary Table III. Epigenomic datasets identified with 723 upregulated transcripts in human Tau-KO cells (Adj P<.01). Analysis performed August 4th 2022.

Epigenomics Roadmap HM ChIP Term	Adj P	Comment
H3K27me3 H1	6.4E-23	H3K27me3
H3K27me3 Colonic Mucosa	1.2E-18	H3K27me3
H3K27me3 Mobilized CD34 Primary Cells	2.9E-16	H3K27me3
H3K27me3 Fetal Brain	1.8E-15	H3K27me3
H3K27me3 iPS-20b	1.2E-11	H3K27me3
H3K27me3 iPS DF 19.11	7.3E-11	H3K27me3
H3K27me3 CD34 Primary Cells	3.1E-10	H3K27me3
H3K27me3 H9	4.2E-10	H3K27me3
H3K27me3 CD8 Memory Primary Cells	3.1E-09	H3K27me3
H3K27me3 iPS DF 6.9	1.4E-08	H3K27me3
H3K27me3 CD4+ CD25- CD45RA+ Naive Primary Cells	2.2E-08	H3K27me3
H3K27me3 CD8 Naive Primary Cells	3.2E-08	H3K27me3
H3K27me3 Rectal Smooth Muscle	4.0E-08	H3K27me3
H3K27me3 H1 BMP4 Derived Mesendoderm Cultured Cells	9.7E-08	H3K27me3
H2BK20ac IMR90	1.7E-07	H2BK20ac
H3K27me3 CD4+ CD25int CD127+ Tmem Primary Cells	2.6E-07	H3K27me3
H3K27me3 Duodenum Mucosa	3.1E-07	H3K27me3
H3K27me3 iPS-15b	1.3E-06	H3K27me3
H3K27me3 H1 BMP4 Derived Trophoblast Cultured Cells	1.9E-06	H3K27me3
H3K4me1 CD4+ CD25- CD45RA+ Naive Primary Cells	9.5E-06	H3K4me1
H3K27me3 Rectal Mucosa	1.6E-05	H3K27me3
H3K4me1 H1	3.2E-05	H3K4me1
H3K4me1 Brain Germinal Matrix	3.4E-05	H3K4me1
H2BK20ac H1	3.5E-05	H2BK20ac
H3K27me3 Brain Germinal Matrix	4.6E-05	H3K27me3
H3K4me1 IMR90	5.8E-05	H3K4me1
H3K27me3 CD4+ CD25- CD45RO+ Memory Primary Cells	1.4E-04	H3K27me3
H3K27me3 Pancreatic Islets	1.9E-04	H3K27me3
H3K27me3 CD3 Primary Cells	2.4E-04	H3K27me3
H3K27me3 Neurosphere Cultured Cells Cortex Derived	2.5E-04	H3K27me3
H2BK12ac IMR90	2.7E-04	H2BK12ac
H3K4me1 CD4+ CD25- Th Primary Cells	2.7E-04	H3K4me1
H3K4me1 Fetal Brain	2.8E-04	H3K4me1
H3K27me3 CD4 Naive Primary Cells	3.2E-04	H3K27me3
H3K27me3 Stomach Mucosa	4.3E-04	H3K27me3
H3K27me3 CD4+ CD25+ CD127- Treg Primary Cells	5.2E-04	H3K27me3
H3K27me3 Fetal Lung	7.6E-04	H3K27me3
H3K27me3 CD4+ CD25- Th Primary Cells	8.1E-04	H3K27me3
H3K27me3 Duodenum Smooth Muscle	0.0011	H3K27me3
H2BK15ac IMR90	0.0018	H2BK15ac
H3K27me3 Brain Hippocampus Middle	0.0021	H3K27me3
H3K27me3 CD4 Memory Primary Cells	0.0028	H3K27me3
H2BK120ac IMR90	0.0031	H2BK120ac
H3K27me3 Brain Substantia Nigra	0.0031	H3K27me3
H3K4me1 iPS DF 6.9	6.6E-03	H3K4me1

Tau Protein Modulates an Epigenetic Mechanism of Cellular Senescence

Claudia Magrin[1,2], Martina Sola[1,2], Ester Piovesana[1,2], Marco Bolis[3], Andrea Rinaldi[4], Stéphanie Papin[1,†], Paolo Paganetti[1, 2,†,*]

[1]Laboratory for Aging Disorders, Laboratories for Translational Research, Ente Cantonale Ospedaliero, Bellinzona, Switzerland.

[2]PhD Program in Neurosciences, Faculty of Biomedical Sciences, Università della Svizzera Italiana, Lugano, Switzerland.

[3]Functional Cancer Genomics Laboratory, Institute of Oncology Research, Bellinzona, Switzerland. Bioinformatics Core Unit, Swiss Institute of Bioinformatics, Bellinzona, Switzerland. Università della Svizzera Italiana, Lugano, Switzerland. Laboratory of Molecular Biology, Istituto di Ricerche Farmacologiche Mario Negri IRCCS, Milano, Italy.

[4]Lymphoma and Genomics Research Program, Institute of Oncology Research, Bellinzona, Switzerland

[†]These authors share last authorship

*** Correspondence:**

Prof. Paolo Paganetti, Laboratory for Aging Disorders, LRT EOC, Via Chiesa 5, 6500 Bellinzona, Switzerland. Phone +4158 666 7103.
paolo.paganetti@eoc.ch

Keywords: Tau, PRC2, transcription, IGFBP3, senescence, aging, disease

Supplementary Table IV: qPCR primers

mRNA	Forward primer (5'-3')	Reverse primer (5'-3')
EZH2	GACCTCTGTCTTACTTGTGGAGC	CGTCAGATGGTGCCAGCAATAG
SUZ12	CCATGCAGGAAATGGAAGAATGTC	CTGTCCAACGAAGAGTGAACTGC
IGFBP3	CGCTACAAAGTTGACTACGAGTC	GTCTTCCATTTCTCTACGGCAGG
GPR37	TTCTGCCTTCCGCTGGTCATCT	TGAAGGTGGTGACTCCCAGAGA
ITGA3	GCCTGACAACAAGTGTGAGAGC	GGTGTTCGTCACGTTGATGCTC
MRC2	GGCAAGGACAAGAAGTGCGTGT	CTTTGGTGACGTTGCTGCGCTT
IRF6	AGAGAAGCAGCCACCGTTTGAG	GATCATCCGAGCCACTACTGGA

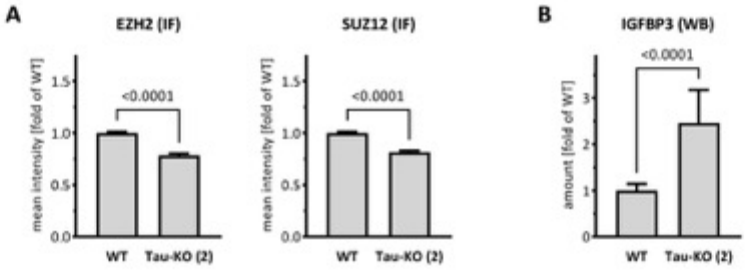

Supplementary Figure 1. Reduced EZH2/SUZ12 and increased IGFBP3 in an independent Tau-KO SH-SY5Y cell line.

(**A**). Nuclear EZH2 or SUZ12 mean fluorescent intensity was analyzed by immune fluorescence staining and laser confocal microscopy with EZH2 or SUZ12 antibodies revealed with an anti-rabbit AlexaFluor 488 antibody. Data obtained with a DAPI nuclear mask (ImageJ) are reported as fold of WT; mean ± sem of 202-208 nuclei (EZH2) or 182-184 nuclei (SUZ12), unpaired Mann-Whitney test. (**B**). IGFBP3 was determined by western blot for matched protein amounts of parental (WT) or Tau-KO (2) cell lysates (biological triplicates on a single gel). Data are reported as fold of WT, mean ± SD of 9 biological replicates, unpaired Mann-Whitney test.

Chapter 5

1. Discussion and perspectives

The main features of Tau can be concisely described with its two main roles in health and disease. These two features span between physiology, when regulating cytoskeletal activities as a microtubule-binding protein, and pathology, when becoming a cause of proteinotoxicity. In the two chapters summarizing the data collected during my research, I investigated whether emerging, non-canonical functions of Tau may represent pieces of the puzzle that we are still missing towards completing our understanding of the biology of a protein identified more than 50 years ago. To address this challenging task, I developed my project on a simple model based on the *MAPT* gene deletion in a human neuroblastoma cell, which has been intensively studied over the years to describe the main features of Tau mentioned above. First, I discovered that by depleting Tau from the cells, a loss-of-function of Tau, possibly associated to a pathogenic mechanism, is revealed only when the cells are exposed to a toxic insult, somehow mimicking the aging process. Indeed, exposure of Tau knockout cells to a DNA damage had a profound effect on P53 stabilization and the role of this latter in balancing cell fate. Then, I applied a bioinformatic analysis of the transcriptome of Tau knockout cells to discover that Tau is involved in an epigenetic mechanism regulating the induction of cellular senescence, another potentially pathogenic process. I also contributed during the course of my project to produce evidence that Tau expression correlated to survival, drug efficacy, and cellular pathways as main cancer traits. Discovering that depending on the cancer type the correlation was either positive or negative suggests that both Tau depletion and Tau overexpression may lead to a profound disturbance of the equilibrium existing between cell death and cell growth. Moreover, the data imply that Tau action on P53 and the epigenetic regulator PRC2 may contribute not only to a neurodegeneration but also to neoplastic conditions, major aging-associated disorders.

1.1 Tau affects P53 function and cell fate during the DNA damage response

We first present novel findings supporting the role of Tau as a regulator of cell fate in response to DNA double-strand breaks (DSBs). Our study highlights how Tau influences this process by modulating the activity of $P53^{288}$. These findings are significant in the context of understanding human aging-related diseases, as a potential loss of Tau function may

contribute to their development. Additionally, since P53 activity dysregulation is implicated in cancer, our observations propose the involvement of Tau in this group of disease as well. The possible role of apoptosis in neurodegenerative cell loss has been well-documented[289], but the role of Tau in modulating this process remains uncertain[290,291]. Our findings shed new light on this process revealing that an acute and brief DNA damage event triggers a positive correlation between Tau and programmed cell death, while negatively affecting cellular senescence. The accumulation of senescent cells with age contributes to tissue deterioration and neuronal dysfunction[292,293]. Notably, a tauopathy model characterized by reduced soluble Tau exhibited increased numbers of senescent glial cells, and intriguingly, the removal of these senescent cells prevented functional decline in neurons[294]. However, direct evidence demonstrating that Tau loss-of-function promotes senescence has not been reported to date. The delicate balance between apoptosis and senescence is regulated by a complex mechanism that can vary depending on different stressors[295]. Upon DNA damage, critical factors such as the type and intensity of the stress influence cell fate.

P53 is considered the key player in both apoptosis and senescence induction through changes in P53 kinetics and transcriptional activity both controlled by post-translational modifications[296]. Our finding that Tau modifies P53 protein level and the equilibrium between cell death and senescence suggests that Tau acts as a modifier of P53 post-translational modifications by influencing P53 modulators. Subsequent investigations focused on MDM2, a major interactor of P53 that regulates its degradation through its ubiquitin-ligase activity. Surprisingly, Tau knockout cells presented lower levels of MDM2 even after Etoposide treatment, which should typically result in increased P53 expression. This led to the conclusion that the decreased P53 expression in Tau-KO cells may be attributed to an effect of Tau on MDM2 expression level and/or activity. To further investigate the possible link between Tau and MDM2, we utilized Nutlin-3, a small molecule known to disrupt the p53/MDM2 complex thereby promoting activation of P53. When the Etoposide-treated cells were incubated with Nutlin-3, P53 expression was restored to a similar level in both Tau-KO and Tau-expressing cells. However, it only partially reversed the reduced activation of the apoptotic pathway. These findings suggest that Tau is involved in regulating the stability of the p53/MDM2 complex. In addition to its role in ubiquitinating P53[297], MDM2 inhibits P53 transcriptional activity though the binding to the amino-terminal domain of P53[298]. Furthermore, the stability, activity, and degradation of both proteins are controlled by a complex network of post-translational modifications, such as phosphorylation at different sites by multiple kinases[299]. Recent data in our laboratory

demonstrated that Tau binds to MDM2 and this interaction results in the inhibition of MDM2-mediated ubiquitination of P53. In conclusion, the possible molecular mechanism explaining the higher levels of stress-induced P53 stabilization in Tau-expressing cells, compared to Tau knockout cells, can be attributed to the inhibitory function of Tau on MDM2-dependent P53 ubiquitination.

The role of Tau in regulating the biology of P53/MDM2 may represent an important mechanism in neurodegenerative diseases, as abnormal P53 species are found in AD and represent potential biomarkers of AD[300–302]. Furthermore, genetic manipulation of P53 family members in mice affects aging, cognitive decline, and Tau phosphorylation[116,303,304]. In addition, these results strengthen the possible implication of Tau in cancers, evidenced by the observed correlation between Tau expression and survival in various cancer types[305,306].

1.2 Tau Protein Modulates Epigenetic-Mediated Induction of Cellular Senescence

In the second part of the project, we described a non-canonical function of Tau as a modulator of the epigenetic activity of PRC2, leading to the induction of cellular senescence in neuroblastoma SH-SY5Y cells. Specifically, we found, through a bioinformatic analysis, that the genes upregulated in Tau knockout cells were mainly genes normally repressed by PRC2. Our experimental findings confirm the bioinformatics results, as we observed that Tau depletion resulted in decreased cellular levels of PRC2 and its epigenetics mark H3K27me3. Furthermore, we were able to replicate the increased senescence phenotype observed in Tau knockout cells by pharmacologically inhibiting PRC2 in cells expressing Tau. Lastly, our study reports that by reversing, in Tau-deficient cells, the up-regulation of IGFBP3, a known target of PRC2, we were able to impair the induction of senescence. In a recent study conducted on a mouse model of tauopathy, compelling evidence was found to support the correlation between cell senescence and cognitive decline. In particular, the study revealed the presence of p16INK4A-positive senescent glial cells surrounding Tau lesions. Blocking the buildup of microglia cells led to the reduced Tau hyperphosphorylation and Tau fibril deposition as well as the preservation of neurons and cognitive functions[307]. These findings highlight the impact of cell senescence on the progression of tauopathies and suggest that targeting senescent cells may represent a promising therapeutic strategy for preserving cognitive function and preventing neuronal loss in disease. In this respect, our data offer a molecular mechanism driven by Tau, PRC2, IGFBP3, and senescence possibly involved in aging disorders such as neurodegeneration and cancer. Our data are supported by recent findings demonstrating that the repression of H3K27me3 activity of PRC2 leads

to induction of p16 (*CDKN2A*) gene expression with the consequence upregulation of the SASP phenotype and senescence[308,309]. Moreover, Tau has been linked to chromatin remodeling and regulation of gene expression[93,94]. In particular, a study demonstrates a global loss of heterochromatin in mouse and drosophila models of AD as well as in human diseased brain tissue[89]. It has also been found that Tau can bind to histones, contributing to the maintenance of compacted chromatin structure[93]. This suggests that Tau may play a role in promoting chromatin compaction to prevent aberrant gene transcription. However, in tauopathies, misfolding, hyperphosphorylation, or sequestration of Tau in oligomers and fibrils, which are characteristic features of these diseases, may negatively regulate this non-canonical function of Tau. In our study, we demonstrate an additional mechanism involving PRC2, which serves as an instrument for modifying histones and modulating chromatin compaction. Previous research has established the independent role of PRC2 and IGFBP3 in senescence. However, our research is the first to demonstrate that IGFBP3 functions as a key mediator of PRC2-dependent senescence induction, and this in a Tau-regulated manner. Moreover, we found that the levels of Tau protein influence the modulation of IGFBP3.

An implication of PRC2 in PD or AD has been reported[310]. In addition, PRC2 dysfunction is frequently associated with tumor progression and PRC2 represents a valid target for anticancer therapy[311]. Considering the prevalence of these disorders and their impact on society, my findings may help to understand the possible mechanism linking Tau to neurodegeneration and cancer.

The possible link between Tau-dependent modulation of P53 and PRC2 activity could be the newly identified interaction of Tau with MDM2. Recent findings shown that MDM2 can physically interact with PRC2 modulating its activity[312]. MDM2 was shown to enhance the stability of the PRC2 complex and increase its methyltransferase activity, thereby promoting gene silencing[313]. Therefore, the interaction between PRC2 and MDM2 implies the possibility of crosstalk between PRC2-mediated epigenetic regulation and the p53 pathway. However, the precise mechanisms and implications of this interplay are still not fully understood. Further research is needed to fully understand the interplay between PRC2 and MDM2 in different cellular processes and diseases.

1.3 Tau at the interface between neurodegeneration and cancer

Our findings describing a function of Tau as a regulator of P53-dependent cell fate and PRC2-modulation of senescence bring additional insight into the implication of Tau in neurodegeneration but, more importantly, suggest an important contribution of Tau in cancer. Neurodegeneration and cancer are diseases affecting different cell types and having

distinct clinical characteristics[140,314] but recent findings demonstrated that these two diseases are sharing several features. In particular apoptosis and senescence are involved, often in opposite direction, in neurodegeneration and cancer.

Apoptosis plays a crucial role both in neurodegeneration and cancer. In neurodegenerative diseases such as AD and PD an abnormal apoptotic process contributes to the progressive loss of neurons and a cognitive decline[315,316]. However, the dysregulation of apoptosis represents a hallmark of cancer. It is described that cancer cells acquire the ability to evade apoptosis and this leads to an uncontrolled proliferation and contributes to tumor development, progression, and resistance to various therapies[175,317].

Senescence is increased in neurodegeneration and contributes to tissue dysfunction and neuronal loss[318,319]. In cancer, senescence induction of tumor cells represents a useful therapeutic strategy that also presents some adverse effects such as induction of persistent inflammation contributing to disease progression[320]. Preclinical studies have demonstrated that targeting persistent senescent cells, which are responsible for tissue damage, can potentially delay, prevent, or alleviate various disorders. Moreover, the identification of small molecule senolytic drugs that can selectively eliminate these senescent cells has opened up promising avenues for preventing and treating multiple diseases and age-related conditions in humans.

While the similarities between neurodegeneration and cancer are evident, more research is needed to understand the interplay between these two complex and multifaceted disease categories.

2. Outlook

My findings support the hypothesis that the protein Tau exerts noncanonical functions in modulating chromatin maintenance. Moreover, this project led to the discovery of cellular pathways downstream of Tau, one regulating apoptosis though the P53/MDM2 axis and the other regulating cellular senescence through the PRC2/IGFBP3 axis.

The relevance of Tau-dependent regulation of P53 activity, which in the meantime the laboratory has shown to occur through the direct interaction and inhibition of MDM2, requires validation in more complex models of disease. One possibility is to make use of organoids as a model of tauopathy. The laboratory is planning to generate organoids starting from isogenic stem cells expressing wilt-type or P301-mutated Tau. It is expected that the presence of the FTD-Tau mutation will accelerate Tau pathology, and this will establish a model for testing the effect of genetic down-regulation of P53 or MDM2. In addition, the laboratory is implementing a screening assay for compounds interfering with the binding of

Tau to MDM2, and positive hits could be tested in the same model. Alternatively, the laboratory has identified several cancer cell lines expressing Tau. The generation of Tau knockdown lines will allow to test the relevance of Tau in xenograft mouse models of cancer. The molecular mechanism by which Tau modulates the activity of PRC2, particularly its impact on the stability of the complex, is a crucial aspect that needs to be addressed in future studies. Understanding the molecular details of how Tau influences PRC2 stability can provide valuable insights into the underlying mechanisms of the non-canonical function of Tau. One possibility is to perform a co-immunoprecipitation and protein-protein interaction assays in order to examine a possible physical association between Tau and the various subunits of PRC2. The same assay could also inform on the regions or domains involved in this interaction. Furthermore, protein stability assays could be utilized to confirm that Tau affects the stability of PRC2. Specifically, by comparing the degradation rates of PRC2 components in the presence or absence of Tau, it is possible to establish an effect on the turnover of PRC2 subunits and the overall stability of the complex. This approach could be employed to ask whether the antagonistic function of Tau on the E3 ubiquitin ligase MDM2 may be involved in the regulation of PRC2 stability and activity. Another aspect that needs future attention is elucidating the PRC2 targets that are modulated according to Tau expression level. Functional assays such as chromatin immunoprecipitation (ChIP) or chromatin accessibility assays may be suited for this purpose. By assessing changes in PRC2 occupancy or histone modifications in the presence or absence of Tau, it can be determined whether Tau influences the enzymatic activity and targeting of PRC2 to specific genomic regions. For this reason, I started a ChIP-based genome-wide analysis utilizing antibodies against the PRC2 core component SUZ12 and against H3K27me3.

In addition, it is necessary to characterize and validate the function of Tau as an epigenetic modulator in additional cellular models. Specifically, it would be interesting firstly to validate in other neuroblastoma cell lines such as IMR5 or IMR32. This will help confirm whether the regulatory role of Tau on PRC2-mediated epigenetic activity and cellular senescence is a consistent phenomenon across different neuroblastoma cell types. To extend the relevance of the findings to a more clinically relevant context, we plan to validate our findings in induced neurons generated from fibroblasts derived directly from patients, a method established in the laboratory. By conducting these validations, a more comprehensive understanding of the role of Tau in the epigenetic modulation of cellular senescence can be achieved. This knowledge would contribute to advancing our

understanding of the underlying mechanisms and potential therapeutic targets in neurodegenerative diseases and other conditions associated with cellular senescence.

The data generated in the context of this thesis highlight the importance of conducting further studies to explore the physiological and pathological relevance of the non-canonical functions of Tau. These investigations may turn out crucial for gaining a deeper understanding of these functions and its potential implications in therapeutic development, particularly for addressing major unmet medical needs.

Abbreviations

- 0N / 1N = amino-terminal inserts of Tau protein
- 4R / 3R = microtubules-binding repeats of Tau proteins
- Aβ = β-amyloid peptide
- AD = Alzheimer's disease
- AEBP2 = adipocyte enhancer-binding protein 2
- AGD = argyrophilic grain disease
- ATM = ataxia telangiectasia mutated
- ATR = RAD3-related
- CBD = corticobasal degeneration
- CGIs = hypomethylated CpG islands
- Chk1= checkpoint kinase 1
- Chk2 = checkpoint kinase 2
- CNS = central nervous system
- cPRC1= canonical PRC1
- DDR = DNA Damage Response
- DLBCL = diffuse large cell B-cell lymphomas
- DNA = deoxyribonucleic acid
- DSBs = DNA double-strand breaks
- EED = embryonic ectoderm development
- EVs = extracellular vesicles
- EZH2/1 = enhancer of zeste homolog 2 or 1
- FL = follicular lymphomas
- fMRI = functional magnetic resonance imaging
- FTD = frontotemporal dementia
- GCB = germinal center B-cell
- GGT = globular glial tauopathy
- GSK3 = glycogen synthase kinase-3
- H2AK119ub = histone H2A lysine 119 mono-ubiquitination
- H3K9me3= trimethylated Lys9 of histone H3
- HD = Huntington's disease
- HMGA1/HMGA2 = high mobility group protein A
- HP1 = heterochromatin protein 1

- Htt = huntingtin
- JARID2 = Jumonji and AT-rich interaction domain 2
- LOAD = late-onset Alzheimer’s disease
- MAPK = mitogen-activated protein kinase
- MAPT = microtubule associated protein Tau gene
- MBD = microtubule-binding domain
- MDM2= Murine Double Minute 2
- MDMX/MDM4 = murine double minute X protein
- mESCs = mouse embryonic stem cells
- MPNST = malignant peripheral nerve sheath tumor
- ncPRC1 = non-canonical PRC1
- NFTs = neurofibrillary tangles
- NHEJ = non homologous end joining
- p-Tau = phosphorylated Tau
- P301L = Proline 301 to leucine mutation in Tau
- PAI-1 = plasminogen activator type 1
- PcG = Polycomb Group components
- PCGF = Polycomb group ring finger proteins
- PCH = pericentromeric heterochromatin
- PCL1/PCL2/PCL3= Polycomb-like proteins
- PD = Parkinson’s disease
- PDPK = proline-directed protein kinase
- PET = position emission tomography
- PFF = pre-formed fibrils
- PHFs = B-sheets-rich paired helical filaments
- PID = Pick's disease
- PRC1 = Polycomb repressive complex 1
- PRC2 = Polycomb repressive complex 2
- PRE = polycomb response element
- PREs = Polycomb response elements
- PSP = progressive supranuclear palsy
- PTEN = phosphatase and tensin homolog
- PTMs = post-translational modifications
- RNA = ribonucleic acid

- RS = replicative senescence
- SA-b-gal = senescence-associated b-galactosidase
- SAHF = senescence-associated heterochromatin foci
- SASP = senescence-associated secretory pathway
- SIPS = stress-induced premature senescence
- SPECT = single-photon emission computed tomography
- SUZ12 = suppressor of zeste 12
- TBI = traumatic brain injury
- TDP-43 = TAR DNA-binding protein 43
- TNFR = tumor necrosis factor receptor
- WHO = World Health Organization
- γH2AX = histone variant H2AX at Ser 139

Bibliography

1. Erkkinen, M. G., Kim, M. O. & Geschwind, M. D. Clinical Neurology and Epidemiology of the Major Neurodegenerative Diseases. *Cold Spring Harb Perspect Biol* **10**, (2018).
2. The Cost of Dementia | Institute for Neurodegenerative Diseases. https://ind.ucsf.edu/supporting-our-work/cost-dementia.
3. Mercier, L., Audet, T., Hébert, R., Rochette, A. & Dubois, M. F. Impact of motor, cognitive, and perceptual disorders on ability to perform activities of daily living after stroke. *Stroke* **32**, 2602–2608 (2001).
4. Hebert, L. E., Scherr, P. A., McCann, J. J., Beckett, L. A. & Evans, D. A. Is the risk of developing Alzheimer's disease greater for women than for men? *Am J Epidemiol* **153**, 132–136 (2001).
5. Edlow, B. L. & Wu, O. Advanced neuroimaging in traumatic brain injury. *Semin Neurol* **32**, 374–400 (2012).
6. Camprodon, J. A. & Stern, T. A. Selecting Neuroimaging Techniques: A Review for the Clinician. *Prim Care Companion CNS Disord* **15**, (2013).
7. Chen, J. J. Functional MRI of brain physiology in aging and neurodegenerative diseases. *Neuroimage* **187**, 209–225 (2019).
8. Wilkins, J. M. & Trushina, E. Application of Metabolomics in Alzheimer's Disease. *Front Neurol* **8**, 1 (2017).
9. Dugger, B. N. & Dickson, D. W. Pathology of Neurodegenerative Diseases. *Cold Spring Harb Perspect Biol* **9**, (2017).
10. Kovacs, G. G. Molecular Pathological Classification of Neurodegenerative Diseases: Turning towards Precision Medicine. *Int J Mol Sci* **17**, (2016).
11. Kovacs, G. G. Current Concepts of Neurodegenerative Diseases. *EMJ Neurol Neurology 1.1 2014* **1**, 10–11 (2014).
12. Lee, V. M. Y., Goedert, M. & Trojanowski, J. Q. Neurodegenerative tauopathies. *Annu Rev Neurosci* **24**, 1121–1159 (2001).
13. Spillantini, M. G. & Goedert, M. Tau pathology and neurodegeneration. *Lancet Neurol* **12**, 609–622 (2013).
14. Praticò, D. The Functional Role of microRNAs in the Pathogenesis of Tauopathy. *Cells* **9**, (2020).

15. Imbimbo, B. P., Ippati, S., Watling, M. & Balducci, C. A critical appraisal of tau-targeting therapies for primary and secondary tauopathies. *Alzheimers Dement* **18**, 1008–1037 (2022).
16. Chung, D. eun C., Roemer, S., Petrucelli, L. & Dickson, D. W. Cellular and pathological heterogeneity of primary tauopathies. *Molecular Neurodegeneration 2021 16:1* **16**, 1–20 (2021).
17. Austin, T. O., Qiang, L. & Baas, P. W. Mechanisms of Neuronal Microtubule Loss in Alzheimer's Disease. *Neuroprotection in Alzheimer's Disease* 59–71 (2017) doi:10.1016/B978-0-12-803690-7.00004-1.
18. Lee Virginia, M. Y. *et al.* Mutation-specific functional impairments in distinct tau isoforms of hereditary FTDP-17. *Science* **282**, 1914–1917 (1998).
19. Barghorn, S. *et al.* Structure, microtubule interactions, and paired helical filament aggregation by tau mutants of frontotemporal dementias. *Biochemistry* **39**, 11714–11721 (2000).
20. Wolfe, M. S. Tau mutations in neurodegenerative diseases. *J Biol Chem* **284**, 6021–6025 (2009).
21. Holtzman, D. M., Mandelkow, E. & Selkoe, D. J. Alzheimer disease in 2020. *Cold Spring Harb Perspect Med* **2**, (2012).
22. Weingarten, M. D., Lockwood, A. H., Hwo, S. Y. & Kirschner, M. W. A protein factor essential for microtubule assembly. *Proc Natl Acad Sci U S A* **72**, 1858 (1975).
23. Cleveland, D. W., Hwo, S. Y. & Kirschner, M. W. Purification of tau, a microtubule-associated protein that induces assembly of microtubules from purified tubulin. *J Mol Biol* **116**, 207–225 (1977).
24. Ksiezak-Reding, H. *et al.* Ultrastructural alterations of Alzheimer's disease paired helical filaments by grape seed-derived polyphenols. *Neurobiol Aging* **33**, 1427–1439 (2012).
25. Wang, Y. & Mandelkow, E. Tau in physiology and pathology. *Nat Rev Neurosci* **17**, 5–21 (2016).
26. Merezhko, M., Uronen, R. L. & Huttunen, H. J. The Cell Biology of Tau Secretion. *Front Mol Neurosci* **13**, (2020).
27. Dixit, R., Ross, J. L., Goldman, Y. E. & Holzbaur, E. L. F. Differential regulation of dynein and kinesin motor proteins by tau. *Science* **319**, 1086–1089 (2008).

28. Tau blocks traffic of organelles, neurofilaments, and APP vesicles in neurons and enhances oxidative stress - PMC. https://www.ncbi.nlm.nih.gov/pmc/articles/PMC2173473/.
29. Caceres, A. & Kosik, K. S. Inhibition of neurite polarity by tau antisense oligonucleotides in primary cerebellar neurons. *Nature 1990 343:6257* **343**, 461–463 (1990).
30. Janning, D. *et al.* Single-molecule tracking of tau reveals fast kiss-and-hop interaction with microtubules in living neurons. **25**, (2014).
31. Morris, M., Maeda, S., Vossel, K. & Mucke, L. The many faces of tau. *Neuron* **70**, 410–426 (2011).
32. Ittner, L. M. *et al.* Dendritic function of tau mediates amyloid-beta toxicity in Alzheimer's disease mouse models. *Cell* **142**, 387–397 (2010).
33. Hefti, M. M. *et al.* High-resolution temporal and regional mapping of MAPT expression and splicing in human brain development. (2018) doi:10.1371/journal.pone.0195771.
34. Andreadis, A., Brown, W. M. & Kosik, K. S. Structure and novel exons of the human tau gene. *Biochemistry* **31**, 10626–10633 (1992).
35. Mukrasch, M. D. *et al.* Structural Polymorphism of 441-Residue Tau at Single Residue Resolution. *PLoS Biol* **7**, e1000034 (2009).
36. Mandelkow, E. M. & Mandelkow, E. Biochemistry and cell biology of tau protein in neurofibrillary degeneration. *Cold Spring Harb Perspect Med* **2**, 1–25 (2012).
37. Wu, X. L., Piña-Crespo, J., Zhang, Y. W., Chen, X. C. & Xu, H. X. Tau-mediated neurodegeneration and potential implications in diagnosis and treatment of Alzheimer's disease. *Chin Med J (Engl)* **130**, 2978–2990 (2017).
38. Goedert, M., Spillantini, M. G., Jakes, R., Rutherford, D. & Crowther, R. A. Multiple isoforms of human microtubule-associated protein tau: sequences and localization in neurofibrillary tangles of Alzheimer's disease. *Neuron* **3**, 519–526 (1989).
39. Boyarko, B. & Hook, V. Human Tau Isoforms and Proteolysis for Production of Toxic Tau Fragments in Neurodegeneration. *Front Neurosci* **15**, 1293 (2021).
40. Goedert, M., Spillantini, M. G., Potier, M. C., Ulrich, J. & Crowther, R. A. Cloning and sequencing of the cDNA encoding an isoform of microtubule-associated protein tau containing four tandem repeats: differential expression of tau protein mRNAs in human brain. *EMBO J* **8**, 393–399 (1989).

41. Binder, L. I., Frankfurter, A. & Rebhun, L. I. The distribution of tau in the mammalian central nervous system. *J Cell Biol* **101**, 1371–1378 (1985).
42. Kowall, N. W. & Kosik, K. S. Axonal disruption and aberrant localization of tau protein characterize the neuropil pathology of Alzheimer's disease. *Ann Neurol* **22**, 639–643 (1987).
43. Lopresti, P., Szuchet, S., Papasozomenos, S. C., Zinkowski, R. P. & Binder, L. I. Functional implications for the microtubule-associated protein tau: localization in oligodendrocytes. *Proc Natl Acad Sci U S A* **92**, 10369–10373 (1995).
44. Lee, G., Neve, R. L. & Kosik, K. S. The microtubule binding domain of tau protein. *Neuron* **2**, 1615–1624 (1989).
45. Chen, X. & Jiang, H. Tau as a potential therapeutic target for ischemic stroke. *Aging* **11**, 12827–12843 (2019).
46. Beharry, C. *et al.* Tau-induced neurodegeneration: mechanisms and targets. *Neurosci Bull* **30**, 346 (2014).
47. Buée, L. *et al.* From tau phosphorylation to tau aggregation: what about neuronal death? *Biochem Soc Trans* **38**, 967–972 (2010).
48. Neddens, J. *et al.* Phosphorylation of different tau sites during progression of Alzheimer's disease. *Acta Neuropathol Commun* **6**, 52 (2018).
49. Morris, M. *et al.* Tau post-translational modifications in wild-type and human amyloid precursor protein transgenic mice. *Nat Neurosci* **18**, 1183–1189 (2015).
50. Biswas, S. & Kalil, K. The Microtubule-Associated Protein Tau Mediates the Organization of Microtubules and Their Dynamic Exploration of Actin-Rich Lamellipodia and Filopodia of Cortical Growth Cones. *J Neurosci* **38**, 291–307 (2018).
51. Jovanov-Milošević, N. *et al.* Human fetal tau protein isoform: Possibilities for Alzheimer's disease treatment. *Int J Biochem Cell Biol* **44**, 1290 (2012).
52. Hefti, M. M. *et al.* Tau Phosphorylation and Aggregation in the Developing Human Brain. *J Neuropathol Exp Neurol* **78**, 930–938 (2019).
53. Avila, J. Tau kinases and phosphatases. *J Cell Mol Med* **12**, 258–259 (2008).
54. Fan, X. *et al.* Tau Acts in Concert With Kinase/Phosphatase Underlying Synaptic Dysfunction. *Front Aging Neurosci* **14**, 507 (2022).
55. Cohen, T. J. *et al.* The acetylation of tau inhibits its function and promotes pathological tau aggregation. *Nat Commun* **2**, 252 (2011).

56. Caballero, B. *et al.* Acetylated tau inhibits chaperone-mediated autophagy and promotes tau pathology propagation in mice. *Nature Communications 2021 12:1* **12**, 1–18 (2021).
57. Cohen, T. J., Friedmann, D., Hwang, A. W., Marmorstein, R. & Lee, V. M. Y. The microtubule-associated tau protein has intrinsic acetyltransferase activity. *Nat Struct Mol Biol* **20**, 756–762 (2013).
58. Cohen, T. J., Constance, B. H., Hwang, A. W., James, M. & Yuan, C. X. Intrinsic Tau Acetylation Is Coupled to Auto-Proteolytic Tau Fragmentation. *PLoS One* **11**, (2016).
59. Min, S. W. *et al.* Critical role of acetylation in tau-mediated neurodegeneration and cognitive deficits. *Nat Med* **21**, 1154–1162 (2015).
60. Cook, C. *et al.* Acetylation of the KXGS motifs in tau is a critical determinant in modulation of tau aggregation and clearance. *Hum Mol Genet* **23**, 104–116 (2014).
61. Min, S. W. *et al.* Acetylation of tau inhibits its degradation and contributes to tauopathy. *Neuron* **67**, 953–966 (2010).
62. Gong, C.-X. & Iqbal, K. Hyperphosphorylation of Microtubule-Associated Protein Tau: A Promising Therapeutic Target for Alzheimer Disease. *Curr Med Chem* **15**, 2321 (2008).
63. Clavaguera, F. *et al.* Transmission and spreading of tauopathy in transgenic mouse brain. *Nat Cell Biol* **11**, 909–913 (2009).
64. Lasagna-Reeves, C. A. *et al.* Alzheimer brain-derived tau oligomers propagate pathology from endogenous tau. *Sci Rep* **2**, (2012).
65. Zanier, E. R. *et al.* Induction of a transmissible tau pathology by traumatic brain injury. *Brain* **141**, 2685–2699 (2018).
66. Clavaguera, F. *et al.* Brain homogenates from human tauopathies induce tau inclusions in mouse brain. *Proc Natl Acad Sci U S A* **110**, 9535–9540 (2013).
67. Edwards, G., Zhao, J., Dash, P. K., Soto, C. & Moreno-Gonzalez, I. Traumatic Brain Injury Induces Tau Aggregation and Spreading. *J Neurotrauma* **37**, 80 (2020).
68. Guo, J. L. & Lee, V. M. Y. Seeding of normal Tau by pathological Tau conformers drives pathogenesis of Alzheimer-like tangles. *J Biol Chem* **286**, 15317–15331 (2011).
69. Calafate, S. *et al.* Synaptic Contacts Enhance Cell-to-Cell Tau Pathology Propagation. *Cell Rep* **11**, 1176–1183 (2015).

70. Iba, M. *et al.* Synthetic tau fibrils mediate transmission of neurofibrillary tangles in a transgenic mouse model of Alzheimer's-like tauopathy. *J Neurosci* **33**, 1024–1037 (2013).
71. Holmes, B. B. *et al.* Heparan sulfate proteoglycans mediate internalization and propagation of specific proteopathic seeds. *Proc Natl Acad Sci U S A* **110**, E3138–E3147 (2013).
72. Takeda, S. *et al.* Neuronal uptake and propagation of a rare phosphorylated high-molecular-weight tau derived from Alzheimer's disease brain. *Nature Communications 2015 6:1* **6**, 1–15 (2015).
73. Dujardin, S. *et al.* Tau molecular diversity contributes to clinical heterogeneity in Alzheimer's disease. *Nat Med* **26**, 1256–1263 (2020).
74. Pedrioli, G. *et al.* Tau Seeds in Extracellular Vesicles Induce Tau Accumulation in Degradative Organelles of Cells. *DNA Cell Biol* **40**, 1185–1199 (2021).
75. Violet, M. *et al.* A major role for Tau in neuronal DNA and RNA protection in vivo under physiological and hyperthermic conditions. *Front Cell Neurosci* **8**, (2014).
76. Camero, S. *et al.* Thermodynamics of the Interaction between Alzheimer's Disease Related Tau Protein and DNA. *PLoS One* **9**, e104690 (2014).
77. Leroy, K. *et al.* Lack of tau proteins rescues neuronal cell death and decreases amyloidogenic processing of APP in APP/PS1 mice. *Am J Pathol* **181**, 1928–1940 (2012).
78. Wang, Y., Loomis, P. A., Zinkowski, R. P. & Binder, L. I. A novel tau transcript in cultured human neuroblastoma cells expressing nuclear tau. *J Cell Biol* **121**, 257–267 (1993).
79. Loomis, P. A., Howard, T. H., Castleberry, R. P. & Binder, L. I. Identification of nuclear tau isoforms in human neuroblastoma cells. *Proc Natl Acad Sci U S A* **87**, 8422–8426 (1990).
80. Wei, Y. *et al.* Binding to the Minor Groove of the Double-Strand, Tau Protein Prevents DNA from Damage by Peroxidation. *PLoS One* **3**, (2008).
81. Sultan, A. *et al.* Nuclear tau, a key player in neuronal DNA protection. *J Biol Chem* **286**, 4566–4575 (2011).
82. Violet, M. *et al.* A major role for Tau in neuronal DNA and RNA protection in vivo under physiological and hyperthermic conditions. *Front Cell Neurosci* **8**, (2014).
83. Oyama, F. *et al.* Gem GTPase and tau: morphological changes induced by gem GTPase in cho cells are antagonized by tau. *J Biol Chem* **279**, 27272–27277 (2004).

84. Siano, G. *et al.* Gene Expression of Disease-related Genes in Alzheimer's Disease is Impaired by Tau Aggregation. *J Mol Biol* **432**, 166675 (2020).
85. Siano, G. *et al.* Modulation of Tau Subcellular Localization as a Tool to Investigate the Expression of Disease-related Genes. *J Vis Exp* **2019**, (2019).
86. Montalbano, M. *et al.* Tau Modulates mRNA Transcription, Alternative Polyadenylation Profiles of hnRNPs, Chromatin Remodeling and Spliceosome Complexes. *Front Mol Neurosci* **14**, 302 (2021).
87. Sjöberg, M. K., Shestakova, E., Mansuroglu, Z., Maccioni, R. B. & Bonnefoy, E. Tau protein binds to pericentromeric DNA: a putative role for nuclear tau in nucleolar organization. *J Cell Sci* **119**, 2025–2034 (2006).
88. Sjöberg, M. K., Shestakova, E., Mansuroglu, Z., Maccioni, R. B. & Bonnefoy, E. Tau protein binds to pericentromeric DNA: a putative role for nuclear tau in nucleolar organization. *J Cell Sci* **119**, 2025–2034 (2006).
89. Frost, B., Hemberg, M., Lewis, J. & Feany, M. B. Tau promotes neurodegeneration through global chromatin relaxation. *Nat Neurosci* **17**, 357–366 (2014).
90. Benhelli-Mokrani, H. *et al.* Genome-wide identification of genic and intergenic neuronal DNA regions bound by Tau protein under physiological and stress conditions. *Nucleic Acids Res* **46**, 11405–11422 (2018).
91. Gil, L. *et al.* Aging dependent effect of nuclear tau. *Brain Res* **1677**, 129–137 (2017).
92. Payão, S. L. M., De Smith, M. A. C. & Bertolucci, P. H. F. Differential chromosome sensitivity to 5-azacytidine in Alzheimer's disease. *Gerontology* **44**, 267–271 (1998).
93. Rico, T. *et al.* Tau Stabilizes Chromatin Compaction. *Front Cell Dev Biol* **9**, (2021).
94. Rossi, G. *et al.* A new function of microtubule-associated protein tau: Involvement in chromosome stability. *http://dx.doi.org/10.4161/cc.7.12.6012* **7**, 1788–1794 (2008).
95. Rossi, G. *et al.* Mutations in MAPT gene cause chromosome instability and introduce copy number variations widely in the genome. *J Alzheimers Dis* **33**, 969–982 (2013).
96. Violet, M. *et al.* A major role for Tau in neuronal DNA and RNA protection in vivo under physiological and hyperthermic conditions. *Front Cell Neurosci* **8**, (2014).
97. Sultan, A. *et al.* Nuclear tau, a key player in neuronal DNA protection. *J Biol Chem* **286**, 4566–4575 (2011).
98. Mansuroglu, Z. *et al.* Loss of Tau protein affects the structure, transcription and repair of neuronal pericentromeric heterochromatin. *Sci Rep* **6**, (2016).
99. Violet, M. *et al.* A major role for Tau in neuronal DNA and RNA protection in vivo under physiological and hyperthermic conditions. *Front Cell Neurosci* **8**, (2014).

100. Zheng-Fischhöfer, Q. *et al.* Sequential phosphorylation of Tau by glycogen synthase kinase-3beta and protein kinase A at Thr212 and Ser214 generates the Alzheimer-specific epitope of antibody AT100 and requires a paired-helical-filament-like conformation. *Eur J Biochem* **252**, 542–552 (1998).
101. Goedert, M., Jakes, R. & Vanmechelen, E. Monoclonal antibody AT8 recognises tau protein phosphorylated at both serine 202 and threonine 205. *Neurosci Lett* **189**, 167–170 (1995).
102. Wu, C., Bassett, A. & Travers, A. A variable topology for the 30-nm chromatin fibre. *EMBO Rep* **8**, 1129–1134 (2007).
103. Federico, C. *et al.* Phosphorylated nucleolar Tau protein is related to the neuronal in vitro differentiation. *Gene* **664**, 1–11 (2018).
104. Sjöberg, M. K., Shestakova, E., Mansuroglu, Z., Maccioni, R. B. & Bonnefoy, E. Tau protein binds to pericentromeric DNA: a putative role for nuclear tau in nucleolar organization. *J Cell Sci* **119**, 2025–2034 (2006).
105. Wei, Y. *et al.* Binding to the Minor Groove of the Double-Strand, Tau Protein Prevents DNA from Damage by Peroxidation. *PLoS One* **3**, e2600 (2008).
106. West, R. L., Lee, J. M. & Maroun, L. E. Hypomethylation of the amyloid precursor protein gene in the brain of an Alzheimer's disease patient. *J Mol Neurosci* **6**, 141–146 (1995).
107. Wang, S. C., Oeize, B. & Schumacher, A. Age-Specific Epigenetic Drift in Late-Onset Alzheimer's Disease. *PLoS One* **3**, (2008).
108. Kilgore, M. *et al.* Inhibitors of class 1 histone deacetylases reverse contextual memory deficits in a mouse model of Alzheimer's disease. *Neuropsychopharmacology* **35**, 870–880 (2010).
109. Lee, J. H., Kim, E. W., Croteau, D. L. & Bohr, V. A. Heterochromatin: an epigenetic point of view in aging. *Exp Mol Med* **52**, 1466 (2020).
110. Alonso, A. D. *et al.* Hyperphosphorylation of Tau Associates with changes in its function beyond microtubule stability. *Front Cell Neurosci* **12**, 397506 (2018).
111. Maldonado, E., Morales-Pison, S., Urbina, F. & Solari, A. Aging Hallmarks and the Role of Oxidative Stress. *Antioxidants* **12**, (2023).
112. Wilson, D. M. *et al.* Hallmarks of neurodegenerative diseases. *Cell* **186**, 693–714 (2023).
113. McHugh, D. & Gil, J. Senescence and aging: Causes, consequences, and therapeutic avenues. *Journal of Cell Biology* **217**, 65–77 (2018).

114. Hoeijmakers, J. H. J. DNA damage, aging, and cancer. *N Engl J Med* **361**, 1475–1485 (2009).
115. López-Otín, C., Blasco, M. A., Partridge, L., Serrano, M. & Kroemer, G. The Hallmarks of Aging. *Cell* **153**, 1194–1217 (2013).
116. Finicelli, M. & Liu, R.-M. Aging, Cellular Senescence, and Alzheimer's Disease. *International Journal of Molecular Sciences 2022, Vol. 23, Page 1989* **23**, 1989 (2022).
117. Sinsky, J., Pichlerova, K. & Hanes, J. Tau Protein Interaction Partners and Their Roles in Alzheimer's Disease and Other Tauopathies. *Int J Mol Sci* **22**, (2021).
118. Rose, M. R. Adaptation, aging, and genomic information. *Aging (Albany NY)* **1**, 444 (2009).
119. Amaro-Ortiz, A., Yan, B. & D'Orazio, J. A. Ultraviolet Radiation, Aging and the Skin: Prevention of Damage by Topical cAMP Manipulation. *Molecules* **19**, 6202 (2014).
120. Rocca, W. A. *et al.* Trends in the incidence and prevalence of Alzheimer's disease, dementia, and cognitive impairment in the United States. *Alzheimers Dement* **7**, 80–93 (2011).
121. Schrijvers, E. M. C. *et al.* Is dementia incidence declining?: Trends in dementia incidence since 1990 in the Rotterdam Study. *Neurology* **78**, 1456–1463 (2012).
122. Madabhushi, R., Pan, L. & Tsai, L. H. DNA damage and its links to neurodegeneration. *Neuron* **83**, 266–282 (2014).
123. Konopka, A. & Atkin, J. D. The Role of DNA Damage in Neural Plasticity in Physiology and Neurodegeneration. *Front Cell Neurosci* **16**, 268 (2022).
124. López-Otín, C., Blasco, M. A., Partridge, L., Serrano, M. & Kroemer, G. The Hallmarks of Aging. *Cell* **153**, 1194 (2013).
125. Chow, H. M. & Herrup, K. Genomic integrity and the ageing brain. *Nat Rev Neurosci* **16**, 672–684 (2015).
126. O'Sullivan, R. J., Kubicek, S., Schreiber, S. L. & Karlseder, J. Reduced histone biosynthesis and chromatin changes arising from a damage signal at telomeres. *Nat Struct Mol Biol* **17**, 1218–1225 (2010).
127. Hu, Z. *et al.* Nucleosome loss leads to global transcriptional up-regulation and genomic instability during yeast aging. *Genes Dev* **28**, 396–408 (2014).

128. Day, K. *et al.* Differential DNA methylation with age displays both common and dynamic features across human tissues that are influenced by CpG landscape. *Genome Biol* **14**, (2013).
129. Lemoine, M. The Evolution of the Hallmarks of Aging. *Front Genet* **12**, (2021).
130. van der Rijt, S., Molenaars, M., McIntyre, R. L., Janssens, G. E. & Houtkooper, R. H. Integrating the Hallmarks of Aging Throughout the Tree of Life: A Focus on Mitochondrial Dysfunction. *Front Cell Dev Biol* **8**, 1422 (2020).
131. Tabarés-Seisdedos, R. *et al.* No paradox, no progress: inverse cancer comorbidity in people with other complex diseases. *Lancet Oncol* **12**, 604–608 (2011).
132. Driver, J. A. *et al.* Inverse association between cancer and Alzheimer's disease: results from the Framingham Heart Study. *BMJ* **344**, 19 (2012).
133. Inzelberg, R. & Jankovic, J. Are Parkinson disease patients protected from some but not all cancers? *Neurology* **69**, 1542–1550 (2007).
134. Olsen, J. H. *et al.* Atypical cancer pattern in patients with Parkinson's disease. *Br J Cancer* **92**, 201–205 (2005).
135. Olsen, J. H., Friis, S. & Frederiksen, K. Malignant melanoma and other types of cancer preceding Parkinson disease. *Epidemiology* **17**, 582–587 (2006).
136. Driver, J. A., Logroscino, G., Buring, J. E., Gaziano, J. M. & Kurth, T. A prospective cohort study of cancer incidence following the diagnosis of Parkinson's disease. *Cancer Epidemiol Biomarkers Prev* **16**, 1260–1265 (2007).
137. Moller, H., Mellemkjaer, L., McLaughlin, J. K. & Olsen, J. H. Occurrence of different cancers in patients with Parkinson's disease. *BMJ : British Medical Journal* **310**, 1500 (1995).
138. Ospina-Romero, M. *et al.* Association Between Alzheimer Disease and Cancer With Evaluation of Study Biases: A Systematic Review and Meta-analysis. *JAMA Netw Open* **3**, (2020).
139. Ibáñez, K., Boullosa, C., Tabarés-Seisdedos, R., Baudot, A. & Valencia, A. Molecular Evidence for the Inverse Comorbidity between Central Nervous System Disorders and Cancers Detected by Transcriptomic Meta-analyses. *PLoS Genet* **10**, e1004173 (2014).
140. Klus, P., Cirillo, D., Botta Orfila, T. & Gaetano Tartaglia, G. Neurodegeneration and Cancer: Where the Disorder Prevails. *Scientific Reports 2015 5:1* **5**, 1–7 (2015).

141. Sankowski, R., Mader, S. & Valdés-Ferrer, S. I. Systemic inflammation and the brain: Novel roles of genetic, molecular, and environmental cues as drivers of neurodegeneration. *Front Cell Neurosci* **9**, 28 (2015).
142. Acharya, A., Das, I., Chandhok, D. & Saha, T. Redox Regulation in Cancer: A Double-edged Sword with Therapeutic Potential. *Oxid Med Cell Longev* **3**, 23–34 (2010).
143. Lee, J.-H. & Ryu, H. Epigenetic modification is linked to Alzheimer's disease: is it a maker or a marker? *BMB Rep* **43**, 649–655 (2010).
144. Liou, Y. C. *et al.* Role of the prolyl isomerase Pin1 in protecting against age-dependent neurodegeneration. *Nature 2003 424:6948* **424**, 556–561 (2003).
145. Kandoth, C. *et al.* Mutational landscape and significance across 12 major cancer types. *Nature 2013 502:7471* **502**, 333–339 (2013).
146. Duffy, M. J., Synnott, N. C. & Crown, J. Mutant p53 as a target for cancer treatment. *Eur J Cancer* **83**, 258–265 (2017).
147. Bieging, K. T., Mello, S. S. & Attardi, L. D. Unravelling mechanisms of p53-mediated tumour suppression. *Nature Reviews Cancer 2014 14:5* **14**, 359–370 (2014).
148. Jazvinšćak Jembrek, M., Slade, N., Hof, P. R. & Šimić, G. The interactions of p53 with tau and Aß as potential therapeutic targets for Alzheimer's disease. *Prog Neurobiol* **168**, 104–127 (2018).
149. Farmer, K. M. *et al.* P53 aggregation, interactions with tau, and impaired DNA damage response in Alzheimer's disease. *Acta Neuropathol Commun* **8**, (2020).
150. Szybinska, A. & Lesniak, W. P53 Dysfunction in Neurodegenerative Diseases - The Cause or Effect of Pathological Changes? *Aging Dis* **8**, 506 (2017).
151. Burguillos, M. A. *et al.* Caspase signalling controls microglia activation and neurotoxicity. *Nature 2011 472:7343* **472**, 319–324 (2011).
152. Tatton, N. A. Increased Caspase 3 and Bax Immunoreactivity Accompany Nuclear GAPDH Translocation and Neuronal Apoptosis in Parkinson's Disease. *Exp Neurol* **166**, 29–43 (2000).
153. Wolfrum, P., Fietz, A., Schnichels, S. & Hurst, J. The function of p53 and its role in Alzheimer's and Parkinson's disease compared to age-related macular degeneration. *Front Neurosci* **16**, 2206 (2022).
154. Lanni, C. *et al.* Conformationally altered p53: a novel Alzheimer's disease marker? *Mol Psychiatry* **13**, 641–647 (2008).

155. Buizza, L. *et al.* Conformational altered p53 affects neuronal function: relevance for the response to toxic insult and growth-associated protein 43 expression. *Cell Death & Disease 2013 4:2* **4**, e484–e484 (2013).
156. Rossi, G. *et al.* Tau mutations serve as a novel risk factor for cancer. *Cancer Res* **78**, 3731–3739 (2018).
157. Rossi, G. *et al.* Mutations in MAPT gene cause chromosome instability and introduce copy number variations widely in the genome. *J Alzheimers Dis* **33**, 969–982 (2013).
158. Smoter, M. *et al.* The role of Tau protein in resistance to paclitaxel. *Cancer Chemother Pharmacol* **68**, 553–557 (2011).
159. Kerr, J. F. R., Wyllie, A. H. & Currie, A. R. Apoptosis: a basic biological phenomenon with wide-ranging implications in tissue kinetics. *Br J Cancer* **26**, 239–257 (1972).
160. Norbury, C. J. & Hickson, I. D. Cellular responses to DNA damage. *Annu Rev Pharmacol Toxicol* **41**, 367–401 (2001).
161. Norbury, C. J. & Hickson, I. D. Cellular responses to DNA damage. *Annu Rev Pharmacol Toxicol* **41**, 367–401 (2001).
162. Ge, Y., Huang, M. & Yao, Y. M. Efferocytosis and Its Role in Inflammatory Disorders. *Front Cell Dev Biol* **10**, (2022).
163. Kerr, J. F. R., Wyllie, A. H. & Currie, A. R. Apoptosis: a basic biological phenomenon with wide-ranging implications in tissue kinetics. *Br J Cancer* **26**, 239–257 (1972).
164. Li, J. & Yuan, J. Caspases in apoptosis and beyond. *Oncogene* **27**, 6194–6206 (2008).
165. Thornberry, N. A. & Lazebnik, Y. Caspases: Enemies within. *Science (1979)* **281**, 1312–1316 (1998).
166. Nicholson, D. W. Caspase structure, proteolytic substrates, and function during apoptotic cell death. *Cell Death & Differentiation 1999 6:11* **6**, 1028–1042 (1999).
167. Stennicke, H. R. & Salvesen, G. S. Caspases - controlling intracellular signals by protease zymogen activation. *Biochim Biophys Acta* **1477**, 299–306 (2000).
168. Guicciardi, M. E. & Gores, G. J. Life and death by death receptors. *The FASEB Journal* **23**, 1625–1637 (2009).
169. Pitti, R. M. *et al.* Induction of apoptosis by Apo-2 ligand, a new member of the tumor necrosis factor cytokine family. *Journal of Biological Chemistry* **271**, 12687–12690 (1996).
170. Green, D. R. & Kroemer, G. The pathophysiology of mitochondrial cell death. *Science (1979)* **305**, 626–629 (2004).

171. Danial, N. N. & Korsmeyer, S. J. Cell Death: Critical Control Points. *Cell* **116**, 205–219 (2004).
172. Zeiss, C. J. The apoptosis-necrosis continuum: insights from genetically altered mice. *Vet Pathol* **40**, 481–495 (2003).
173. Nijhawan, D., Honarpour, N. & Wang, X. Apoptosis in neural development and disease. *Annu Rev Neurosci* **23**, 73–87 (2000).
174. Greenhalgh, D. G. The role of apoptosis in wound healing. *Int J Biochem Cell Biol* **30**, 1019–1030 (1998).
175. Carson, D. A. & Ribeiro, J. M. Apoptosis and disease. *Lancet* **341**, 1251–1254 (1993).
176. Thompson, C. B. Apoptosis in the pathogenesis and treatment of disease. *Science* **267**, 1456–1462 (1995).
177. Hayflick, L. & Moorhead, P. S. The serial cultivation of human diploid cell strains. *Exp Cell Res* **25**, 585–621 (1961).
178. Courtois-Cox, S., Jones, S. L. & Cichowski, K. Many roads lead to oncogene-induced senescence. *Oncogene 2008 27:20* **27**, 2801–2809 (2008).
179. Toussaint, O., Medrano, E. E. & Von Zglinicki, T. Cellular and molecular mechanisms of stress-induced premature senescence (SIPS) of human diploid fibroblasts and melanocytes. *Exp Gerontol* **35**, 927–945 (2000).
180. Von Zglinicki, T., Petrie, J. & Kirkwood, T. B. L. Telomere-driven replicative senescence is a stress response. *Nature Biotechnology 2003 21:3* **21**, 229–230 (2003).
181. Sikora, E., Arendt, T., Bennett, M. & Narita, M. Impact of cellular senescence signature on ageing research. *Ageing Res Rev* **10**, 146–152 (2011).
182. Campisi, J. Aging, Cellular Senescence, and Cancer. *https://doi.org/10.1146/annurev-physiol-030212-183653* **75**, 685–705 (2013).
183. Kurz, D. J., Decary, S., Hong, Y. & Erusalimsky, J. D. Senescence-associated (beta)-galactosidase reflects an increase in lysosomal mass during replicative ageing of human endothelial cells. *J Cell Sci* **113**, 3613–3622 (2000).
184. Lee, B. Y. *et al.* Senescence-associated β-galactosidase is lysosomal β-galactosidase. *Aging Cell* **5**, 187–195 (2006).
185. Coppé, J. P., Desprez, P. Y., Krtolica, A. & Campisi, J. The Senescence-Associated Secretory Phenotype: The Dark Side of Tumor Suppression. *Annu Rev Pathol* **5**, 99 (2010).

186. Zhang, R. *et al.* Formation of MacroH2A-containing senescence-associated heterochromatin foci and senescence driven by ASF1a and HIRA. *Dev Cell* **8**, 19–30 (2005).
187. Narita, M. *et al.* Rb-mediated heterochromatin formation and silencing of E2F target genes during cellular senescence. *Cell* **113**, 703–716 (2003).
188. Zhang, R., Chen, W. & Adams, P. D. Molecular dissection of formation of senescence-associated heterochromatin foci. *Mol Cell Biol* **27**, 2343–2358 (2007).
189. Sadaie, M. *et al.* Redistribution of the Lamin B1 genomic binding profile affects rearrangement of heterochromatic domains and SAHF formation during senescence. *Genes Dev* **27**, 1800–1808 (2013).
190. Swanson, E. C., Manning, B., Zhang, H. & Lawrence, J. B. Higher-order unfolding of satellite heterochromatin is a consistent and early event in cell senescence. *J Cell Biol* **203**, 929–942 (2013).
191. Lengefeld, J. *et al.* Cell size is a determinant of stem cell potential during aging. *Sci Adv* **7**, 271 (2021).
192. Acosta, J. C. *et al.* A complex secretory program orchestrated by the inflammasome controls paracrine senescence. *Nature Cell Biology 2013 15:8* **15**, 978–990 (2013).
193. Sharpless, N. E. & Sherr, C. J. Forging a signature of in vivo senescence. *Nature Reviews Cancer 2015 15:7* **15**, 397–408 (2015).
194. Demaria, M. *et al.* An Essential Role for Senescent Cells in Optimal Wound Healing through Secretion of PDGF-AA. *Dev Cell* **31**, 722–733 (2014).
195. Adams, P. D. Healing and Hurting: Molecular Mechanisms, Functions, and Pathologies of Cellular Senescence. *Mol Cell* **36**, 2–14 (2009).
196. Lecot, P., Alimirah, F., Desprez, P. Y., Campisi, J. & Wiley, C. Context-dependent effects of cellular senescence in cancer development. *British Journal of Cancer 2016 114:11* **114**, 1180–1184 (2016).
197. Campisi, J. Aging, cellular senescence, and cancer. *Annu Rev Physiol* **75**, 685–705 (2013).
198. Chinta, S. J. *et al.* Cellular Senescence Is Induced by the Environmental Neurotoxin Paraquat and Contributes to Neuropathology Linked to Parkinson's Disease. *Cell Rep* **22**, 930–940 (2018).
199. Bussian, T. J. *et al.* Clearance of senescent glial cells prevents tau-dependent pathology and cognitive decline. *Nature 2018 562:7728* **562**, 578–582 (2018).

200. Bussian, T. J. *et al.* Clearance of senescent glial cells prevents tau-dependent pathology and cognitive decline. *Nature 2018 562:7728* **562**, 578–582 (2018).
201. Soto-Gamez, A., Quax, W. J. & Demaria, M. Regulation of Survival Networks in Senescent Cells: From Mechanisms to Interventions. *J Mol Biol* **431**, 2629–2643 (2019).
202. Atamna, H., Cheung, I. & Ames, B. N. A method for detecting abasic sites in living cells: age-dependent changes in base excision repair. *Proc Natl Acad Sci U S A* **97**, 686–691 (2000).
203. Ciccia, A. & Elledge, S. J. The DNA Damage Response: Making it safe to play with knives. *Mol Cell* **40**, 179 (2010).
204. Jackson, S. P. & Bartek, J. The DNA-damage response in human biology and disease. *Nature* **461**, 1071–1078 (2009).
205. Giglia-Mari, G., Zotter, A. & Vermeulen, W. DNA Damage Response. *Cold Spring Harb Perspect Biol* **3**, 1–19 (2011).
206. Clay, D. E. & Fox, D. T. DNA Damage Responses during the Cell Cycle: Insights from Model Organisms and Beyond. *Genes (Basel)* **12**, (2021).
207. Huang, R. X. & Zhou, P. K. DNA damage response signaling pathways and targets for radiotherapy sensitization in cancer. *Signal Transduction and Targeted Therapy 2020 5:1* **5**, 1–27 (2020).
208. Matsuoka, S. *et al.* ATM and ATR substrate analysis reveals extensive protein networks responsive to DNA damage. *Science (1979)* **316**, 1160–1166 (2007).
209. Maréchal, A. & Zou, L. DNA damage sensing by the ATM and ATR kinases. *Cold Spring Harb Perspect Biol* **5**, (2013).
210. Bartek, J. & Lukas, J. Chk1 and Chk2 kinases in checkpoint control and cancer. *Cancer Cell* **3**, 421–429 (2003).
211. Goodarzi, A. A. *et al.* ATM signaling facilitates repair of DNA double-strand breaks associated with heterochromatin. *Mol Cell* **31**, 167–177 (2008).
212. Ahmed, K. A. & Xiang, J. Mechanisms of cellular communication through intercellular protein transfer. *J Cell Mol Med* **15**, 1458 (2011).
213. Liu, Y., Tavana, O. & Gu, W. P53 modifications: Exquisite decorations of the powerful guardian. *J Mol Cell Biol* **11**, 564–577 (2019).
214. Kruse, J. P. & Gu, W. SnapShot: p53 posttranslational modifications. *Cell* **133**, (2008).

215. DeVine, T. & Dai, M.-S. Targeting the ubiquitin-mediated proteasome degradation of p53 for cancer therapy. *Curr Pharm Des* **19**, 3248 (2013).
216. Brooks, C. L. & Gu, W. p53 ubiquitination: Mdm2 and beyond. *Mol Cell* **21**, 307–315 (2006).
217. Bode, A. M. & Dong, Z. Post-translational modification of p53 in tumorigenesis. *Nat Rev Cancer* **4**, 793–805 (2004).
218. Hoe, K. K., Verma, C. S. & Lane, D. P. Drugging the p53 pathway: understanding the route to clinical efficacy. *Nat Rev Drug Discov* **13**, 217–236 (2014).
219. Hoh, J. *et al.* The p53MH algorithm and its application in detecting p53-responsive genes. *Proc Natl Acad Sci U S A* **99**, 8467 (2002).
220. Shvarts, A. *et al.* MDMX: a novel p53-binding protein with some functional properties of MDM2. *EMBO J* **15**, 5349 (1996).
221. Marine, J. C. & Jochemsen, A. G. Mdmx as an essential regulator of p53 activity. *Biochem Biophys Res Commun* **331**, 750–760 (2005).
222. Hock, A. K. & Vousden, K. H. The role of ubiquitin modification in the regulation of p53. *Biochimica et Biophysica Acta (BBA) - Molecular Cell Research* **1843**, 137–149 (2014).
223. Nag, S., Qin, J., Srivenugopal, K. S., Wang, M. & Zhang, R. The MDM2-p53 pathway revisited. *J Biomed Res* **27**, 254 (2013).
224. Mirza-Aghazadeh-Attari, M. *et al.* DNA damage response and repair in colorectal cancer: Defects, regulation and therapeutic implications. *DNA Repair (Amst)* **69**, 34–52 (2018).
225. Hwang, J. Y., Aromolaran, K. A. & Zukin, R. S. The emerging field of epigenetics in neurodegeneration and neuroprotection. *Nat Rev Neurosci* **18**, 347 (2017).
226. Moosavi, A. & Ardekani, A. M. Role of Epigenetics in Biology and Human Diseases. *Iran Biomed J* **20**, 246 (2016).
227. Butenko, Y. & Ohad, N. Polycomb-group mediated epigenetic mechanisms through plant evolution. *Biochim Biophys Acta Gene Regul Mech* **1809**, 395–406 (2011).
228. Lewis, E. B. *review article A gene complex controlling segmentation in Drosophila*. *Nature* vol. 276 (1978).
229. Lewis, E. B. A gene complex controlling segmentation in Drosophila. *Nature 1978 276:5688* **276**, 565–570 (1978).

230. Loubiere, V., Martinez, A. M. & Cavalli, G. Cell Fate and Developmental Regulation Dynamics by Polycomb Proteins and 3D Genome Architecture. *BioEssays* **41**, 1800222 (2019).
231. Schuettengruber, B., Chourrout, D., Vervoort, M., Leblanc, B. & Cavalli, G. Genome Regulation by Polycomb and Trithorax Proteins. *Cell* **128**, 735–745 (2007).
232. Schuettengruber, B., Bourbon, H. M., di Croce, L. & Cavalli, G. Genome Regulation by Polycomb and Trithorax: 70 Years and Counting. *Cell* **171**, 34–57 (2017).
233. Klein, D. C. & Hainer, S. J. Chromatin regulation and dynamics in stem cells. *Curr Top Dev Biol* **138**, 1 (2020).
234. Simon, J. A. & Kingston, R. E. Occupying Chromatin: Polycomb Mechanisms for Getting to Genomic Targets, Stopping Transcriptional Traffic, and Staying Put. *Mol Cell* **49**, 808–824 (2013).
235. Wang, W. *et al.* Polycomb Group (PcG) Proteins and Human Cancers: Multifaceted Functions and Therapeutic Implications. *Med Res Rev* **35**, 1220 (2015).
236. Cohen, I., Bar, C. & Ezhkova, E. Activity of PRC1 and Histone H2AK119 Monoubiquitination: Revising Popular Misconceptions. *BioEssays* **42**, 1900192 (2020).
237. de Napoles, M. *et al.* Polycomb Group Proteins Ring1A/B Link Ubiquitylation of Histone H2A to Heritable Gene Silencing and X Inactivation. *Dev Cell* **7**, 663–676 (2004).
238. Gao, Z. *et al.* PCGF homologs, CBX proteins, and RYBP define functionally distinct PRC1 family complexes. *Mol Cell* **45**, 344–356 (2012).
239. Wang, R. *et al.* Polycomb group targeting through different binding partners of RING1B C-terminal domain. *Structure* **18**, 966–975 (2010).
240. Hauri, S. *et al.* A High-Density Map for Navigating the Human Polycomb Complexome. *Cell Rep* **17**, 583–595 (2016).
241. Pemberton, H. *et al.* Genome-wide co-localization of Polycomb orthologs and their effects on gene expression in human fibroblasts. *Genome Biol* **15**, 1–16 (2014).
242. Tavares, L. *et al.* RYBP-PRC1 Complexes Mediate H2A Ubiquitylation at Polycomb Target Sites Independently of PRC2 and H3K27me3. *Cell* **148**, 664 (2012).
243. Garcia, E., Marcos-Gutiérrez, C., del Mar Lorente, M., Moreno, J. C. & Vidal, M. RYBP, a new repressor protein that interacts with components of the mammalian Polycomb complex, and with the transcription factor YY1. *EMBO J* **18**, 3404–3418 (1999).

244. Boyer, L. A. *et al.* Polycomb complexes repress developmental regulators in murine embryonic stem cells. *Nature* **441**, 349–353 (2006).
245. Thornton, S. R., Butty, V. L., Levine, S. S. & Boyer, L. A. Polycomb Repressive Complex 2 Regulates Lineage Fidelity during Embryonic Stem Cell Differentiation. *PLoS One* **9**, e110498 (2014).
246. von Schimmelmann, M. *et al.* Polycomb repressive complex 2 (PRC2) silences genes responsible for neurodegeneration. *Nat Neurosci* **19**, 1321–1330 (2016).
247. Czermin, B. *et al.* Drosophila enhancer of Zeste/ESC complexes have a histone H3 methyltransferase activity that marks chromosomal Polycomb sites. *Cell* **111**, 185–196 (2002).
248. Cao, R. *et al.* Role of histone H3 lysine 27 methylation in polycomb-group silencing. *Science (1979)* **298**, 1039–1043 (2002).
249. Margueron, R. *et al.* Role of the polycomb protein EED in the propagation of repressive histone marks. *Nature 2009 461:7265* **461**, 762–767 (2009).
250. Moritz, L. E. & Trievel, R. C. Structure, mechanism, and regulation of polycomb-repressive complex 2. *J Biol Chem* **293**, 13805–13814 (2018).
251. Kasinath, V. *et al.* Structures of human PRC2 with its cofactors AEBP2 and JARID2. *Science* **359**, 940–944 (2018).
252. Ciferri, C. *et al.* Molecular architecture of human polycomb repressive complex 2. *Elife* **1**, (2012).
253. Yang, X. *et al.* Structure-Activity Relationship Studies for Enhancer of Zeste Homologue 2 (EZH2) and Enhancer of Zeste Homologue 1 (EZH1) Inhibitors. *J Med Chem* **59**, 7617–7633 (2016).
254. Jiao, L. & Liu, X. Structural basis of histone H3K27 trimethylation by an active polycomb repressive complex 2. *Science* **350**, (2015).
255. Do´, D. *et al.* The Polycomb -Group Gene Ezh2 Is Required for Early Mouse Development . *Mol Cell Biol* **21**, 4330–4336 (2001).
256. Pasini, D., Bracken, A. P., Jensen, M. R., Denchi, E. L. & Helin, K. Suz12 is essential for mouse development and for EZH2 histone methyltransferase activity. *EMBO J* **23**, 4061–4071 (2004).
257. Moritz, L. E. & Trievel, R. C. Structure, mechanism, and regulation of polycomb-repressive complex 2. *J Biol Chem* **293**, 13805–13814 (2018).
258. Piunti, A. & Shilatifard, A. Epigenetic balance of gene expression by Polycomb and COMPASS families. *Science* **352**, (2016).

259. Kim, H., Kang, K. & Kim, J. AEBP2 as a potential targeting protein for Polycomb Repression Complex PRC2. *Nucleic Acids Res* **37**, 2940–2950 (2009).
260. Schmitges, F. W. *et al.* Histone methylation by PRC2 is inhibited by active chromatin marks. *Mol Cell* **42**, 330–341 (2011).
261. Aranda, S., Mas, G. & di Croce, L. Regulation of gene transcription by Polycomb proteins. *Sci Adv* **1**, (2015).
262. Moritz, L. E. & Trievel, R. C. Structure, mechanism, and regulation of polycomb-repressive complex 2. *J Biol Chem* **293**, 13805–13814 (2018).
263. Blackledge, N. P., Rose, N. R. & Klose, R. J. Targeting polycomb systems to regulate gene expression: modifications to a complex story. *Nat Rev Mol Cell Biol* **16**, 643 (2015).
264. Aranda, S., Mas, G. & Di Croce, L. Regulation of gene transcription by Polycomb proteins. *Sci Adv* **1**, (2015).
265. Laugesen, A., Højfeldt, J. W. & Helin, K. Role of the Polycomb Repressive Complex 2 (PRC2) in Transcriptional Regulation and Cancer. *Cold Spring Harb Perspect Med* **6**, (2016).
266. Moritz, L. E. & Trievel, R. C. Structure, mechanism, and regulation of polycomb-repressive complex 2. *J Biol Chem* **293**, 13805–13814 (2018).
267. Moritz, L. E. & Trievel, R. C. Structure, mechanism, and regulation of polycomb-repressive complex 2. *J Biol Chem* **293**, 13805 (2018).
268. Grijzenhout, A. *et al.* Functional analysis of AEBP2, a PRC2 Polycomb protein, reveals a Trithorax phenotype in embryonic development and in ESCs. *Development* **143**, 2716 (2016).
269. Vizán, P., Beringer, M., Ballaré, C. & Di Croce, L. Role of PRC2-associated factors in stem cells and disease. *FEBS J* **282**, 1723–1735 (2015).
270. Sanulli, S. *et al.* Jarid2 Methylation via the PRC2 Complex Regulates H3K27me3 Deposition during Cell Differentiation. *Mol Cell* **57**, 769 (2015).
271. Margueron, R. & Reinberg, D. The Polycomb complex PRC2 and its mark in life. *Nature 2011 469:7330* **469**, 343–349 (2011).
272. Ding, M. *et al.* The polycomb group protein enhancer of zeste 2 is a novel therapeutic target for cervical cancer. *Clin Exp Pharmacol Physiol* **42**, 458–464 (2015).
273. Kleer, C. G. *et al.* EZH2 is a marker of aggressive breast cancer and promotes neoplastic transformation of breast epithelial cells. *Proc Natl Acad Sci U S A* **100**, 11606–11611 (2003).

274. Yap, D. B. *et al.* Somatic mutations at EZH2 Y641 act dominantly through a mechanism of selectively altered PRC2 catalytic activity, to increase H3K27 trimethylation. *Blood* **117**, 2451–2459 (2011).
275. Kurmasheva, R. T. *et al.* Initial testing (stage 1) of tazemetostat (EPZ-6438), a novel EZH2 inhibitor, by the Pediatric Preclinical Testing Program. *Pediatr Blood Cancer* **64**, e26218 (2017).
276. Campbell, J. E. *et al.* EPZ011989, A Potent, Orally-Available EZH2 Inhibitor with Robust in Vivo Activity. *ACS Med Chem Lett* **6**, 491–495 (2015).
277. Soumyanarayanan, U. & Dymock, B. W. Recently discovered EZH2 and EHMT2 (G9a) inhibitors. *Future Med Chem* **8**, 1635–1654 (2016).
278. Bracken, A. P. *et al.* EZH2 is downstream of the pRB-E2F pathway, essential for proliferation and amplified in cancer. *EMBO J* **22**, 5323–5335 (2003).
279. Varambally, S. *et al.* The polycomb group protein EZH2 is involved in progression of prostate cancer. *Nature* **419**, 624–629 (2002).
280. Ernst, T. *et al.* Inactivating mutations of the histone methyltransferase gene EZH2 in myeloid disorders. *Nat Genet* **42**, 722–726 (2010).
281. Nikoloski, G. *et al.* Somatic mutations of the histone methyltransferase gene EZH2 in myelodysplastic syndromes. *Nat Genet* **42**, 665–667 (2010).
282. Margueron, R. & Reinberg, D. The Polycomb complex PRC2 and its mark in life. *Nature* **469**, 343–349 (2011).
283. Cholewa-Waclaw, J. *et al.* The Role of Epigenetic Mechanisms in the Regulation of Gene Expression in the Nervous System. *J Neurosci* **36**, 11427–11434 (2016).
284. Jung, M. & Pfeifer, G. P. Aging and DNA methylation. *BMC Biol* **13**, 1–8 (2015).
285. Li, J. *et al.* EZH2-mediated H3K27 trimethylation mediates neurodegeneration in ataxia-telangiectasia. *Nat Neurosci* **16**, 1745–1753 (2013).
286. Chaudhry, M. *et al.* Genetic variation in imprinted genes is associated with risk of late-onset Alzheimer's disease. *J Alzheimers Dis* **44**, 989–994 (2015).
287. Kouznetsova, V. L., Tchekanov, A., Li, X., Yan, X. & Tsigelny, I. F. Polycomb repressive 2 complex—Molecular mechanisms of function. *Protein Sci* **28**, 1387 (2019).
288. Vousden, K. H. & Prives, C. Blinded by the Light: The Growing Complexity of p53. *Cell* **137**, 413–431 (2009).
289. Chi, H., Chang, H. Y. & Sang, T. K. Neuronal Cell Death Mechanisms in Major Neurodegenerative Diseases. *Int J Mol Sci* **19**, (2018).

290. Liu, X. A. *et al.* Tau dephosphorylation potentiates apoptosis by mechanisms involving a failed dephosphorylation/activation of Bcl-2. *J Alzheimers Dis* **19**, 953–962 (2010).
291. Li, H. L. *et al.* Phosphorylation of tau antagonizes apoptosis by stabilizing beta-catenin, a mechanism involved in Alzheimer's neurodegeneration. *Proc Natl Acad Sci U S A* **104**, 3591–3596 (2007).
292. Kritsilis, M. *et al.* Ageing, Cellular Senescence and Neurodegenerative Disease. *Int J Mol Sci* **19**, (2018).
293. Baker, D. J. & Petersen, R. C. Cellular senescence in brain aging and neurodegenerative diseases: evidence and perspectives. *J Clin Invest* **128**, 1208–1216 (2018).
294. Bussian, T. J. *et al.* Clearance of senescent glial cells prevents tau-dependent pathology and cognitive decline. *Nature 2018 562:7728* **562**, 578–582 (2018).
295. Childs, B. G., Baker, D. J., Kirkland, J. L., Campisi, J. & Deursen, J. M. Senescence and apoptosis: dueling or complementary cell fates? *EMBO Rep* **15**, 1139–1153 (2014).
296. Clark, J. S. *et al.* Post-translational Modifications of the p53 Protein and the Impact in Alzheimer's Disease: A Review of the Literature. *Front Aging Neurosci* **14**, 268 (2022).
297. Brooks, C. L. & Gu, W. p53 Ubiquitination: Mdm2 and Beyond. *Mol Cell* **21**, 307 (2006).
298. Inoue, K., Fry, E. A. & Frazier, D. P. Transcription factors that interact with p53 and Mdm2. *International journal of cancer. Journal international du cancer* **138**, 1577 (2016).
299. Meek, D. W. & Anderson, C. W. Posttranslational Modification of p53: Cooperative Integrators of Function. *Cold Spring Harb Perspect Biol* **1**, (2009).
300. Lanni, C. *et al.* Conformationally altered p53: a novel Alzheimer's disease marker? *Mol Psychiatry* **13**, 641–647 (2008).
301. Clark, J. S. *et al.* Post-translational Modifications of the p53 Protein and the Impact in Alzheimer's Disease: A Review of the Literature. *Front Aging Neurosci* **14**, (2022).
302. Abate, G. *et al.* The pleiotropic role of p53 in functional/dysfunctional neurons: focus on pathogenesis and diagnosis of Alzheimer's disease. *Alzheimers Res Ther* **12**, (2020).

303. Clark, J. S. *et al.* Post-translational Modifications of the p53 Protein and the Impact in Alzheimer's Disease: A Review of the Literature. *Front Aging Neurosci* **14**, (2022).
304. Merlo, P. *et al.* P53 prevents neurodegeneration by regulating synaptic genes. *Proc Natl Acad Sci U S A* **111**, 18055–18060 (2014).
305. Lei, C. *et al.* Analysis of Tau Protein Expression in Predicting Pathological Complete Response to Neoadjuvant Chemotherapy in Different Molecular Subtypes of Breast Cancer. *J Breast Cancer* **23**, 47 (2020).
306. Hedna, R. *et al.* Tau Protein as Therapeutic Target for Cancer? Focus on Glioblastoma. *Cancers (Basel)* **14**, (2022).
307. Cai, Y., Liu, J., Wang, B., Sun, M. & Yang, H. Microglia in the Neuroinflammatory Pathogenesis of Alzheimer's Disease and Related Therapeutic Targets. *Front Immunol* **13**, (2022).
308. Ito, T., Teo, Y. V., Evans, S. A., Neretti, N. & Sedivy, J. M. Regulation of Cellular Senescence by Polycomb Chromatin Modifiers through Distinct DNA Damage- and Histone Methylation-Dependent Pathways. *Cell Rep* **22**, 3480–3492 (2018).
309. Chu, L. *et al.* Induction of senescence-associated secretory phenotype underlies the therapeutic efficacy of PRC2 inhibition in cancer. *Cell Death & Disease 2022 13:2* **13**, 1–14 (2022).
310. Kouznetsova, V. L., Tchekanov, A., Li, X., Yan, X. & Tsigelny, I. F. Polycomb repressive 2 complex—Molecular mechanisms of function. *Protein Science* **28**, 1387–1399 (2019).
311. Parreno, V., Martinez, A. M. & Cavalli, G. Mechanisms of Polycomb group protein function in cancer. *Cell Research 2022 32:3* **32**, 231–253 (2022).
312. Wienken, M. *et al.* MDM2 Associates with Polycomb Repressor Complex 2 and Enhances Stemness-Promoting Chromatin Modifications Independent of p53. *Mol Cell* **61**, 68 (2016).
313. Wienken, M., Moll, U. M. & Dobbelstein, M. Mdm2 as a chromatin modifier. *J Mol Cell Biol* **9**, 74 (2017).
314. Klus, P., Cirillo, D., Botta Orfila, T. & Gaetano Tartaglia, G. Neurodegeneration and Cancer: Where the Disorder Prevails. *Scientific Reports 2015 5:1* **5**, 1–7 (2015).
315. Kumari, S., Dhapola, R. & Reddy, D. H. K. Apoptosis in Alzheimer's disease: insight into the signaling pathways and therapeutic avenues. *Apoptosis* **1**, 1–15 (2023).
316. Erekat, N. S. Apoptosis and its therapeutic implications in neurodegenerative diseases. *Clinical Anatomy* **35**, 65–78 (2022).

317. Pfeffer, C. M. & Singh, A. T. K. Apoptosis: A Target for Anticancer Therapy. *Int J Mol Sci* **19**, (2018).
318. Holloway, K., Neherin, K., Dam, K. U. & Zhang, H. Cellular senescence and neurodegeneration. *Hum Genet* (2023) doi:10.1007/S00439-023-02565-X.
319. Martínez-Cué, C. & Rueda, N. Cellular Senescence in Neurodegenerative Diseases. *Front Cell Neurosci* **14**, (2020).
320. Wang, L., Lankhorst, L. & Bernards, R. Exploiting senescence for the treatment of cancer. *Nature Reviews Cancer 2022 22:6* **22**, 340–355 (2022).

List of publication and other activities

Published:

'Tau affects P53 function and cell fate during the DNA damage response'
Communication Biology– May 2020
Martina Sola & **Claudia Magrin**, Giona Pedrioli, Sandra Pinton, Agnese Salvadè, Stèphanie Papin&PaoloPaganetti
https://doi.org/10.1038/s42003-020-0975-4

'Tau seed in extracellular vesicles induce Tau accumulation in degradative organelles of cells'
DNA and cell biology - September 2021
Giona Pedrioli, Marialuisa Barberis, **Claudia Magrin**, Diego Morone, Ester Piovesana, Giorgia Senesi, Martina Sola, Stèphanie Papin & Paolo Paganetti https://doi.org/10.1089/dna.2021.0485

Submitted:

'Tau protein modulates epigenetic-mediated induction of cellular senescence'
Fr Cell Dev Biol– submitted 2023
Claudia Magrin, Martina Sola,Ester Piovesana, Marco Bolis, Andrea Rinaldi, Stéphanie Papin, Paolo Paganetti https://doi.org/10.1038/s42003-020-0975-4

Posters at National and International Congress

- BeNeFri Workshop – February 2020
- BeNeFri Workshop – February 2021
- 10° Giornata della Ricerca della Svizzera Italiana – June 2021
- Synapsis Forum – September 2021
- PhD Day – October 2019
- PhD Day – October 2020
- PhD Day – October 2021 (Oral Presentation)
- ADPD 2022- March 2022 (Oral Presentation)